

Stony Brook University



OFFICIAL COPY

The official electronic file of this thesis or dissertation is maintained by the University Libraries on behalf of The Graduate School at Stony Brook University.

© All Rights Reserved by Author.

Potts Model and Generalizations: Exact Results and Statistical Physics

A Dissertation Presented

by

Yan Xu

to

The Graduate School

in Partial Fulfillment of the Requirements

for the Degree of

Doctor of Philosophy

in

Physics

Stony Brook University

May 2012

Stony Brook University

The Graduate School

Yan Xu

We, the dissertation committee for the above candidate for the Doctor of Philosophy degree, hereby recommend acceptance of this dissertation.

Robert Shrock – Dissertation Advisor
Professor, C. N. Yang Institute for Theoretical Physics,
Department of Physics and Astronomy

Alexander Abanov – Chairperson of Defense
Associate Professor, Department of Physics and Astronomy

Jin Wang – Committee Member
Associate Professor, Affiliated to Department of Physics and Astronomy
Department of Chemistry

Jiangyong Jia – Outside Member
Assistant Professor, Department of Chemistry

This dissertation is accepted by the Graduate School.

Charles Taber
Interim Dean of the Graduate School

Abstract of the Dissertation

Potts Model and Generalizations: Exact Results and Statistical Physics

by

Yan Xu

Doctor of Philosophy

in

Physics

Stony Brook University

2012

The q -state Potts model is a spin model that has been of longstanding interest as a many body system in statistical mechanics. Via a cluster expansion, the Potts model partition function $Z(G, q, v)$, defined on a graph $G = (V, E)$, where V is the set of vertices (sites) and E is the set of edges (bonds), is expressed as a polynomial in terms of q and a temperature-dependent Boltzmann variable v . An important special case ($v = -1$) is the zero-temperature Potts antiferromagnet, for which $Z(G, q, -1) = P(G, q)$, where $P(G, q)$ is the chromatic polynomial, counting the number of ways of assigning q colors to the vertices of graph G such that no two adjacent vertices have the same color.

A natural generalization is to consider this model in a generalized external field that favors or disfavors spin values in a subset $I_s = \{1, \dots, s\}$ of the total set of q -state spin values. In this dissertation, we calculate the exact partition functions of the generalized Potts model $Z(G, q, s, v, w)$, where w is a field-dependent Boltz-

mann variable, for certain families of graphs. We also investigate its special case, viz. $Z(G, q, s, -1, w) = Ph(G, q, s, w)$, which describes a weighted-set graph coloring problem.

Nonzero ground-state entropy (per lattice site), $S_0 \neq 0$, is an important subject in statistical physics, as an exception to the third law of thermodynamics and a phenomenon involving large disorder even at zero temperature. The q -state Potts antiferromagnet is a model exhibiting ground-state entropy for sufficiently large q on a given lattice graph. Another part of the dissertation is devoted to the study of ground-state entropy, for which lower bounds on slabs of the simple cubic lattice and exact results on homeomorphic expansions of kagomé lattice strips are presented. Next, we focus on the structure of chromatic polynomials for a particular class of graphs, viz. planar triangulations $\{G_{pt}\}$, and discuss implications for chromatic zeros and some asymptotic limiting quantities.

Contents

List of Figures	viii
List of Tables	ix
Acknowledgements	x
1 Introduction to Potts Model and Generalizations	1
1.1 The Zero-Field Potts Model and Its Partition Function as a Cluster Expansion	3
1.2 Ground State Entropy of the Potts Antiferromagnet and Its Connection with the Chromatic Polynomial	4
1.3 Potts Model in a Generalized External Field and Weighted-Set Graph Colorings	6
2 Exact Results on the Generalized Potts Model Partition Function and Weighted-Set Graph Colorings for Certain Families of Graphs	10
2.1 General Properties of $Z(G, q, s, v, w)$ and $Ph(G, q, s, w)$	10
2.2 Star Graphs S_n	15
2.3 Path graphs L_n	16
2.4 Circuit Graphs C_n	18
2.5 Complete Graphs K_n	20
2.6 The p -Wheel graphs $Wh_n^{(p)} = K_p + C_{n-p}$	22
2.7 Upper and Lower Bounds on $Z(G, q, s, v, w)$ for $v \geq 0$	26
2.8 Use of $Z(G, q, s, v, w)$ and $Ph(G, q, s, w)$ to Distinguish Between Tutte-Equivalent and Chromatically Equivalent Graphs	31
3 Ground State Entropy of the Potts Antiferromagnet: I. Lower Bounds for Slabs of the Simple Cubic Lattice	37
3.1 Computational Method	37
3.2 Results for Slab of Thickness $L_z = 2$ with FBC_z	41

3.3	Comparison with Large- q Series Expansions	42
3.4	Results for Slabs of Thickness $L_z = 3, 4$ with FBC_z	45
3.5	Result for Slab of Thickness $L_z = 3$ with PBC_z	45
3.6	Discussion	46
4	Ground State Entropy of the Potts Antiferromagnet: II. Exact Calculations of Homeomorphic Expansions of Kagomé Lattice Strips	49
4.1	Homeomorphic Expansions of Kagomé Lattice Strips	49
4.2	Computational Method	52
4.3	Strips with Free Longitudinal Boundary Conditions	53
4.4	Cyclic Strip $[H_k(kag)]_{m,c}$	56
4.5	Locus \mathcal{B}	58
4.5.1	Case of Free Longitudinal Boundary Conditions	58
4.5.2	Case of Cyclic Longitudinal Boundary Conditions	59
5	Chromatic Polynomials of Planar Triangulation Graphs: I. The Tutte Upper Bound and One-Parameter Families	61
5.1	Chromatic Polynomials of Planar Triangulations and the Tutte Upper Bound	61
5.2	General Properties of One-Parameter Families of Planar Trian- gulations	63
5.2.1	General	63
5.2.2	Families with $P(G_{pt,m}, q)$ Consisting of a Power of a Sin- gle Polynomial	64
5.2.3	Families with $P(G_{pt,m}, q)$ Consisting of Powers of Several Functions	65
5.2.4	Asymptotic Behavior as $m \rightarrow \infty$	66
5.3	Properties of a Class of $G_{pt,m}$ with $P(G_{pt,m}, q)$ Having $j_{max} = 3$ and Certain $\lambda_{G_{pt},j}$	67
5.3.1	Structure of Coefficients $c_{G_{pt},j}$ in $P(G_{pt,m}, q)$	67
5.3.2	Properties of Real Chromatic Zeros	70
5.3.3	Properties of Complex Chromatic Zeros	73
5.4	The Family $R_m = P_m + P_2$	75
5.5	The Cylindrical Strip of the Triangular Lattice with $L_y = 3$	76
5.6	Iterated Icosahedron Graphs	77
5.7	The Bipyramid Family B_m	79
5.8	The Family H_m	80
5.9	The Family L_m	83
5.10	The Family F_m	84

6	Chromatic Polynomials of Planar Triangulation Graphs: II. Multi-Parameter Families and Implications for Statistical Physics	90
6.1	Two-Parameter Families of Planar Triangulations, G_{pt,m_1,m_2}	90
6.2	General Form of $P(G_{pt,m}, q)$	94
6.3	The Two-Parameter Family D_{m_1,m_2}	95
6.4	The Family $D_{m-4,0}$	102
6.5	The Family $D_{m-4,1}$	103
6.6	The Family $D_{m-4,2}$	104
6.7	The Family $D_{m-4,3}$	106
6.8	The Family $D_{0,m-2}$	108
6.9	A Symmetric Two-Parameter Family S_{m_1,m_2}	108
6.10	Families of the form G_{pt,m_1,m_2} with $m_1 = m_2$	111
6.11	The Families D_{m_1,m_2} and S_{m_1,m_2} with $m_1 = m_2$	112
6.12	Some Implications for Statistical Physics	114
6.13	Comparative Discussion	116
6.14	Summary of Chapter	117
	Bibliography	119

List of Figures

1.1	An illustration of the cluster expansion of C_3 graph.	5
1.2	Physical ranges of w with the weighted-set colorings of C_3 graph as an illustration.	8
1.3	Potts model and generalizations, as well as implications for statistical physics: the distribution of chapters.	9
2.1	Representatives for several families of graphs: S_n , L_n , Y_n , C_n and Wh_n	15
2.2	The complete graphs K_4 and K_5	20
2.3	Use of $Z(G, q, s, v, w)$ to distinguish between Tutte/chromatic equivalent tree graphs S_n and L_n	33
3.1	Equivalence between simple cubic slab graph $sc[2_F \times 2_F \times (L_y)_F]$ and square lattice strip graph $sq[4_P \times (L_y)_F]$, using $L_y = 3$ as an illustration.	41
4.1	The minimal-width Kagomé lattice strip with free ($[H_0(kag)]_{3,f}$) and periodic ($[H_0(kag)]_{3,f}$) boundary conditions, and its $k = 1$ homeomorphic expansion ($[H_1(kag)]_{3,BC}$). All strips illustrated here are comprised of $m = 3$ subgraphs.	51
5.1	Graphs R_3 and R_4	76
5.2	Octahedron as planar triangulation graph, TC_2	77
5.3	Icosahedron as planar triangulation graph, I_1	78
5.4	Graphs B_5 and B_6	79
5.5	Graphs H_3 and H_4	82
5.6	Graphs L_3 and L_4	83
5.7	Graphs F_3 and F_4	85
5.8	Graphs F_5 and F_6	86
6.1	Graphs $D_{0,0}$ and $D_{1,2}$	96
6.2	Graphs $D_{2,2}$ and $D_{2,3}$	97
6.3	Graphs $S_{0,0}$ and $S_{2,1}$	109

List of Tables

3.1	Comparison of lower bounds $W(S_{(L_z)_{BCz}}, q)_\ell$ for $(L_z)_{BCz} = 2_F = 2_P, 3_F, 4_F, 3_P$ with approximate values of $W(\Lambda, q)$ for the square (sq) and simple cubic (sc) lattices Λ , as determined from large- q series expansions, denoted $W(\Lambda, q)_{ser.}$ and, where available, Monte Carlo simulations, denoted $W(\Lambda, q)_{MC}$. We also list $W(\text{sq}, q)_\ell$ for reference. See text for further details.	48
4.1	Values of $W(\{kag\}, q) \equiv W(\{H_0(kag)\}, q)$, $W(\{H_1(kag)\}, q)$, and $W(\{H_2(kag)\}, q)$ for $3 \leq q \leq 10$. For comparison, we also show $W(\{sq\}, q) \equiv W(\{H_0(sq)\}, q)$, $W(\{H_1(sq)\}, q)$, and $W(\{H_2(sq)\}, q)$ for the square-lattice ladder strips. To save space, we omit the argument q in these W functions below. See text for further details	55
5.1	Location of zeros q_z of $P(B_m, q)$ closest to $\tau+1 = 2.6180339887..$ for m from 4 to 18. Notation $ae-n$ means $a \times 10^{-n}$	81
6.1	Values of the ratio $r(D_{m_1, m_2})$. The rows and columns list m_1 and m_2 , respectively, so that, for example, $r(D_{1,2})$ is the entry 0.3769.	100
6.2	Values of the ratios $r(D_{m_1, \infty})$ and $r(D_{\infty, m_2})$. Note that $r(D_{k, \infty}) = r(D_{\infty, k-2})$ for $k \geq 2$	102
6.3	Location of real zeros of $P(D_{m-4,2}, q)$ in the interval $q \in [q_w, 3)$, as a function of the number of vertices, $n = m + 7$. Here the notation nz means that there is no second real zero in the interval $[q_w, 3)$	105
6.4	Location of real zeros of $P(D_{m-4,3}, q)$ in the interval $q \in [q_w, 3)$, as a function of the number of vertices, $n = m + 8$. Notation nz means that there is no second zero in this interval.	107
6.5	Some asymptotic limiting quantities for one-parameter families of planar triangulations. The shorthand notation $3me, 4mo$ means $\chi = 3$ if m is even and $\chi = 4$ if m is odd. Additional information for χ values is $\chi(R_3) = 3$, $\chi(F_1) = 4$, and $\chi(F_2) = 3$. Numerical values are quoted to three significant figures.	118

Acknowledgements

I am grateful to my dissertation advisor, Prof. Robert Shrock, for his guidance and support.

Chapter 1

Introduction to Potts Model and Generalizations

In this dissertation, we are interested in calculating and analyzing the partition function of the Potts model and its generalizations for various families of graphs $\{G\}$. Our results on this were published in Refs. [66] and [67]. We also study an important special case, namely the partition function of the zero-temperature Potts antiferromagnet, which is the chromatic polynomial. Our results on this were published in Refs. [68], [69] and [70], together with a paper in press, Ref. [71].

The main new results in this thesis work are as follows. We derive a powerful exact general formula for the partition function of the q -state Potts model on various families of graphs G in a generalized external magnetic field that favors or disfavors spin values in a subset $I_s = \{1, \dots, s\}$ of the total set of possible spin values, $Z(G, q, s, v, w)$, where v and w are temperature- and field-dependent Boltzmann variables. An important property of this formula is that it expresses $Z(G, q, s, v, w)$ in a graph-theoretic manner as a sum of contributions from spanning subgraphs G' of the graph G , rather than as a sum over spin configurations, as in the original Hamiltonian formulation. It thus allows one to generalize q from positive integer values to positive real values (and also to complex values, as is necessary for the analysis of the zeros of $Z(G, q, s, v, w)$). Using this general formula, we derive a number of exact properties of $Z(G, q, s, v, w)$. These include new upper and lower bounds on $Z(G, q, s, v, w)$ for the ferromagnetic case in terms of zero-field Potts partition functions with certain transformed arguments. We also prove general inequalities for $Z(G, q, s, v, w)$ on different families of tree graphs. We remark on differences in thermodynamic behavior between our model with a generalized external magnetic field and the Potts model with a conventional magnetic field that favors or disfavors a single spin value. We also analyze an interesting spe-

cial case of the zero-temperature Potts antiferromagnet, corresponding to a set-weighted chromatic polynomial $Ph(G, q, s, w)$ that counts the number of colorings of the vertices of G subject to the condition that colors of adjacent vertices are different, with a weighting w that favors or disfavors colors in the interval I_s . As part of our analysis, we elucidate how the field-dependent Potts partition function and weighted-set chromatic polynomial distinguish, respectively, between Tutte-equivalent and chromatically equivalent pairs of graphs.

This dissertation work also includes new results on chromatic polynomials $P(G, q)$ and ground-state entropy of the q -state Potts antiferromagnet on families of graphs. We calculate rigorous lower bounds for the ground state degeneracy per site, W , of this model on slabs of the simple cubic lattice that are infinite in two directions and finite in the third, which thus interpolate between the square (sq) and simple cubic (sc) lattices. We give a comparison with large- q series expansions for the sq and sc lattices and also present numerical comparisons. Moreover, it is of interest to study how the ground-state entropy of the Potts antiferromagnet depends on various properties of a graph. To elucidate this, we present exact calculations of the chromatic polynomial and resultant ground state entropy of the q -state Potts antiferromagnet on lattice strips that are homeomorphic expansions of a strip of the kagomé lattice. The dependence of the ground state entropy on the form of homeomorphic expansion is elucidated.

It is noteworthy to mention that, in general, the time required for the calculation of these functions (polynomials) grows exponentially with the number of vertices $n = n(G)$, rendering the calculation intractable even for moderate n . Hence, it is quite valuable to develop techniques to handle complexity in calculations and to compute these quantities exactly for arbitrarily large n for certain families of graphs. It is also of great interest to discuss implications of these results in statistical physics.

A *graph* G is defined as a network $G = (V, E)$, where V is the set of vertices (also called sites or nodes), and E is the set of edges (also called bonds or links). We denote the number of vertices of G as $n = n(G) = |V|$ and the number of edges of G as $e(G) = |E|$. Further, $k(G)$ denotes the number of (connected) components of G . $H = (V', E')$ is a *subgraph* of $G = (V, E)$ if $V' \subseteq V$ and $E' \subseteq E$. A *spanning subgraph* is a subgraph containing (or spanning) all the vertices of G , i.e. $G' = (V, E')$ is a spanning subgraph of $G = (V, E)$ if and only if $E' \subseteq E$, and it is denoted as $G' \subseteq G$. We shall use these definitions and notations hereafter.

1.1 The Zero-Field Potts Model and Its Partition Function as a Cluster Expansion

In this chapter we introduce the (zero-field) Potts model and its generalizations, as well as a general discussion of the statistical physics of these models. The q -state Potts model has served as a valuable model for the study of a many-body spin system in statistical mechanics [42], [85]. On a general graph $G = (V, E)$, at temperature T , this model is defined by the partition function

$$Z(G, q, T) = \sum_{\{\sigma\}} e^{-\beta\mathcal{H}}, \quad (1.1)$$

with the (zero-field) Hamiltonian describing a local spin-spin interaction between nearest-neighbors:

$$\mathcal{H} = -J \sum_{\langle ij \rangle \in E} \delta_{\sigma_i \sigma_j}, \quad (1.2)$$

where $\sigma_i = 1, \dots, q$ are the discrete (classical) spin variables on each vertex $i \in V$. $\langle ij \rangle$ denotes pairs of adjacent (nearest-neighbor) vertices, viz. each $\langle ij \rangle$ is an edge in the edge set E . $\delta_{\sigma_i \sigma_j} = 1$ for $\sigma_i = \sigma_j$, and $\delta_{\sigma_i \sigma_j} = 0$ otherwise. $\beta = 1/(k_B T)$ and k_B is the Boltzmann constant. J is the spin-spin interaction constant.

For convenience, we use the notation

$$K = \beta J, \quad v = e^K - 1, \quad (1.3)$$

so that the physical ranges for this temperature-dependent Boltzmann variable v are (i) $v \geq 0$, corresponding to $\infty \geq T \geq 0$ for the Potts ferromagnet ($J > 0$), and (ii) $-1 \leq v \leq 0$, corresponding to $0 \leq T \leq \infty$ for the Potts antiferromagnet ($J < 0$). Thus the (zero-field) Potts model partition function $Z(G, q, v)$ is a function of variables q and v , also depending on the graph G .

One can express $Z(G, q, v)$ as the following

$$Z(G, q, v) = \sum_{\{\sigma\}} \prod_{\langle ij \rangle \in E} (1 + v \delta_{\sigma_i \sigma_j}). \quad (1.4)$$

Then $Z(G, q, v)$ can be written as the sum of spanning subgraphs $G' \subseteq G$, instead of summation over spin configurations $\{\sigma\}$, via a cluster expansion [31]:

$$Z(G, q, v) = \sum_{G' \subseteq G} v^{e(G')} q^{k(G')}, \quad (1.5)$$

where $e(G')$ and $k(G')$ denote the number of edges and components of G' , respectively. Hence, we see that $Z(G, q, v)$ is a polynomial in q and v .

Consider, for example, $G = C_3$, where C_n is the circuit graph with n vertices. See Fig. (1.1). Then we have

$$\begin{aligned}
Z(C_3, q, v) &= \sum_{\{\sigma\}} \prod_{\langle ij \rangle \in E} (1 + v\delta_{\sigma_i \sigma_j}) \\
&= \sum_{\{\sigma\}} (1 + v\delta_{\sigma_1 \sigma_2})(1 + v\delta_{\sigma_2 \sigma_3})(1 + v\delta_{\sigma_3 \sigma_1}) \\
&= \sum_{\{\sigma\}} [1 + v(\delta_{\sigma_1 \sigma_2} + \delta_{\sigma_2 \sigma_3} + \delta_{\sigma_3 \sigma_1}) \\
&\quad + v^2(\delta_{\sigma_1 \sigma_2} \delta_{\sigma_2 \sigma_3} + \delta_{\sigma_2 \sigma_3} \delta_{\sigma_3 \sigma_1} + \delta_{\sigma_3 \sigma_1} \delta_{\sigma_1 \sigma_2}) \\
&\quad + v^3(\delta_{\sigma_1 \sigma_2} \delta_{\sigma_2 \sigma_3} \delta_{\sigma_3 \sigma_1})] \tag{1.6}
\end{aligned}$$

From this figure, as a graphical representation of Eq. (1.6), we see that the contribution to $Z(G, q, v)$ in Eq.(1.4) consists of N_{SSG} terms, each of the form $v^{e(G')}q^{k(G')}$, for each of the spanning subgraphs $G' \subseteq G$, where $N_{SSG} = 2^{e(G)}$ is the total number of spanning subgraphs of G . Thus, for this illustration,

$$Z(C_3, q, v) = q^3 + 3q^2v + 3qv^2 + qv^3 = (q + v)^3 + (q - 1)v^3 \tag{1.7}$$

1.2 Ground State Entropy of the Potts Antiferromagnet and Its Connection with the Chromatic Polynomial

In this section we discuss an important special case for $Z(G, q, v)$. For the Potts antiferromagnet (PAF), $J < 0$ so that, as $T \rightarrow 0$ with $\beta J = -\infty$, viz. $v = -1$; hence, in this limit, the only contributions to the partition function are from spin configurations in which adjacent spins have different values. The resultant $T = 0$ PAF partition function is therefore precisely the chromatic polynomial $P(G, q)$ of the graph G :

$$Z(G, q, T = 0)_{PAF} = Z(G, q, v = -1) = P(G, q) , \tag{1.8}$$

where $P(G, q)$ counts the number of ways of assigning q colors to the vertices of G subject to the condition that no two adjacent vertices have the same color (for references and reviews on the chromatic polynomial, see [14], [43], [44] and

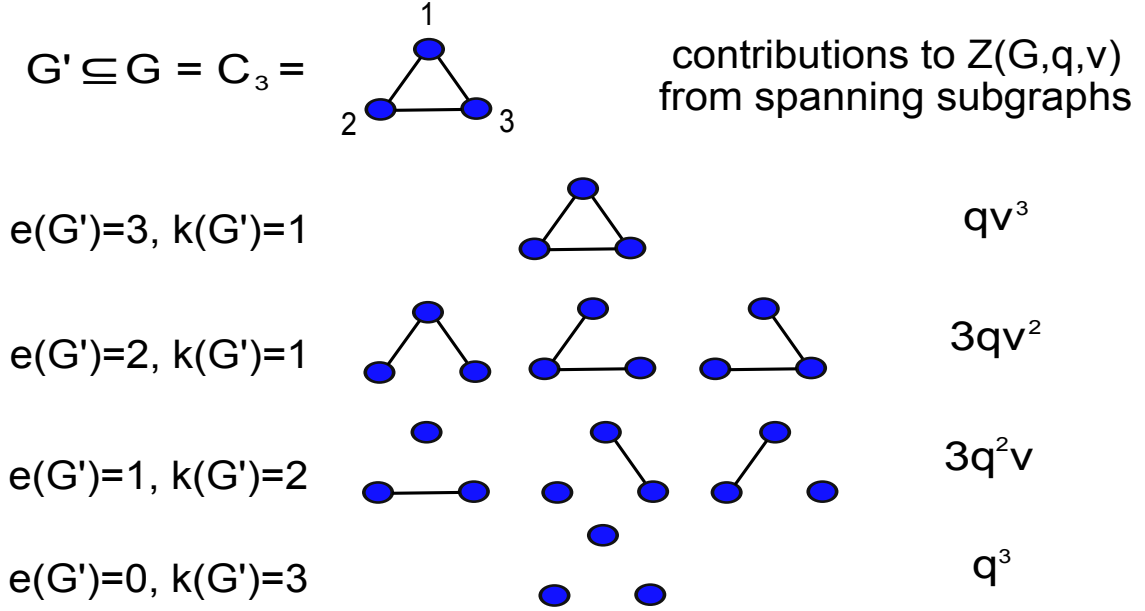


Figure 1.1: An illustration of the cluster expansion of C_3 graph.

[29]). This is called a proper q -coloring of (the vertices of) graph G . Thus, the ground state degeneracy (per site) is connected to the chromatic polynomial via the following relation

$$W(\{G\}, q) = \lim_{n \rightarrow \infty} P(G, q)^{1/n}. \quad (1.9)$$

Nonzero ground state entropy (per lattice site), $S_0 \neq 0$, is an important subject in statistical mechanics, as an exception to the third law of thermodynamics and a phenomenon involving large disorder even at zero temperature [41]. Since $S_0 = k_B \ln W$, where $W = \lim_{n \rightarrow \infty} W_{tot}^{1/n}$ and n denotes the number of lattice sites, $S_0 \neq 0$ is equivalent to $W > 1$, i.e., a total ground state degeneracy W_{tot} that grows exponentially rapidly as a function of n . One physical example is provided by H_2O ice, for which the measured residual entropy per site (at 1 atm. pressure) is $S_0 = (0.41 \pm 0.03)k_B$, or equivalently, $W = 1.51 \pm 0.05$ [41] [32] [1] (a recent theoretical study is [7], which gets $W = 1.50738 \pm 0.00016$). In ice, the ground state entropy occurs without frustration; that is, each of the ground state configurations of the hydrogen atoms on the hydrogen bonds between water molecules minimizes the internal energy of the crystal. This is in contrast to systems where nonzero ground state entropy is associated with frustration, including the Ising antiferromagnet on the triangular lattice.

Here the q -state Potts antiferromagnet (PAF) serves as a model that exhibits ground state entropy without frustration and hence provides a useful framework in which to study this phenomenon [85],[4] on a given lattice Λ or, more generally, a graph G , for sufficiently large q . An interesting question concerns how this ground state entropy, or equivalently, the ground state degeneracy per site, W , depends on properties of the graph. One can study this using such methods as Monte Carlo simulations, calculations of rigorous upper and lower bounds, and large- q series [53] [55]. One can also gain considerable insight from exact solutions for W on the $n \rightarrow \infty$ limits of certain families of graphs.

The determination of $W(\{G\}, q)$ is thus equivalent to the determination of $S_0(\{G\}, q)$, and we shall generally give results in terms of $W(\{G\}, q)$. The minimal integer value of q for which one can carry out a proper q -coloring of G is the chromatic number, $\chi(G)$ [34]. In general, for certain special values of q , denoted q_s , one has the following noncommutativity of limits [52]

$$\lim_{n \rightarrow \infty} \lim_{q \rightarrow q_s} P(G, q)^{1/n} \neq \lim_{q \rightarrow q_s} \lim_{n \rightarrow \infty} P(G, q)^{1/n}, \quad (1.10)$$

and hence it is necessary to specify which order of limits one takes in defining $W(\{G\}, q)$. This will be indicated below, where it is not obvious. For the families of graphs considered here, the set $\{q_s\}$ includes $\{0, 1, 2\}$. For lattice strips that are m -fold repetitions of some basic subgraph, one can take a limit $n \rightarrow \infty$ by taking the limit $m \rightarrow \infty$ [46].

1.3 Potts Model in a Generalized External Field and Weighted-Set Graph Colorings

A natural generalization is to study the q -state Potts model in a generalized external magnetic field that favors or disfavors a certain subset of spin values $I_s = \{1, \dots, s\}$, out of the total set of spin values $I_q = \{1, \dots, q\}$ [66] and [67]. The full Hamiltonian of this generalized Potts model contains two parts: the local (nearest-neighbor) spin-spin interaction and the global spin-field interaction, viz.

$$\mathcal{H} = -J \sum_{\langle ij \rangle} \delta_{\sigma_i \sigma_j} - \sum_{p=1}^q H_p \sum_l \delta_{\sigma_l, p}, \quad (1.11)$$

where the external field is defined as the following: $H_p = H$ for $1 \leq p \leq s$ and $H_p = 0$ for $s + 1 \leq p \leq q$.

We employ the notation $h = \beta H$, $w = e^h$, so w is a field-dependent Boltzmann variable. It is very useful to obtain a general graph-theoretic formula

for $Z(G, q, s, v, w)$ that does not make any explicit reference to the spins σ_i , or the summation over spin configurations, but instead expresses this function as a sum of terms arising from the spanning subgraphs $G' \subseteq G$:

$$Z(G, q, s, v, w) = \sum_{G' \subseteq G} v^{e(G')} \prod_{i=1}^{k(G')} u_{n(G'_i)} \quad (1.12)$$

where

$$u_m = q - s + sw^m = q + s(w^m - 1) \quad (1.13)$$

This is a major part of the present dissertation work. The derivation of this result and studies of properties of $Z(G, q, s, v, w)$ and applications are given in [66] and [67]. Our results generalize earlier work for the case $s = 1$ by F. Y. Wu [84] [85] and by Chang and Shrock [25] [27]. In the special case $H = 0$, Eq. (1.1) reduces to the cluster formula for the zero-field Potts model partition function Eq. (1.5).

An important special case is the zero-temperature Potts antiferromagnet in a generalized field, i.e., $v = -1$, and we denote

$$Ph(G, q, s, w) \equiv Z(G, q, s, -1, w) . \quad (1.14)$$

In this case the only contributions to Z are those such that no two adjacent spins have the same value. Thus, $Ph(G, q, s, w)$ counts the number of proper q -colorings of the vertices of G with a vertex weighting that either disfavors (for $0 \leq w < 1$) or favors (for $w > 1$) colors in the interval I_s . We have denoted these coloring problems as DFSCP and FSCP for disfavored or favored weighted-set graph vertex coloring problems [66]. The associated set-weighted chromatic polynomial constitutes a generalization of the conventional (unweighted) chromatic polynomial, which counts the number of proper q -colorings of a graph G [66].

For $w = 0$, one is prevented from assigning any of the s disfavored colors to any of the vertices, so that the problem reduces to that of a proper coloring of the vertices of G with $q - s$ colors, without any weighting among them. This is described by the usual (unweighted) chromatic polynomial $P(G, q - s)$, so

$$Ph(G, q, s, 0) = P(G, q - s) . \quad (1.15)$$

Thus, the DFSCP, described by $Ph(G, q, s, w)$ may be regarded as interpolating between $P(G, q)$ and $P(G, q - s)$ as w decreases through real values from $w = 1$ to $w = 0$. (The case of no weighting, $w = 1$, may be considered to be the border between the DFSCP and FSCP regimes.) See Fig. (1.2) as an

Physical ranges of w for $\text{Ph}(G,q,s,w)$
with the $q=5, s=2$ weighted-set colorings of C_3 graph as an illustration

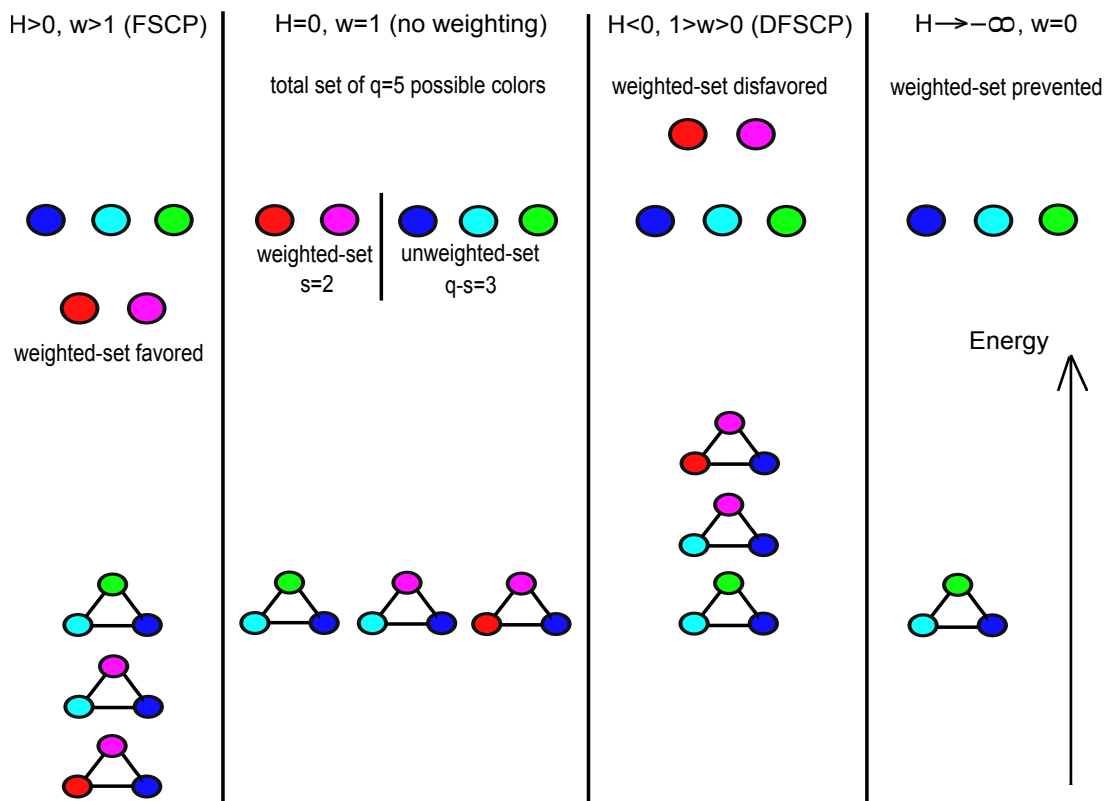


Figure 1.2: Physical ranges of w with the weighted-set colorings of C_3 graph as an illustration.

illustration of DFSCP and FSCP as well as the borderline cases $w = 0$ and $w = 1$.

There are several motivations for the study of weighted-set graph colorings, arising from the areas of mathematics, physics, and engineering. One motivation is the intrinsic mathematical interest in graph coloring problems. Indeed, we are not aware of previous study of weighted-set graph coloring. A second motivation stems from the equivalence to the statistical mechanics of the Potts antiferromagnet in a set of magnetic fields that disfavor or favor a corresponding set of spin values. Third, although we focus here on theoretical properties of weighted-set graph coloring, there are real-world situations that could be modeled by this type of restricted coloring. For example, the weighted-set graph coloring problem with $0 \leq w < 1$ (i.e., the DFSCP) describes, among

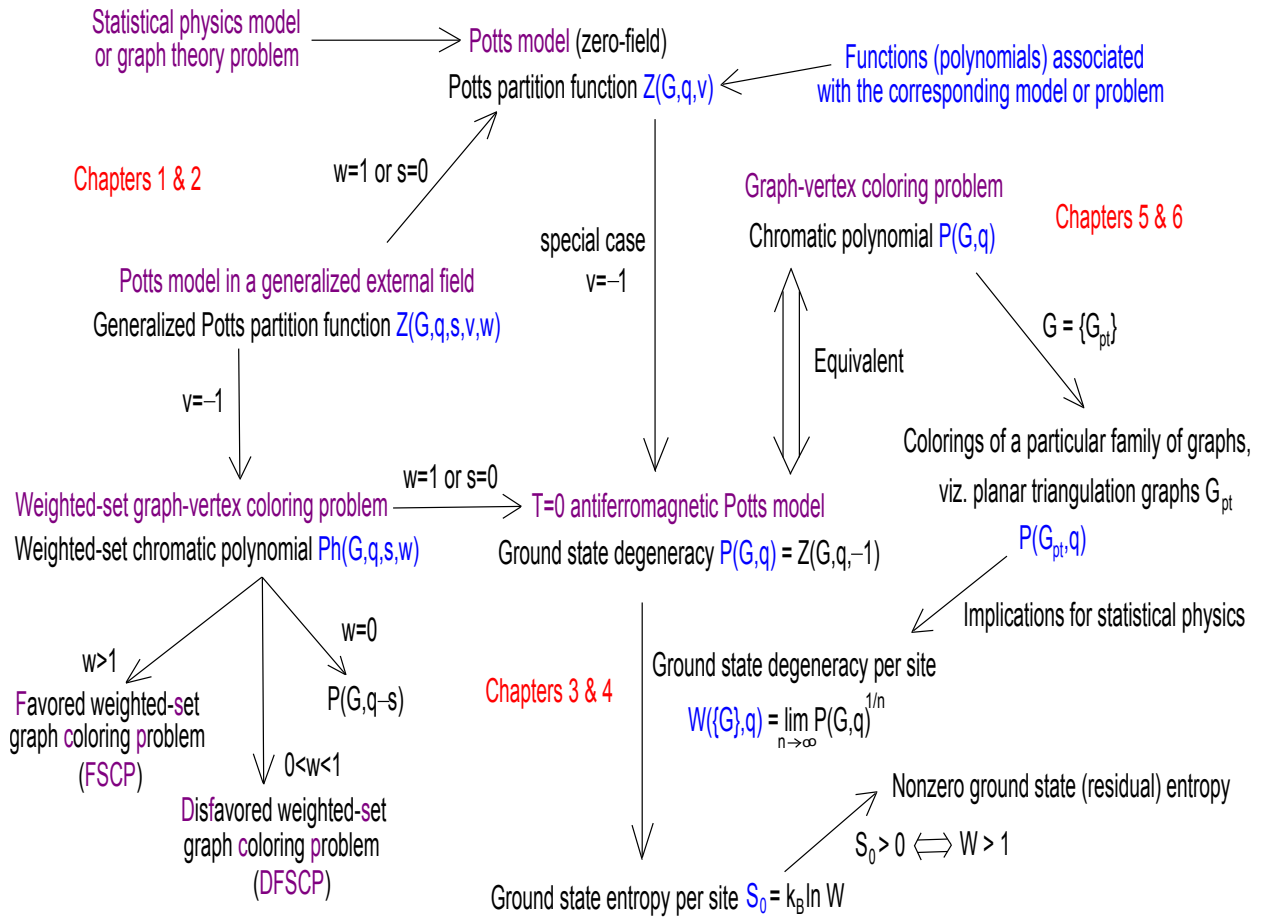


Figure 1.3: Potts model and generalizations, as well as implications for statistical physics: the distribution of chapters.

other things, the assignment of frequencies to commercial radio broadcasting stations in an area such that (i) adjacent stations must use different frequencies to avoid interference and (ii) stations prefer to avoid transmitting on a set of s specific frequencies, e.g., because these are used for data-taking by a nearby radio astronomy antenna. The weighted-set graph coloring problem with $w > 1$ (i.e., the FSCP) describes this frequency assignment process with a preference for a set of s frequencies, e.g., because these are most free of interference.

For the relations among Potts model and generalizations, as well as various special cases and implications for statistical physics, the reader may refer to Fig. (1.3).

Chapter 2

Exact Results on the Generalized Potts Model Partition Function and Weighted-Set Graph Colorings for Certain Families of Graphs

2.1 General Properties of $Z(G, q, s, v, w)$ and $Ph(G, q, s, w)$

First we discuss some basic results about $Z(G, q, s, v, w)$ and $Ph(G, q, s, w)$ that will be needed in subsequent discussion. These are from our Refs. [66] and [67], generalizing [25] and [27]. Applying the factorization

$$w^m - 1 = (w - 1) \sum_{j=0}^{m-1} w^j \quad (2.1)$$

in Eq. (1.12) with $m = n(G'_i)$, one sees that the variable s enters in $Z(G, q, s, v, w)$, and $Ph(G, q, s, w)$ only in the combination

$$t = s(w - 1) . \quad (2.2)$$

Since $I_s \subseteq I_q$, whence $0 \leq s \leq q$, and since $w \geq 0$ for any real external field H , it follows that

$$u_m = q - s + sw^m \geq 0 . \quad (2.3)$$

Therefore, for the ferromagnetic case $v \geq 0$, each term in the sum over spanning subgraphs in Eq. (1.12) is nonnegative. For a given spanning

subgraph $G' \subseteq G$, consisting of a sum of $k(G')$ connected components G'_i , where $i = 1, \dots, k(G')$, the contribution to $Z(G, q, s, v, w)$ in Eq. (1.12) is the number of spanning subgraphs G' of a particular topology, $N_{G'}$, times $v^{e(G')} \prod_{i=1}^{k(G')} u_{n(G'_i)}$, which has the generic form

$$N_{G'} v^{e(G')} \prod_{j=1}^{k(G')} u_{n(G'_j)} . \quad (2.4)$$

Here

$$\sum_{i=1}^{k(G')} n(G'_i) = n . \quad (2.5)$$

Since some of the components G'_i and G'_j may have the same number of vertices, $n(G'_i) = n(G'_j)$, the product in Eq. (2.4) can also be written as $\prod_j (u_{r_j})^{p_j}$, where r_j takes on certain values in the set $\{1, \dots, n\}$ and the exponents p_j are integers taking on certain values in the set $\{1, \dots, k(G')\}$. As a consequence of Eq. (2.5), these satisfy the relation

$$\sum_j p_j r_j = n . \quad (2.6)$$

Note that u_m satisfies the identity

$$u_m(q, s, w) = w^m u_m(q, q - s, w^{-1}) \quad (2.7)$$

where we have written u_m as a function of its three arguments q, s, w . A given spanning subgraph G' corresponds to a partition of the total set of vertices depending on which edges are present and which are absent. The sum of the coefficients $N_{G'}$ of the various terms $N_{G'} \prod_j (u_{r_j})^{p_j}$ that multiply a given power $v^{e(G')}$ in Eq. (1.12) is $\binom{e(G)}{e(G')}$ since this is the number of ways of choosing $e(G')$ edges out of a total of $e(G)$ edges. These satisfy the relation

$$\sum_{e(G')=0}^{e(G)} \binom{e(G)}{e(G')} = 2^{e(G)} . \quad (2.8)$$

This reflects the fact that there are $2^{e(G)}$ spanning subgraphs of G , as follows from the property that these are classified by choosing whether each edge is present or absent, and there are $2^{e(G)}$ such choices. In mathematical graph theory, a loop is defined as an edge that connects a vertex to itself and a cycle is a closed circuit along the edges of G . In the following we restrict to

loopless graphs. For any such n -vertex graph G , the terms in $Z(G, q, s, v, w)$ proportional to v^0 , v^1 , and $v^{e(G)}$ can be given in general, as

$$Z(G, q, s, v, w) = u_1^n + e(G)vu_2u_1^{n-2} + \dots + v^{e(G)}u_n . \quad (2.9)$$

The partition function $Z(G, q, s, v, w)$ satisfies the following identities [25] [27] [66]

$$Z(G, q, s, v, 1) = Z(G, q, 0, v, w) = Z(G, q, v) , \quad (2.10)$$

(where, as above, $Z(G, q, v)$ is the zero-field Potts partition function),

$$Z(G, q, s, v, w) = w^n Z(G, q, q - s, v, w^{-1}) , \quad (2.11)$$

(c.f. Eq. (2.7)) and

$$Z(G, q, q, v, w) = w^n Z(G, q, v) . \quad (2.12)$$

Setting $v = -1$ in these identities yields the corresponding relations for $Ph(G, q, s, w)$; for example, Eq. (2.11) yields

$$Ph(G, q, s, w) = w^n Ph(G, q, q - s, w^{-1}) . \quad (2.13)$$

There are a number of equivalent ways of writing $Z(G, q, s, v, w)$ as sums of powers of a given variable with coefficients depending on the rest of the variables in the set $\{q, s, v, w\}$. The basic spanning subgraph formula (1.12) is a sum of powers of v . A second convenient form in which to express $Z(G, q, s, v, w)$ is as a sum of powers of w with coefficients, denoted as $\beta_{Z,G,j}(q, s, v)$, which are polynomials in q , s , and v :

$$Z(G, q, s, v, w) = \sum_{j=0}^n \beta_{Z,G,j}(q, s, v) w^j . \quad (2.14)$$

The symmetry (2.11) implies the following relation among the coefficients:

$$\beta_{Z,G,j}(q, s, v) = \beta_{Z,G,n-j}(q, q - s, v) \quad \text{for } 0 \leq j \leq n . \quad (2.15)$$

For the special case $v = -1$, we write

$$Ph(G, q, s, w) = \sum_{j=0}^n \beta_{G,j}(q, s) w^j , \quad (2.16)$$

where

$$\beta_{G,j}(q, s) \equiv \beta_{Z,G,j}(q, s, -1) . \quad (2.17)$$

From (2.15), we have

$$\beta_{G,j}(q, s) = \beta_{G,n-j}(q, q - s) \quad \text{for } 0 \leq j \leq n . \quad (2.18)$$

We have proved further that [66]

$$\beta_{Z,G,n}(q, s, v) = Z(G, s, v) \quad (2.19)$$

and

$$\beta_{Z,G,0}(q, s, v) = Z(G, q - s, v) , \quad (2.20)$$

so that for $v = -1$, $\beta_{G,0}(q, s) = P(G, q - s)$ and $\beta_{G,n}(q, s) = P(G, s)$. Various general factorization results were also given in Ref. [66] for these coefficients $\beta_{Z,G,j}(q, s, v)$ and $\beta_{G,j}(q, s)$, including the following:

$$\text{For } 1 \leq j \leq n, \quad \beta_{Z,G,j}(q, s, v) \text{ and } \beta_{G,j}(q, s) \text{ contain a factor of } s . \quad (2.21)$$

$$\text{For } 0 \leq j \leq n-1, \quad \beta_{Z,G,j}(q, s, v) \text{ and } \beta_{G,j}(q, s) \text{ contain a factor } (q-s) . \quad (2.22)$$

The minimum number of colors needed for a proper q -coloring of a graph G is the chromatic number, $\chi(G)$. A further factorization property is that

$$\beta_{G,n}(q, s) \text{ contains the factor } \prod_{j=0}^{\chi(G)-1} (s - j) , \quad (2.23)$$

and

$$\beta_{G,0}(q, s) \text{ contains the factor } \prod_{j=0}^{\chi(G)-1} (q - s - j) . \quad (2.24)$$

A third useful type of expression for $Z(G, q, s, v, w)$ is

$$Z(G, q, s, v, w) = \sum_{j=0}^n \alpha_{Z,G,n-j}(s, v, w) q^{n-j} . \quad (2.25)$$

With the notation

$$\alpha_{G,n-j}(s, w) \equiv \alpha_{Z,G,n-j}(s, -1, w) , \quad (2.26)$$

we then have

$$Ph(G, q, s, w) = \sum_{j=0}^n \alpha_{G,n-j}(s, w) q^{n-j} . \quad (2.27)$$

This form is particularly convenient for comparisons with the conventional

unweighted chromatic polynomial $P(G, q) = Ph(G, q, 0, w) = Ph(G, q, s, 1)$.

For a graph G , the number of linearly independent cycles, $c(G)$ (the cyclomatic number), satisfies the relation

$$c(G) = e(G) + k(G) - n(G) . \quad (2.28)$$

A connected n -vertex graph with no cycles is a tree graph, T_n , while a general graph with no cycles, which can be disconnected, is called a forest graph. We denote a graph G with no cycles as G_{nc} and define

$$q' \equiv \frac{q}{s} , \quad v' \equiv \frac{v}{s} . \quad (2.29)$$

In Ref. [66] we proved that for such a cycle-free graph G_{nc} ,

$$Z(G_{nc}, q, s, v, w) = s^n Z(G_{nc}, q', 1, v', w) . \quad (2.30)$$

This relation allows us to obtain $Z(G_{nc}, q, s, v, w)$ from $Z(G_{nc}, q, 1, v, w)$ for any cycle-free graph G_{nc} . In particular, all of the results for $Z(G, q, s, v, w)$ for various types of tree graphs calculated in Ref. [27] for $s = 1$ can be used to obtain the analogous results for general s .

For a graph G , let us denote the graph obtained by deleting an edge $e \in E$ as $G - e$ and the graph obtained by deleting this edge and identifying the two vertices that had been connected by it as G/e . The Potts model partition function satisfies the deletion-contraction relation (DCR)

$$Z(G, q, v) = Z(G - e, q, v) + vZ(G/e, q, v) , \quad (2.31)$$

and, setting $v = -1$, the chromatic polynomial thus satisfies the DCR

$$P(G, q) = P(G - e, q) - P(G/e, q) . \quad (2.32)$$

However, as we showed in Ref. [66], in general, neither $Z(G, q, s, v, w)$ nor $Ph(G, q, s, w)$ satisfies the respective deletion-contraction relation, i.e., in general, $Z(G, q, s, v, w)$ is not equal to $Z(G - e, q, s, v, w) + vZ(G/e, q, s, v, w)$. The only cases where this deletion-contraction relation holds are for the values $s = 0$, $w = 1$, and $w = 0$ where $Z(G, q, s, v, w)$ reduces to a zero-field Potts model partition function.

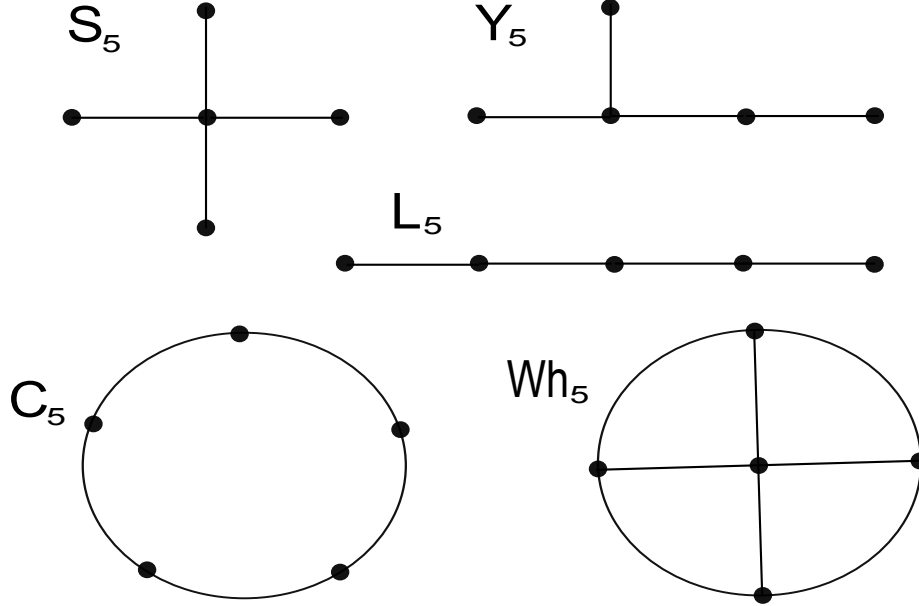


Figure 2.1: Representatives for several families of graphs: S_n , L_n , Y_n , C_n and Wh_n .

2.2 Star Graphs S_n

A star graph S_n consists of one central vertex with degree $n - 1$ connected by edges with $n - 1$ outer vertices, each of which has degree 1 (see Fig. (2.1)).

The graph S_2 is degenerate in the sense that it has no central vertex but instead coincides with L_2 . The graph S_3 is nondegenerate, and coincides with L_3 , while the S_n for $n \geq 4$ are distinct graphs not coinciding with those of other families. For $n \geq 2$, the chromatic number is $\chi(S_n) = 2$. By the use of combinatorics and Eq.(2.4), we have derived the following general formula for $Z(S_n, q, s, v, w)$:

$$\begin{aligned}
 Z(S_n, q, s, v, w) &= \sum_{j=0}^{n-1} \binom{n-1}{j} v^j u_{j+1} u_1^{n-1-j} \\
 &= \sum_{j=0}^{n-1} \binom{n-1}{j} (q-s)v^j u_1^{n-1-j} + \sum_{j=0}^{n-1} \binom{n-1}{j} sw(wv)^j u_1^{n-1-j} \\
 &= (q-s)(u_1 + v)^{n-1} + sw(u_1 + wv)^{n-1}
 \end{aligned}$$

$$= (q-s) \left[q + s(w-1) + v \right]^{n-1} + sw \left[q + s(w-1) + wv \right]^{n-1}. \quad (2.33)$$

Here j is the number of edges in a given spanning subgraph G' , and the numerical prefactor $\binom{n-1}{j}$ in the first line of Eq. (2.33) is the number of ways of choosing j edges out of the total number of edges, $n-1$, in S_n . Evaluating Eq. (2.33) for $v = -1$ yields $Ph(S_n, q, s, w)$.

As an explicit example, for the graph S_4 , we calculate

$$\begin{aligned} Z(S_4, q, s, v, w) &= q(q+v)^3 w^4 + s(q-s)(4s^2 + 6sv + 3v^2)w^3 \\ &+ 3s(q-s)[2s(q-s) + qv]w^2 + s(q-s) \left[4(q-s)^2 + 6(q-s)v + 3v^2 \right] w \\ &+ (q-s)(q-s+v)^3. \end{aligned} \quad (2.34)$$

2.3 Path graphs L_n

The path graph L_n is the graph consisting of n vertices with each vertex connected to the next one by one edge (see Fig. (2.1)). One may picture this graph as forming a line, and in the physics literature this is commonly called a line graph. We use the alternate term “path graph” here because in mathematical graph theory the line graph $L(G)$ of a graph G refers to a different object (namely the graph obtained by an isomorphism in which one maps the edges of G to the vertices of $L(G)$ and connects these resultant vertices by edges if the edges of G are connected to the same vertex of G). For $n \geq 2$, the chromatic number is $\chi(L_n) = 2$. Here we present a general formula for this partition function. Let

$$T_{Z,1,0} = \begin{pmatrix} q-s+v & sw \\ q-s & w(s+v) \end{pmatrix} \quad (2.35)$$

$$H_{1,0} = \begin{pmatrix} 1 & 0 \\ 0 & sw \end{pmatrix} \quad (2.36)$$

$$\omega_1 = \begin{pmatrix} q-s \\ 1 \end{pmatrix} \quad (2.37)$$

and

$$s_1 = \begin{pmatrix} 1 \\ 1 \end{pmatrix}. \quad (2.38)$$

Then

$$Z(L_n, q, s, v, w) = \omega_1^T H_{1,0} (T_{Z,1,0})^{n-1} s_1 \quad (2.39)$$

and $Ph(L_n, q, s, w) = Z(L_n, q, s, -1, w)$. It is straightforward to verify that our result for $Z(L_n, q, s, v, w)$ satisfies the relation (2.30). We note that

$$\det(T_{Z,1,0}) = v(q + v)w, \quad (2.40)$$

independent of s , and

$$\text{Tr}(T_{Z,1,0}) = q - s + v + w(s + v). \quad (2.41)$$

The eigenvalues of $T_{Z,1,0}$ are the same as the eigenvalues with coefficients of degree $d = 0$ for the circuit graph C_n , which will be given in Eq. (2.47) of the next section, namely

$$\lambda_{Z,1,0,\pm} = \frac{1}{2} \left[q - s + v + w(s + v) \pm \left[\{q - s + v + w(s + v)\}^2 - 4vw(q + v) \right]^{1/2} \right]. \quad (2.42)$$

Thus, we can also write

$$Z(C_n, q, s, v, w) = \text{Tr}[(T_{Z,1,0})^n] + (s - 1)(vw)^n + (q - s - 1)v^n. \quad (2.43)$$

The graphs L_n , C_n , and, more generally, lattice strip graphs of some transverse width L_y and length $L_x = m$ are examples of recursive families of graphs, i.e., graphs G_m that have the property that G_{m+1} can be constructed by starting with G_m and adding a given graph H or, if necessary, cutting and gluing in H . For these graphs, $Z(G_m, q, s, v, w)$ has the structure of a sum of coefficients that are independent of the length m multiplied by m 'th powers of some algebraic functions.

Note that, by Eq. (2.9), the term in $Z(C_n, q, s, v, w)$ of highest order in v is $v^n u_n = [q + s(w - 1) \sum_{j=0}^{n-1} w^j] v^n$, part of which gives rise to the last two terms in Eq. (2.47). We note that for $s = 0$ or $w = 1$, one can check that our expressions for $Z(L_n, q, s, v, w)$ and $Z(C_n, q, s, v, w)$ simplify, respectively, to $Z(L_n, q, v) = q(q + v)^{n-1}$ and $Z(C_n, q, v) = (q + v)^n + (q - 1)v^n$. Going from the case of $sw(w - 1) = 0$ to $sw(w - 1) \neq 0$, $Z(L_n, q, s, v, w)$ expands from a sum of one power to a sum involving two powers, and $Z(C_n, q, s, v, w)$ expands from a sum of two powers to a sum of four powers.

As our exact solutions for $Z(L_n, q, s, v, w)$ and $Z(C_n, q, s, v, w)$ (see the next section) show, the field-dependent Potts partition functions $Z(G, q, s, v, w)$ do not, in general, have any common factor. This contrasts with the case of

the zero-field Potts partition function, which always has an overall factor of q . Similarly, in the $v = -1$ special case defining the set-weighted chromatic polynomial, the resultant polynomials $Ph(G, q, s, w)$ do not, in general, have a common factor. For special values of s , $Ph(G, q, s, w)$ may reduce to a form with a common factor. The case $s = 0$ (and the case $w = 1$) for which this reduces to the conventional chromatic polynomial is well-known; in this case $P(G, q)$ has, as a common factor, $\prod_{j=0}^{\chi(G)-1} (q - j)$. Similarly, for $s = q$, $Ph(G, q, q, w)$ has this common factor multiplied by w^n . For the special case $s = 1$ and for a connected graph G with at least one edge, it was shown in Ref. [27] that $Ph(G, q, 1, w)$ contains a factor $(q - 1)$. However, it is not true that for a special case such as $s = 2$, a connected graph G with at least one edge contains a factor of $(q - s)$. For example, using the elementary result

$$Z(L_2, q, s, v, w) = s(s + v)w^2 + 2s(q - s)w + (q - s)(q - s + v) \quad (2.44)$$

$$\begin{aligned} Z(L_3, q, s, v, w) &= s(s + v)^2 w^3 + s(q - s)(3s + 2v)w^2 \\ &+ s(q - s) \left[3(q - s) + 2v \right] w + (q - s)(q - s + v)^2 \end{aligned} \quad (2.45)$$

$$\begin{aligned} Z(L_4, q, s, v, w) &= s(s + v)^3 w^4 + 2s(q - s)(s + v)(2s + v)w^3 \\ &+ s(q - s) \left[-3(s^2 + (q - s)^2) + 3q(q + v) + 2v^2 \right] w^2 \\ &+ 2s(q - s)(q - s + v)[2(q - s) + v]w \\ &+ (q - s)(q - s + v)^3. \end{aligned} \quad (2.46)$$

One sees that $Ph(L_2, q, 1, w) = (q - 1)(q - 2 + 2w)$, but $Ph(L_2, q, 2, w) = 2w^2 + 4(q - 2)w + (q - 2)(q - 3)$, which has no common factor.

2.4 Circuit Graphs C_n

The circuit graph C_n , or equivalently, the 1D lattice with periodic boundary conditions, see Fig. (2.1), has chromatic number $\chi(C_n) = 2$ if $n \geq 2$ is even and $\chi(C_n) = 3$ if $n \geq 3$ is odd.

In general, $Z(C_n, q, s, v, w)$ has the structure

$$Z(C_n, q, s, v, w) = \sum_{j=1}^2 [\lambda_{Z,1,0,j}]^n + (s-1)(vw)^n + (q-s-1)v^n. \quad (2.47)$$

where $\lambda_{Z,1,0,j}$ has been defined in Eq. (2.42), with $j = 1, 2$ corresponding to \pm here. It is readily checked that this expression for $Z(C_n, q, s, v, w)$ (i) reduces to the zero-field Potts model partition function

$$Z(C_n, q, v) = (q+v)^n + (q-1)v^n \quad (2.48)$$

for $s = 0$ or $w = 1$, (ii) satisfies the general symmetry property (2.11), and (iii) reduces to $w^n Z(C_n, q, v)$ for $s = q$, in agreement with Eq. (2.12).

The result (2.47) shows a qualitative difference between the case $s = 1$ considered previously [27] and the more general set of cases with $s \geq 2$ in the interval I_s , namely the fact that the third term, $(s-1)(vw)^n$, is absent for $s = 1$ but is present for other values of $s \in I_s$. By the $s \leftrightarrow q-s$ symmetry in Eq.(2.11), this also means that another term vanishes identically for $s = q-1$ but is present for other values of $s \in I_s$; this is the last term in (2.47), $(q-s-1)v^n$. It is interesting to observe that the symmetry (2.11) applies not just to the total $Z(C_n, q, s, v, w)$, but also to parts of this function. Specifically, under the replacement $s \rightarrow q-s$, one sees that (i) the sum of the last two terms in (2.47), $(s-1)(vw)^n + (q-s-1)v^n$, transforms into $w^n[(q-s-1)v^n + (s-1)(vw^{-1})^n]$ and (ii) the first two terms, $\sum_{j=1}^2 [\lambda_{Z,1,0,j}(q, s, v, w)]^n$ transform into $w^n \sum_{j=1}^2 [\lambda_{Z,1,0,j}(q, q-s, v, w^{-1})]^n$, so that each of these parts, (i) and (ii), individually satisfies the symmetry (2.11).

We exhibit $Z(C_n, q, s, v, w)$ for $n = 2$ and $n = 3$ below. To keep the equations as compact as possible, we write the coefficients of the terms of maximal degree in w and of degree 0 in w in terms of zero-field partition functions using the general results (2.19) and (2.20). We find

$$Z(C_2, q, s, v, w) = Z(C_2, s, v)w^2 + 2s(q-s)w + Z(C_2, q-s, v) \quad (2.49)$$

$$\begin{aligned} Z(C_3, q, s, v, w) &= Z(C_3, s, v)w^3 + 3s(q-s)(s+v)w^2 \\ &+ 3s(q-s)(q-s+v)w + Z(C_3, q-s, v) \end{aligned} \quad (2.50)$$

As usual, one obtains the $Ph(C_n, q, s, w)$ for each n by setting $v = -1$ in $Z(C_n, q, s, v, w)$. For $s = 1$, the parts of $Z(C_n, q, 1, v, w)$ were given in Ref. [26] and $Ph(C_n, q, 1, w)$ was given in Ref. [27].

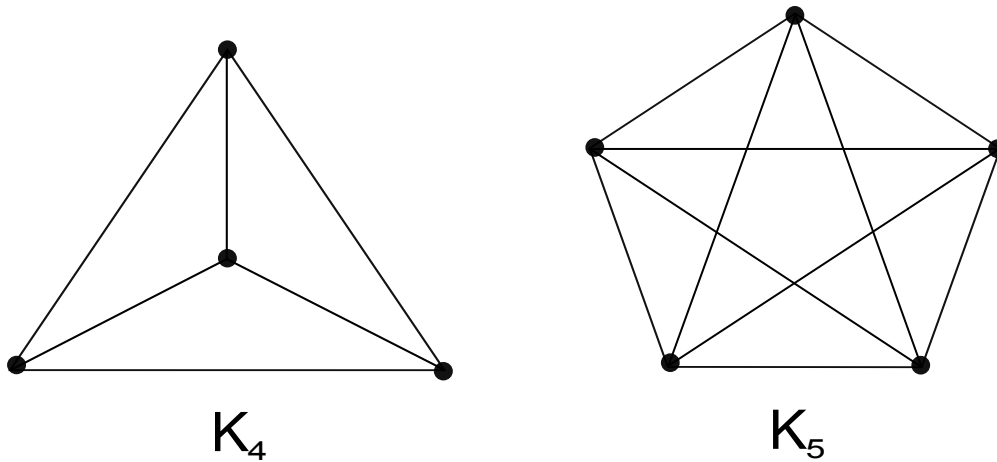


Figure 2.2: The complete graphs K_4 and K_5 .

2.5 Complete Graphs K_n

The complete graph K_n is the graph with n vertices such that each vertex is connected to every other vertex by one edge, see Fig. (2.5) for illustrations of K_4 and K_5 . The chromatic number is $\chi(K_n) = n$ and the number of edges is $e(K_n) = \binom{n}{2}$.

The weighted-set chromatic polynomial for the complete graphs has the following form:

$$Ph(K_n, q, s, w) = \sum_{\ell=0}^n \beta_{K_n, \ell}(q, s) w^\ell \quad (2.51)$$

where

$$\beta_{K_n, \ell}(q, s) = \binom{n}{\ell} \left[\prod_{i=0}^{\ell-1} (s - i) \right] \left[\prod_{j=0}^{n-\ell-1} (q - s - j) \right]. \quad (2.52)$$

Here it is understood that if the upper index on either of the two products in Eq. (2.52) is negative, that product is absent, so that the first product is absent for $\ell = 0$ and the second one is absent for $\ell = n$.

This result is proved by a combinatoric coloring argument. Accordingly, we take q to be a non-negative integer. The resultant Eqs. (2.51) and (2.52) allow the extension of q to \mathbb{R} (and \mathbb{C}). First, if $q < \chi(K_n) = n$, then $Ph(K_n, q, s, w)$ vanishes identically. Hence, we shall formally take $q \geq n$ to begin with; once we have obtained the results (2.51) and (2.52), it will be seen that they allow an extension of q away from this range. If $s \geq n$, then one can assign n different colors to the n vertices of K_n from the set I_s , and this gives rise

to a term with degree n in w . To determine the coefficient of this term, we enumerate the number of ways this color assignment can be made. We pick a given vertex and assign some color from I_s to this vertex, which we can do in any of s ways. Then we go on to the next vertex and assign one of the remaining $s - 1$ colors in I_s to that vertex, and so on for the n vertices. The number of ways of making this color assignment, i.e., the coefficient of the term in $Ph(K_n, q, s, w)$ of maximal degree in w , viz., w^n , is therefore

$$\beta_{K_n, n}(q, s) = \prod_{j=0}^{n-1} (s - j) = P(K_n, s) . \quad (2.53)$$

The fact that this coefficient is $P(K_n, s)$ agrees with the $v = -1$ special case of the general result of Eq. (2.19). Similarly, the term of order w^0 is obtained by assigning n different colors to the n vertices of K_n from the orthogonal set S^\perp . By reasoning analogous to that given above, it follows that the number of ways of doing this is given by replacing s by $q - s$ in Eq. (2.53), so

$$\beta_{K_n, 0}(q, s) = \prod_{j=0}^{n-1} (q - s - j) = P(K_n, q - s) . \quad (2.54)$$

Having illustrated the logic on these two extremal terms, let us next consider the general w^ℓ term with $0 \leq \ell \leq n$. This term arises from color assignments in which we pick ℓ different colors from the set I_s and assign them to ℓ of the n vertices of K_n , and then $n - \ell$ different colors from the orthogonal complement set S^\perp , which are assigned to the remaining $n - \ell$ vertices. The number of ways of doing this is

$$\beta_{K_n, \ell}(q, s) = \left[\prod_{i=0}^{\ell-1} (s - i) \right] \left[\prod_{j=0}^{n-\ell-1} (q - s - j) \right] . \quad (2.55)$$

This proves the result in Eqs. (2.51) and (2.52).

Evidently, with the polynomial $Ph(K_n, q, s, w)$ as specified in these equations, one can extend q and s away from non-negative integer values. Our result in Eqs. (2.51) and (2.52) generalizes the result for the case $s = 1$ given in [27]. As is evident, for $w = 1$ or $s = 0$, $Ph(K_n, q, s, w)$ reduces to the (usual, unweighted) chromatic polynomial

$$P(K_n, q) = \prod_{j=0}^{n-1} (q - j) . \quad (2.56)$$

A corollary of Eqs. (2.51) and (2.52) is that

$$\text{If } s < n \text{ , then } \beta_{K_n,j}(q, s) = 0 \text{ for } s < j \leq n \quad (2.57)$$

and hence

$$\deg_w(Ph(K_n, q, s, w)) = \min(n, s) . \quad (2.58)$$

Note that

$$\beta_{K_n,\ell}(q, s) = \beta_{K_n,n-\ell}(q, q-s) , \quad (2.59)$$

in agreement with the general symmetry (2.18). Substituting this in Eq. (2.51) shows explicitly that our result for $Ph(K_n, q, s, w)$ satisfies the symmetry relation (2.13). Note that K_n is not a recursive family of graphs, so one does not expect $Ph(K_n, q, s, w)$ to have the form of a sum of coefficients multiplied by powers of certain algebraic functions, and it does not, in contrast to $Ph(G_n, q, s, w)$ for recursive families G_n such as C_n or L_n .

The calculation of $Ph(K_n, q, s, w)$ for the cases K_1 and $K_2 = L_2$ are elementary. For $K_3 = C_3$ our general formula (2.51) yields

$$Ph(K_3, q, s, w) = P(K_3, s)w^3 + 3s(s-1)(q-s)w^2 + 3s(q-s)(q-s-1)w + P(K_3, q-s) \quad (2.60)$$

while for K_4 we have

$$\begin{aligned} Ph(K_4, q, s, w) &= P(K_4, s)w^4 + 4s(s-1)(s-2)(q-s)w^3 + 6s(s-1)(q-s)(q-s-1)w^2 \\ &+ 4s(q-s)(q-s-1)(q-s-2)w + P(K_4, q-s) . \end{aligned} \quad (2.61)$$

2.6 The p -Wheel graphs $Wh_n^{(p)} = K_p + C_{n-p}$

The p -wheel graph $Wh_n^{(p)}$ is defined as

$$Wh_n^{(p)} = K_p + C_{n-p} , \quad (2.62)$$

i.e., the join of the complete graph K_p with the circuit graph C_{n-p} . (Given two graphs G and H , the join, denoted $G + H$, is defined as the graph obtained by joining each of the vertices of G to each of the vertices of H). (Here and below, no confusion should result from the use of the symbol H for a graph and H for the external field; the meaning will be clear from context.) The family of $Wh_n^{(p)}$ graphs is a recursive family. For $p = 1$, $Wh_n^{(1)}$ is the wheel graph, see Fig. (2.1). The central vertex can be regarded as forming the axle of the wheel, while the $n - 1$ vertices of the C_{n-1} and their edges form the outer rim of the wheel. This is well-defined for $n \geq 3$, and in this range the

chromatic number is $\chi(Wh_n) = 3$ if n is odd and $\chi(Wh_n) = 4$ if n is even. Although K_p is not defined for $p = 0$, we may formally define $Wh_n^{(0)} \equiv C_n$. For the zero-field case, i.e., for the usual, unweighted chromatic polynomial and for an arbitrary graph G ,

$$P(K_p + G, q) = P(K_p, q)P(G, q - p) = q_{(p)}P(G, q - p) , \quad (2.63)$$

where $q_{(m)}$ is the falling factorial, defined as

$$q_{(m)} = \prod_{j=0}^{m-1} (q - j) . \quad (2.64)$$

This result is a consequence of the fact that in assigning colors to the p vertices of K_p , one must use p different colors, and then, because of the join condition, one must select from the other $q - p$ colors to color the vertices of G . In particular, for $Wh^{(p)}$, this gives

$$\begin{aligned} P(Wh_n^{(p)}, q) &= P(K_p, q)P(C_{n-p}, q - p) \\ &= q_{(p)} \left[(q - 1 - p)^{n-p} + (q - 1 - p)(-1)^{n-p} \right] . \end{aligned} \quad (2.65)$$

Note that, for arbitrary p , this chromatic polynomial consists of the prefactor times the sum of the $(n - p)$ 'th powers of $N_{Wh^{(p)}, \lambda} = 2$ terms. For $p = 1$, this number can be seen to be the $L_y = 1$ special case of a general formula in Eq. (3.2.15) of Ref. [23] for the join of K_1 with a width- L_y cyclic strip.

For the weighted-set chromatic polynomial, we generalize this coloring method as follows. Consider first $K_1 + G$. There are two possible types of choices for the color to be assigned to the vertex of K_1 . One type is to choose this color to lie in the set I_s . There are s ways to make this choice, and each gets a weighting factor of w . For each choice, one then performs the proper coloring of the vertices of G with the remaining $q - 1$ colors, of which only $s - 1$ can be used from the set I_s ; this is determined by $Ph(G, q - 1, s - 1, w)$. The second type of coloring is to choose the color assigned to the K_1 vertex to lie in the orthogonal set I_s^\perp . There are $(q - s)$ ways to make this choice, and since this is not the weighted set, there is no weighting factor of w . For each such choice, one then performs the proper coloring of the vertices of G with the remaining $q - 1$ colors, of which all s colors in the set I_s are available, but only $q - s - 1$ colors in the orthogonal set I_s^\perp are available. This yields the result

$$Ph(K_1 + G, q, s, w) = swPh(G, q - 1, s - 1, w) + (q - s)Ph(G, q - 1, s, w) . \quad (2.66)$$

To calculate $Ph(K_p + G, q, s, w)$ for a given graph G , one first carries out the proper coloring of $K_1 + G$, using the result (2.66). One then joins the next vertex of K_p to $K_1 + G$ to get $K_2 + G$, using the relation $K_1 + (K_r + G) = K_{r+1} + G$ and iteratively applies Eq. (2.66). One continues in this manner to carry out the proper coloring of the full join $K_p + G$. This yields

$$Ph(K_p + G, q, s, w) = \sum_{\ell=0}^p \beta_{K_p, \ell}(q, s) Ph(G, q - p, s - \ell, w) w^\ell . \quad (2.67)$$

Utilizing this coloring method, we have calculated $Ph(Wh_n^{(p)}, q, s, w)$ for arbitrary n . Let us define

$$a(p, q, s, w) = q - s - (p + 1) + (s - 1)w = q - (p + 1) + s(w - 1) - w \quad (2.68)$$

and

$$\lambda_{Wh^{(p)}, \ell, \pm}(q, s, w) = \frac{1}{2} \left[a(p, q, s - \ell, w) \pm [a(p, q, s - \ell, w)^2 + 4w(q - p - 1)]^{1/2} \right] \\ \text{for } 0 \leq \ell \leq p . \quad (2.69)$$

We note that for $\ell = 0$, these $\lambda_{Wh^{(p)}, \ell, \pm}(q, s, w)$ are equal to the $v = -1$ special case of $\lambda_{Z, 1, 0, \pm}$ given in Eq. (2.42) of the earlier section for the circuit graph with the replacement of q by $q - p$. This is in accord with the fact that the effect of the join of K_p with G is that the proper q -coloring of G can only use $q - p$ of the original q colors. We define two additional terms that do not depend on q or s ,

$$\lambda_{Wh^{(p)}, 2p+3} = -w \quad (2.70)$$

and

$$\lambda_{Wh^{(p)}, 2p+4} = -1 . \quad (2.71)$$

The total number of λ 's for $Ph(Wh_n^{(p)}, q, s, w)$ is thus

$$N_{Ph(Wh^{(p)}), \lambda} = 2(p + 2) . \quad (2.72)$$

Note that in contrast to the unweighted chromatic polynomial of $Wh_n^{(p)}$, where the number of λ 's, $N_{P(Wh^{(p)}), \lambda} = 2$, is independent of p , here this number depends on p . In terms of these quantities, we find, for the weighted-set

chromatic polynomial for $Wh_n^{(p)}$, the result

$$\begin{aligned}
Ph(Wh_n^{(p)}, q, s, w) &= \sum_{\ell=0}^p \beta_{K_p, \ell}(q, s) \left[[\lambda_{Wh^{(p)}, \ell, +}(q, s, w)]^{n-p} + [\lambda_{Wh^{(p)}, \ell, -}(q, s, w)]^{n-p} \right] w^\ell \\
&+ \left[\sum_{\ell=0}^p \beta_{K_p, \ell}(q, s) (s - \ell - 1) w^\ell \right] (-w)^{n-p} \\
&+ \left[\sum_{\ell=0}^p \beta_{K_p, \ell}(q, s) (q - s - p + \ell - 1) w^\ell \right] (-1)^{n-p} .
\end{aligned} \tag{2.73}$$

This formula applies for integer $p \geq 1$ and also for $p = 0$ if one sets $\beta_{K_p, \ell}(q, s) \equiv \delta_{\ell, 0}$ for $p = 0$. It can be checked that for $p = 0$, Eq. (2.73) reduces to our result for $Ph(C_n, q, s, w)$ given as the special $v = -1$ case of Eqs. (5.3)-(5.5) in Ref. [66]. It can also be verified that for $p = 1$ and $s = 1$, Eq. (2.73) reduces to the result given for this case in Eqs. (3.30)-(3.32) in Ref. [27]. Furthermore, since the graph $Wh_4^{(1)} = K_1 + K_3 = K_4$, it follows that $Ph(Wh_4^{(1)}, q, s, w) = Ph(K_4, q, s, w)$. The symmetry (2.13) is realized as follows: the summation on the first line of Eq. (2.73) goes into itself, while the sum of the expressions on the two subsequent lines of Eq. (2.73) transforms into itself with the replacement of w by w^{-1} in these expressions and the prefactor w^n appearing overall. One could also study $Z(Wh_n^{(p)}, q, s, v, w)$, but we have focused here on $Ph(Wh_n^{(p)}, q, s, w)$, since its calculation can be performed by combinatoric methods associated with the proper q -coloring condition. For some explicit examples of set-weighted chromatic polynomials $Ph(Wh_n^{(p)}, q, s, w)$ obtained from the general formula (2.73), see Appendix 1 of [67].

Following our notation in Ref. [66] and earlier works, the $n \rightarrow \infty$ limit of a family of n -vertex graphs G_n is denoted $\{G\}$ and the continuous accumulation set of the zeros of $Ph(G_n, q, s, w)$ in the complex q plane is denoted \mathcal{B}_q . For recursive families of graphs, this locus is determined as the solution of the equality in magnitude of two (or more) λ 's of dominant magnitude, as a function of q (with other variables held fixed) [13]. The other loci \mathcal{B}_v , etc. are defined in an analogous manner. These loci are typically comprised of curves and possible line segments. For studies of the $n \rightarrow \infty$ limit of chromatic polynomials and their generalization to weighted-set chromatic polynomials, the locus \mathcal{B}_q is of primary interest. Depending on the family of graphs, the locus \mathcal{B}_q may or may not cross the real q axis. If it does cross the real q axis, we denote the maximum (finite) point at which it crosses this axis as q_c . Extending

our previous result for the $p = 0$ case of $\{G\} = \{Wh^{(p)}\}$ in Eq. (7.17) of Ref. [66], we find the following result for general p :

$$q_c = 2 + p + \frac{s(1-w)}{1+w} \quad \text{for } \{G\} = \{Wh^{(p)}\} \text{ and } 0 \leq w \leq 1 \quad \text{and } 1 \leq s \leq p + 2. \quad (2.74)$$

Regarding connections of this general formula to previously determined special cases, (i) for $s = 0$ or $w = 1$, this reduces to the result $q_c = 2 + p$ for the $n \rightarrow \infty$ limit of the chromatic polynomial $P(Wh^{(p)}, q)$ given in Eq. (22) of Ref. [54]; (ii) for $p = 0$, this reduces to the result for the $n \rightarrow \infty$ limit of $Ph(C_n, q, s, w)$ given in Eq. (7.17) of Ref. [66], and (iii) for $s = 1$, this reduces to the result for the $n \rightarrow \infty$ limit of $Ph(Wh^{(1)}, q, 1, w)$ given in Eq. (10.1) of Ref. [27] (with the obvious notation change $\{C\} \rightarrow \{Wh\}$). For the relevant interval $0 \leq w \leq 1$, the value of q_c in Eq. (2.74) is (a) greater than the value $q_c = 2 + p$ for the unweighted chromatic polynomial; (b) a monotonically increasing function of s for fixed w in this DFSCP interval; and (c) a monotonically decreasing function of w . These properties are consequences of the greater suppression of color values in the set I_s as w decreases in the DFSCP interval, finally restricting the vertex coloring to use colors from the orthogonal set I_s^\perp as w reaches 0. Thus, as w decreases from 1 to 0, q_c increases continuously from $2 + p$ to $2 + p + s$. In contrast, the left-hand part of the boundary locus \mathcal{B}_q changes discontinuously; as w decreases by an arbitrarily small amount below 1, the point on the left where \mathcal{B}_q crosses the real q axis jumps discontinuously from $q = p$ to $q = p + s$. This behavior is in agreement with the fact that in the two limits $w = 1$ and $w = 0$, \mathcal{B}_q is comprised, respectively, of the unit circle centered at $q = 1 + p$ and the unit circle centered at $q = 1 + s + p$. The change in the nature of the locus for $s > 2 + p$ follows via the corresponding generalization of the analysis in Ref. [66] to $p \geq 0$.

2.7 Upper and Lower Bounds on $Z(G, q, s, v, w)$ for $v \geq 0$

In this section we derive powerful new two-sided upper and lower bounds for the generalized field-dependent partition function of the ferromagnetic ($v \geq 0$) Potts model, $Z(G, q, s, v, w)$ on an arbitrary graph G in terms of the zero-field Potts model partition functions $Z(G, u_1, v)$ and $Z(G, u_1/w, v)$, where $u_1 = q + s(w - 1)$ (c.f. Eq. (1.13)). These are especially useful because the zero-field Potts model partition function is considerably easier to calculate than

$Z(G, q, s, v, w)$. Throughout this section, it is understood that $q \geq 0$, $0 \leq s \leq q$, and $v \geq 0$. The former two conditions are obvious for our present analysis, while the latter will often be indicated explicitly.

We first derive a lower bound for $Z(G, q, s, v, w)$ for the range $w \geq 1$. To begin, we observe that, from its definition in Eq. (1.13) and factorization property (2.1), u_m satisfies

$$\begin{aligned} u_m &= q + s(w^m - 1) = q + s(w - 1) \sum_{j=0}^{m-1} w^j \\ &\geq q + s(w - 1) = u_1 \quad \text{for } w \geq 1 . \end{aligned} \quad (2.75)$$

Substituting this inequality into the expression for $Z(G, q, s, v, w)$ in Eq. (1.12) in terms of contributions from spanning subgraphs $G' \subseteq G$, we have, for the same conditions

$$\begin{aligned} Z(G, q, s, v, w) &= \sum_{G' \subseteq G} v^{e(G')} \prod_{i=1}^{k(G')} u_{n(G'_i)} \\ &\geq \sum_{G' \subseteq G} v^{e(G')} (u_1)^{k(G')} \quad \text{for } v \geq 0 \text{ and } w \geq 1 . \end{aligned} \quad (2.76)$$

But the expression on the second line of Eq. (2.76) is just the zero-field Potts model partition function given in Eq. (1.5) with its argument q replaced by u_1 , namely $Z(G, u_1, v)$. Hence, we have derived a lower bound on $Z(G, q, s, v, w)$:

$$Z(G, q, s, v, w) \geq Z(G, u_1, v) \quad \text{for } v \geq 0 \text{ and } w \geq 1 . \quad (2.77)$$

For the interval $0 \leq w \leq 1$, the inequality (2.75) is reversed:

$$u_m \leq u_1 \quad \text{for } 0 \leq w \leq 1 , \quad (2.78)$$

and thus Eq. (2.76) is replaced by

$$Z(G, q, s, v, w) \leq \sum_{G' \subseteq G} v^{e(G')} (u_1)^{k(G')} \quad \text{for } v \geq 0 \text{ and } 0 \leq w \leq 1 \quad (2.79)$$

Therefore, we obtain a second inequality, which is an upper bound:

$$Z(G, q, s, v, w) \leq Z(G, u_1, v) \quad \text{for } v \geq 0 \text{ and } 0 \leq w \leq 1 . \quad (2.80)$$

To derive two-sided inequalities, we make use of the symmetry relation (2.11), which maps the interval $w \geq 1$ to the interval $0 \leq w \leq 1$ and vice versa.

Let us start with the case $w \geq 1$, for which we have proved the lower bound (2.77). Now, from the symmetry relation (2.11) we know that $Z(G, q, s, v, w) = w^n Z(G, q, \hat{s}, v, \hat{w})$ where $\hat{s} \equiv q - s$ and $\hat{w} \equiv w^{-1}$. Since $\hat{w} \in [0, 1]$, we can apply our upper bound (2.80) to $Z(G, q, \hat{s}, v, \hat{w})$, getting the inequality

$$Z(G, q, \hat{s}, v, \hat{w}) \leq Z(G, \hat{u}_1, v) , \quad (2.81)$$

where

$$\hat{u}_1 \equiv q + \hat{s}(\hat{w} - 1) = q + (q - s)(w^{-1} - 1) = \frac{u_1}{w} . \quad (2.82)$$

Combining (2.81) with (2.77), we derive the two-sided inequality

$$Z(G, u_1, v) \leq Z(G, q, s, v, w) \leq w^n Z(G, \frac{u_1}{w}, v) \quad \text{for } v \geq 0 \quad \text{and } w \geq 1 . \quad (2.83)$$

For the interval $0 \leq w \leq 1$, by the same type of reasoning, we extend our upper bound (2.80) to the two-sided inequality

$$w^n Z(G, \frac{u_1}{w}, v) \leq Z(G, q, s, v, w) \leq Z(G, u_1, v) \quad \text{for } v \geq 0 \quad \text{and } 0 \leq w \leq 1 . \quad (2.84)$$

As two-sided inequalities, these are powerful restrictions on the generalized field-dependent Potts model partition function in terms of zero-field Potts model partition functions with q replaced by u_1 and u_1/w .

We next prove some factorization properties of the upper and lower differences in these two-sided inequalities. First, if $w = 1$, then since $Z(G, q, s, v, 1) = Z(G, q, v)$ and $u_1 = q$, it follows that the two-sided inequalities (2.84) and (2.83) reduce to equalities, i.e., both the upper and lower differences vanish. Second, if $v = 0$, then the only contributions in the respective Eqs. (1.12) and (1.5) are from the spanning subgraph with no edges (called the null graph, N_n), so $Z(G, q, s, 0, w) = (u_1)^n$, and $Z(G, q, 0) = q^n$, whence $Z(G, u_1, 0) = (u_1)^n$ and $w^n Z(G, u_1/w, 0) = (u_1)^n$. Hence, again, in this $v = 0$ case, the inequalities (2.84) and (2.83) reduce to equalities and the upper and lower differences vanish. Third, if $s = 0$, then $Z(G, q, 0, v, w) = Z(G, q, v)$ and $u_1 = q$, so that $Z(G, u_1, v) = Z(G, q, v)$. Hence, if $s = 0$, then the lower difference in (2.83) and the upper difference in (2.84) vanish. Fourth, if $w = 0$, then $Z(G, q, s, v, 0) = Z(G, q - s, v)$ and $u_1 = q - s$, so $Z(G, u_1, v) = Z(G, q - s, v)$; therefore, again, the lower difference in (2.83) and the upper difference in (2.84) vanish. Together, these four results prove that the difference

$$Z(G, q, s, v, w) - Z(G, u_1, v) \quad \text{contains the factor} \quad w(w - 1)sv . \quad (2.85)$$

Fifth, if $s = q$, then $Z(G, q, q, v, w) = w^n Z(G, q, v)$ and $u_1 = qw$, so $w^n Z(G, u_1/w, v) =$

$w^n Z(G, q, v)$. Hence, if $s = q$, then the upper difference in (2.83) and the lower difference in (2.84) vanish. Combining this with the first two results above, we have shown that

$$w^n Z(G, \frac{u_1}{w}, v) - Z(G, q, s, v, w) \quad \text{contains the factor} \quad (w-1)(q-s)v. \quad (2.86)$$

It is also useful to characterize the difference between the zero-field Potts model partition functions that constitute the upper and lower bounds in these two-sided inequalities (2.83) and (2.84). For an arbitrary graph G , we have

$$w^n Z(G, \frac{u_1}{w}, v) - Z(G, u_1, v) = \sum_{G' \subseteq G} v^{e(G')} (u_1)^{k(G')} \left[w^{n(G)-k(G')} - 1 \right], \quad (2.87)$$

where G' is a spanning subgraph of G . Now the right-hand side of Eq. (2.87) is nonzero only if G has at least one edge, and, in this case, the only nonvanishing contributions have $n(G) - k(G') \geq 1$. It follows that

$$w^n Z(G, \frac{u_1}{w}, v) - Z(G, u_1, v) \quad \text{contains a factor} \quad vu_1(w-1). \quad (2.88)$$

It is worthwhile to give some illustrations of these two-sided inequalities (2.83) and (2.84). We first do this for tree graphs. For any n -vertex tree graph T_n , if $w \geq 1$, then the inequality (2.83) reads

$$u_1(u_1 + v)^{n-1} \leq Z(T_n, q, s, v, w) \leq u_1(u_1 + wv)^{n-1} \quad \text{for} \quad v \geq 0 \quad \text{and} \quad w \geq 1. \quad (2.89)$$

where we have used $Z(T_n, q, v) = q(q+v)^{n-1}$. If $w \in [0, 1]$, then the inequality (2.84) reads

$$u_1(u_1 + wv)^{n-1} \leq Z(T_n, q, s, v, w) \leq u_1(u_1 + v)^{n-1} \quad \text{for} \quad v \geq 0 \quad \text{and} \quad 0 \leq w \leq 1. \quad (2.90)$$

(This example also shows how the apparent singularity at $w = 0$ arising from the u_1/w argument in $Z(G, u_1/w, v)$ on the left-hand side of the inequality (2.84) is removed by the w^n factor, yielding a nonsingular expression.) One gains further insight by calculating the differences between the polynomials that constitute the upper bound, the middle term, $Z(T_n, q, s, w, v)$, and the lower bound for various tree graphs. For the path graph L_2 and $w \geq 1$, the differences that enter in the two-sided inequality (2.89) are

$$u_1(u_1 + wv) - Z(L_2, q, s, v, w) = (w-1)(q-s)v \geq 0 \quad (2.91)$$

and

$$Z(L_2, q, s, v, w) - u_1(u_1 + v) = w(w - 1)sv \geq 0 . \quad (2.92)$$

For $w \in [0, 1]$ the differences that enter in (2.90) are obvious reversals of these, viz., $u_1(u_1 + v) - Z(L_2, q, s, v, w) = w(1 - w)sv \geq 0$ and $Z(L_2, q, s, v, w) - u_1(u_1 + wv) = (1 - w)(q - s)v \geq 0$. For the path graph L_3 and $w \geq 1$, the differences in (2.89) are

$$u_1(u_1 + wv)^2 - Z(L_3, q, s, v, w) = (w - 1)(q - s)v \left[2u_1 + v(w + 1) \right] \geq 0 \quad (2.93)$$

and

$$Z(L_3, q, s, v, w) - u_1(u_1 + v)^2 = w(w - 1)sv \left[2u_1 + v(w + 1) \right] \geq 0 , \quad (2.94)$$

and similarly for $w \in [0, 1]$.

Among n -vertex tree graphs, the star graph S_n has a particularly simple field-dependent Potts partition function, which was given in Ref. [66] and also has been derived in Eq. (2.33). Here we recall the general formula of S_n (for any v):

$$\begin{aligned} Z(S_n, q, s, v, w) &= (q - s) \left[q + s(w - 1) + v \right]^{n-1} + sw \left[q + s(w - 1) + wv \right]^{n-1} \\ &= (q - s)(u_1 + v)^{n-1} + sw(u_1 + wv)^{n-1} . \end{aligned} \quad (2.95)$$

For $v \geq 0$, substituting this result (2.95) into the two-sided inequalities (2.89) and (2.90), we can derive general formulas for the respective upper and lower differences. If $w \geq 1$ we find, for the lower difference in (2.89),

$$\begin{aligned} Z(S_n, q, s, v, w) - u_1(u_1 + v)^{n-1} &= sw \left[(u_1 + wv)^{n-1} - (u_1 + v)^{n-1} \right] \\ &= sw \sum_{j=0}^{n-1} \binom{n-1}{j} (u_1)^{n-1-j} v^j (w^j - 1) \\ &= sw(w - 1)v \sum_{j=1}^{n-1} \binom{n-1}{j} (u_1)^{n-1-j} v^{j-1} \left[\sum_{\ell=0}^{j-1} w^\ell \right] \\ &\geq 0 . \end{aligned} \quad (2.96)$$

In the same way, if $w \in [0, 1]$, then the upper difference $u_1(u_1 + v)^{n-1} - Z(S_n, q, s, v, w)$ in (2.90) is given by minus the right-hand side of Eq. (2.96).

Similarly, if $w \geq 1$, then for the upper difference in (2.89) we calculate

$$\begin{aligned}
u_1(u_1 + wv)^{n-1} - Z(S_n, q, s, v, w) &= (q - s) \left[(u_1 + wv)^{n-1} - (u_1 + v)^{n-1} \right] \\
&= (q - s)(w - 1)v \sum_{j=1}^{n-1} \binom{n-1}{j} (u_1)^{n-1-j} v^{j-1} \left[\sum_{\ell=0}^{j-1} w^\ell \right] \\
&\geq 0 .
\end{aligned} \tag{2.97}$$

Again, if $w \in [0, 1]$, then the lower difference $Z(S_n, q, s, v, w) - u_1(u_1 + wv)^{n-1}$ in (2.90) is given by minus the right-hand side of Eq. (2.97).

For the circuit graph C_n , if $w \geq 1$, the inequality (2.89) reads $Z(C_n, u_1, v) \leq Z(C_n, q, s, v, w) \leq w^n Z(C_n, u_1/w, v)$. Using the fact that $Z(C_n, q, v) = (q + v)^n + (q - 1)v^n$, we can write this explicitly as

$$(u_1 + v)^n + (u_1 - 1)v^n \leq Z(C_n, q, s, v, w) \leq (u_1 + wv)^n + (u_1 - w)w^{n-1}v^n . \tag{2.98}$$

For C_2 (which has a double edge), the differences that enter in this two-sided inequality are

$$w^2 Z(C_2, u_1/w, v) - Z(C_2, q, s, v, w) = (q - s)(w - 1)v(v + 2) \geq 0 \tag{2.99}$$

and

$$Z(C_2, q, s, v, w) - Z(C_2, u_1, v) = w(w - 1)sv(v + 2) \geq 0 . \tag{2.100}$$

Similar illustrations of the general inequalities (2.89) and (2.90) can be given for L_n and C_n with higher values of n and for other families of graphs.

2.8 Use of $Z(G, q, s, v, w)$ and $Ph(G, q, s, w)$ to Distinguish Between Tutte-Equivalent and Chromatically Equivalent Graphs

Two graphs G and H are defined to be (i) chromatically equivalent if they have the same chromatic polynomial, and (ii) Tutte-equivalent if they have the same Tutte polynomial, or equivalently, zero-field Potts model partition function. Here the Tutte polynomial $T(G, x, y)$ of a graph G is defined as

$$T(G, x, y) = \sum_{G' \subseteq G} (x - 1)^{k(G') - k(G)} (y - 1)^{c(G')} , \tag{2.101}$$

where G' is a spanning subgraph of G (and $c(G')$ and $k(G')$ were defined above as, respectively, the number of linearly independent cycles and the number of connected components of G'). This is equivalent to the zero-field Potts model partition function, via the relation

$$Z(G, q, v) = (x - 1)^{k(G)} (y - 1)^n T(G, x, y) , \quad (2.102)$$

where $y = v + 1$ and $x = 1 + (q/v)$. The Tutte polynomial is of considerable interest in mathematical graph theory, since it encodes much information about a graph [74] [75]. However, although it distinguishes between many graphs, there exist other pairs of graphs G and H that are different but have the same Tutte polynomial. An important property of our generalized field-dependent Potts model partition function $Z(G, q, s, v, w)$ is that it can distinguish between many Tutte-equivalent graphs. Similarly, an important property of the weighted-set chromatic polynomial is that it can distinguish between many chromatically equivalent graphs. We study this further in this section. This property is true for all w and s values except the special values $w = 1$, $w = 0$, $s = 0$, and $s = q$, for which $Z(G, q, s, v, w)$ is reducible to a zero-field Potts partition function (as well as the trivial case $v = 0$) and similarly for $Ph(G, q, s, w)$. reducible to a chromatic polynomial. In Ref. [66] we proved that for any two Tutte-equivalent graphs G and H ,

$$Z(G, q, s, v, w) - Z(H, q, s, v, w) \quad \text{contains the factor} \quad s(q - s)vw(w - 1) . \quad (2.103)$$

In the following, we will generally phrase our analysis in terms of how the field-dependent Potts partition function distinguishes between Tutte-equivalent graphs; the special cases of the various expressions for $v = -1$ then show how the weighted-set chromatic polynomial distinguishes between different chromatically equivalent graphs.

A class of Tutte-equivalent (and, hence also chromatically equivalent) graphs of particular interest is comprised of tree graphs, generically denoted T_n . For these, $T(T_n, x, y) = x^{n-1}$, so

$$Z(T_n, q, v) = q(q + v)^{n-1} \quad \text{and} \quad P(T_n, q) = q(q - 1)^{n-1} . \quad (2.104)$$

Note that $e(T_n) = n - 1$ (and a tree graph cannot have any multiple edges). There is only one tree graph with $n = 1$ vertex, one with $n = 2$ vertices, and one with $n = 3$ vertices. There are two different tree graphs with $n = 4$ vertices, namely the path graph, L_4 , and the star graph, S_4 . Enumerations of tree graphs with larger numbers of vertices are given, e.g., in Refs. [33] and [45]. Let us consider two different n -vertex tree graphs (which thus have $n \geq 4$), denoted


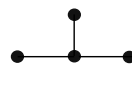
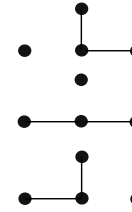
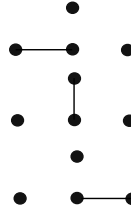

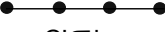

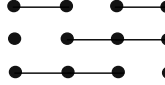
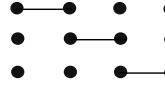

spanning subgraphs	$e(G')=3$	$e(G')=2$	$e(G')=1$	$e(G')=0$
 $G' \subseteq S_4$				
contribution to $Z(S_4, q, s, v, w)$	$v^3 u_4$	$3v^2 u_1 u_3$	$3v u_1^2 u_2$	u_1^4
 $G' \subseteq L_4$				
contribution to $Z(L_4, q, s, v, w)$	$v^3 u_4$	$v^2(2u_1 u_3 + u_2^2)$	$3v u_1^2 u_2$	u_1^4
The difference $Z(S_4) - Z(L_4)$	0	$v^2(u_1 u_3 - u_2^2)$	0	0

Figure 2.3: Use of $Z(G, q, s, v, w)$ to distinguish between Tutte/chromatic equivalent tree graphs S_n and L_n .

G_t and H_t . Since these have the same number of edges, inspection of the general Eq. (2.9) shows that for the difference $Z(G_t, q, s, v, w) - Z(H_t, q, s, v, w)$, not only the v^0 and v^n terms, but also the v^1 terms cancel. Hence,

$$Z(G_t, q, s, v, w) - Z(H_t, q, s, v, w) \quad \text{contains the factor } v^2. \quad (2.105)$$

We recall that $I_s \subseteq I_q$, so that $0 \leq s \leq q$, and that $w \geq 0$, as follows for any physical field H . These properties will be understood implicitly in the following. As preparation for the derivation of an inequality concerning $Z(G_t, q, s, v, w)$ for S_n and L_n graphs, it is useful to give some explicit examples. Let us consider the two tree graphs with $n = 4$ vertices, namely S_4 and L_4 (see Fig. (2.3)). In the following, we will usually omit the arguments q, s, v, w in $Z(G, q, s, v, w)$ for brevity of notation. We have given exact expressions for $Z(S_n)$ in Eq. (3.5) of Ref. [66] and for $Z(L_n)$ in Eq. (2.39) above. For our present purposes, we focus on the expressions in terms of the spanning subgraph expansion. For S_4 , this is

$$Z(S_4) = u_1^4 + 3v u_2 u_1^2 + 3v^2 u_3 u_1 + v^3 u_4, \quad (2.106)$$

while for L_4 we have

$$Z(L_4) = u_1^4 + 3vu_2u_1^2 + v^2(2u_3u_1 + u_2^2) + v^3u_4 . \quad (2.107)$$

The difference in the structure of the term proportional to v^2 arises from the differences in the spanning subgraphs with two edges in S_4 and L_4 . Hence,

$$Z(S_4) - Z(L_4) = v^2(u_3u_1 - u_2^2) = v^2s(q - s)w(w - 1)^2 . \quad (2.108)$$

Since the last expression will appear as a factor in the differences $Z(G_t) - Z(H_t)$ to be presented below, we give it a symbol:

$$\mu \equiv s(q - s)v^2w(w - 1)^2 \quad (2.109)$$

and note that

$$\mu \geq 0 , \quad (2.110)$$

so that $Z(S_4) - Z(L_4) \geq 0$.

There are three different tree graphs with $n = 5$ vertices: S_5 , L_5 , and a graph that we denote as Y_5 , which has the form of a Y , with the vertical part made up of three vertices and two edges (shown in Fig. (2.1)). The graph Y_n is the generalization of this graph in which the vertical part is comprised of $n - 2$ vertices forming a path graph P_{n-2} (so that $Y_4 = S_4$). The spanning subgraph expansions for these graphs, in order of decreasing maximal vertex degree, are

$$Z(S_5) = u_1^5 + 4vu_2u_1^3 + 6v^2u_3u_1^2 + 4v^3u_4u_1 + v^4u_5 , \quad (2.111)$$

$$Z(Y_5) = u_1^5 + 4vu_2u_1^3 + 2v^2(2u_3u_1^2 + u_2^2u_1) + v^3(3u_4u_1 + u_3u_2) + v^4u_5 \quad (2.112)$$

and

$$Z(L_5) = u_1^5 + 4vu_2u_1^3 + 3v^2(u_3u_1^2 + u_2^2u_1) + 2v^3(u_4u_1 + u_3u_2) + v^4u_5 \quad (2.113)$$

Thus, for the differences, we have

$$\begin{aligned} Z(S_5) - Z(Y_5) &= 2v^2(u_3u_1^2 - u_2^2u_1) + v^3(u_4u_1 - u_3u_2) \\ &= \mu[2u_1 + v(w + 1)] , \end{aligned} \quad (2.114)$$

$$\begin{aligned}
Z(S_5) - Z(L_5) &= 3v^2(u_3u_1^2 - u_2^2u_1) + 2v^3(u_4u_1 - u_3u_2) \\
&= \mu[3u_1 + 2v(w + 1)] ,
\end{aligned} \tag{2.115}$$

and

$$\begin{aligned}
Z(Y_5) - Z(L_5) &= v^2(u_3u_1^2 - u_2^2u_1) + v^3(u_4u_1 - u_3u_2) \\
&= \mu[u_1 + v(w + 1)] .
\end{aligned} \tag{2.116}$$

Now (remembering that $0 \leq s \leq q$ and $w \geq 0$), for the ferromagnetic range $v \geq 0$, for nonnegative a and b , one has

$$au_1 + bv(w + 1) \geq 0 . \tag{2.117}$$

Hence, for the ferromagnetic case, each of the differences $Z(S_5) - Z(Y_5)$, $Z(S_5) - Z(L_5)$, and $Z(Y_5) - Z(L_5)$ is non-negative.

From these explicit examples, one sees that the origin of these inequalities can be traced to inequalities among products of the u_r 's. We proceed to prove two lemmas and then a general theorem. Our first lemma is

$$u_{n-1}u_1 \geq u_{n-\ell}u_\ell \quad \text{for } n \geq 2 \text{ and } 2 \leq \ell \leq n - 2 . \tag{2.118}$$

To verify this lemma, we expand and factor the given expression:

$$\begin{aligned}
u_{n-1}u_1 - u_{n-\ell}u_\ell &= s(q-s)w(1 + w^{n-2} - w^{\ell-1} - w^{n-\ell-1}) \\
&= s(q-s)w(w^{n-\ell-1} - 1)(w^{\ell-1} - 1) \\
&= s(q-s)w(w-1)^2 \left[\sum_{i=0}^{n-\ell-2} w^i \right] \left[\sum_{j=0}^{\ell-2} w^j \right] \geq 0 \tag{2.119}
\end{aligned}$$

This lemma shows that the difference $u_3u_1 - u_2^2$ that appears multiplying v^2 in Eqs. (2.108), (2.114), (2.115), and (2.116) is nonnegative, and similarly that the difference $u_4u_1 - u_3u_2$ that appears multiplying v^3 in the last three of these equations is nonnegative.

Differences of the form $Z(G_t) - Z(H_t)$ for higher values of n involve differences of higher products of u_r factors, and there is an analogous inequality for these products. We prove this as a second lemma. Let us consider a generic term in Eq. (1.12), for the spanning subgraph $G' = \oplus G'_i$ with $k(G')$ connected components, G'_i , each with $n(G'_i)$ vertices. This has the form (2.4) satisfying

the relation (2.5). Our second lemma is, with $\ell = n - k(G') + 1$,

$$u_\ell u_1^{n-\ell} \geq \prod_{j=1}^{k(G')} u_{n(G'_j)} \quad \text{for } n \geq 2 \quad \text{and} \quad 1 \leq \ell \leq n, \quad \text{i.e., } 1 \leq k(G') \leq n. \quad (2.120)$$

For example, for the case $n = 6$, this lemma yields the inequalities $u_4 u_1^2 \geq u_3^2$, $u_4 u_1^2 \geq u_2^3$, and $u_4 u_1^2 \geq u_4 u_2$. This lemma is proved by applying Lemma 1 iteratively.

Combining the expression for $Z(S_n, q, s, v, w)$ in the first line of Eq. (2.33) with our other results above, we have the following theorem: For the ferromagnetic case,

$$Z(S_n, q, s, v, w) - Z(T_n, q, s, v, w) \geq 0 \quad \text{for } v \geq 0 \quad (2.121)$$

for any tree graph T_n . This is proved by applying the two lemmas above to the terms in the spanning subgraph expansions of these partition functions for S_n and a generic tree graph T_n . In the second appendix we give further explicit results for differences of field-dependent partition functions for tree graphs with $n = 6$ vertices.

The difference $Z(Y_5) - Z(L_5)$ in Eq. (2.116) (where we omit the arguments for brevity of notation) can also be understood using the recursive relation for $n \geq 5$:

$$\begin{aligned} Z(Y_n) - Z(L_n) &= \sum_{j=1}^{n-4} v^{j-1} u_j [Z(Y_{n-j}) - Z(L_{n-j})] \\ &+ v^{n-4} \left(\sum_{j=0}^{n-4} w^j \right) [Z(Y_4) - Z(L_4)], \end{aligned} \quad (2.122)$$

where $Z(Y_4) - Z(L_4) = Z(S_4) - Z(L_4) = \mu$ was given in Eq. (2.108). For the ferromagnetic range $v \geq 0$, each term on the right-hand side of Eq. (2.122) is nonnegative, and hence this proves the inequality

$$Z(Y_n, q, s, v, w) - Z(L_n, q, s, v, w) \geq 0 \quad \text{for } v \geq 0. \quad (2.123)$$

Combining (2.121) and (2.123), we have

$$Z(S_n, q, s, v, w) \geq Z(Y_n, q, s, v, w) \geq Z(L_n, q, s, v, w) \quad \text{for } v \geq 0. \quad (2.124)$$

Chapter 3

Ground State Entropy of the Potts Antiferromagnet: I. Lower Bounds for Slabs of the Simple Cubic Lattice

In the present chapter we derive lower bounds on $W(\{G\}, q)$ for sections of a three-dimensional lattice, namely the simple cubic lattice, which are of infinite extent in two directions (taken to lie along the x and y axes) and finite in the third direction, z . By comparison with large- q expansions and numerical evaluations, we show how the lower bounds for the W functions for these slabs interpolate between the values for the (respective thermodynamic limits of the) square and simple cubic lattices. The results reported here were published in Ref. [68]. These bounds are of interest partly because one does not know the exact functions $W(\text{sq}, q)$ or $W(\text{sc}, q)$ for general q .

3.1 Computational Method

Let us consider a section (slab) of the simple cubic lattice of dimensions $L_x \times L_y \times L_z$ vertices, which we denote $\text{sc}[(L_x)_{BCx} \times (L_y)_{BCy} \times (L_z)_{BCz}]$, where the boundary conditions (BC) in each direction are indicated by the subscripts. The chromatic polynomial of this lattice will be denoted $P(\text{sc}[(L_x)_{BCx} \times (L_y)_{BCy} \times (L_z)_{BCz}], q)$. We will calculate lower bounds for $W(\text{sc}[(L_x)_{BCx} \times (L_y)_{BCy} \times (L_z)_{BCz}], q)$ in the limit $L_x \rightarrow \infty$ and $L_y \rightarrow \infty$ with L_z fixed. These are independent of the boundary conditions imposed in the directions in which the slab is of infinite extent, and hence, for brevity of notation, we will denote the limit $\lim_{L_x, L_y \rightarrow \infty} \text{sc}[(L_x)_{BCx} \times (L_y)_{BCy} \times (L_z)_{BCz}]$ simply as

$S_{(L_z)BC_z}$, where S stands for “slab”. We will consider both free (F) and periodic (P) boundary conditions in the z direction, and thus slabs such as S_{3F} , S_{3P} , etc. For technical reasons (to get an expression involving a trace of a coloring matrix, as explained below) we will use periodic boundary conditions in the x direction. Note that the proper q -coloring constraint implies that FBC_z and PBC_z are equivalent if $L_z = 2$. The number of vertices for $G = \text{sc}[(L_x)BC_x \times (L_y)BC_y \times (L_z)BC_z]$ is $n = L_x L_y L_z$. The specific form of Eq. (1.9) for our calculation is

$$W(S_{(L_z)BC_z}, q) = \lim_{L_y \rightarrow \infty} \lim_{L_x \rightarrow \infty} [P(\text{sc}[(L_x)P \times (L_y)BC_y \times (L_z)BC_z], q)]^{1/n}. \quad (3.1)$$

To derive a lower bound on $W(S_{(L_z)BC_z}, q)$, we generalize the method of Refs. [53], [55] and [57] from two to three dimensions. We consider two adjacent transverse slices of the slab orthogonal to the x direction, with x values x_0 and $x_0 + 1$. These are thus sections of the square lattice of dimension $L_y \times L_z$, which we denote $G_{x_0} = \text{sq}[(L_y)BC_y \times (L_z)BC_z]_{x_0}$ and $G_{x_0+1} = \text{sq}[(L_y)BC_y \times (L_z)BC_z]_{x_0+1}$. We label a particular color assignment to the vertices of G_{x_0} that is a proper q -coloring of these vertices as $C(G_{x_0})$ and similarly for G_{x_0+1} . The total number of proper q -colorings of G_{x_0} is

$$\mathcal{N} = P(G_{x_0}, q) = P(G_{x_0+1}, q). \quad (3.2)$$

Now let us add the edges in the x direction that join these two adjacent transverse slices of the slab together. Among the \mathcal{N}^2 color configurations that yield proper q -colorings of these two separate yz transverse slices, some will continue to be proper q -colorings after we add these edges that join them in the x direction, while others will not.

We define an $\mathcal{N} \times \mathcal{N}$ -dimensional *coloring compatibility matrix* T (see Refs. [9] and [12]), with entries $T_{C(G_{x_0}), C(G_{x_0+1})}$ equal to (i) 1 if the color assignments $C(G_{x_0})$ and $C(G_{x_0+1})$ are proper q -colorings after the edges in the x direction have been added joining G_{x_0} and G_{x_0+1} , i.e., if the color assigned to each vertex $v(x_0, y, z)$ in G_{x_0} is different from the color assigned to the vertex $v(x_0 + 1, y, z)$ in G_{x_0+1} ; and (ii) 0 if the color assignments $C(G_{x_0})$ and $C(G_{x_0+1})$ are not proper q -colorings after the edges in the x direction have been added, i.e., there exists some color assigned to a vertex $v(x_0, y, z)$ in G_{x_0} that is equal to a color assigned to the vertex $v(x_0 + 1, y, z)$ in G_{x_0+1} . Clearly, $T_{ij} = T_{ji}$. The chromatic polynomial for the slab is then given by the trace

$$P(\text{sc}[(L_x)P \times (L_y)BC_y \times (L_z)BC_z], q) = \text{Tr}(T^{L_x}). \quad (3.3)$$

Since T is a real symmetric matrix, there exists an orthogonal matrix A that diagonalizes T : $ATA^{-1} = T_{diag}$. Let us denote the \mathcal{N} eigenvalues of T as $\lambda_{T,j}$, $1 \leq j \leq \mathcal{N}$. Since T is a real non-negative matrix, we can apply the generalized Perron-Frobenius theorem [36, 39] to infer that T has a real maximal eigenvalue, which we denote $\lambda_{T,max}$. It follows that

$$\lim_{L_x \rightarrow \infty} [P(\text{sc}[(L_x)_P \times (L_y)_{BC_y} \times (L_z)_{BC_z}], q)]^{1/L_x} = \lambda_{T,max} . \quad (3.4)$$

Now for the transverse slices G_{x_0} and G_{x_0+1} , denoted generically as $ts((L_z)_{BC_z})$, the chromatic polynomial has the form

$$P(G_{x_0}, q) = P(G_{x_0+1}, q) = \sum_j c_j (\lambda_{ts((L_z)_{BC_z}),j})^{L_y} \quad (3.5)$$

where the c_j are coefficients whose precise form is not needed here, given the range of $q \geq 3$ for which we apply our bounds. (This range is used because bounds are unnecessary for $q = 2$, since $W(\text{sc}, 2) = 1$ is known exactly.) The set of $\lambda_{ts((L_z)_{BC_z}),j}$'s is independent of the length L_y and although this set depends on BC_y , the maximal one (having the largest magnitude), $\lambda_{ts((L_z)_{BC_z}),max}$, is independent of BC_y . Hence,

$$\begin{aligned} \lim_{L_y \rightarrow \infty} [P(G_{x_0}, q)]^{1/L_y} &\equiv \lim_{L_y \rightarrow \infty} (\mathcal{N})^{1/L_y} \\ &= \lambda_{ts((L_z)_{BC_z}),max} . \end{aligned} \quad (3.6)$$

The two adjacent slices together with the edges in the x direction that join them constitute the graph $\text{sc}[2_F \times (L_y)_{BC_y} \times (L_z)_{BC_z}]$. We denote the chromatic polynomial for this section (tube) of the sc lattice as $P(\text{sc}[2_F \times (L_y)_{BC_y} \times (L_z)_{BC_z}], q)$ (which is equal to $P(\text{sc}[2_P \times (L_y)_{BC_y} \times (L_z)_{BC_z}], q)$ because of the proper q -coloring condition). This has the form

$$\begin{aligned} &P(\text{sc}[2_F \times (L_y)_{BC_y} \times (L_z)_{BC_z}], q) \\ &= \sum_j c'_j (\lambda_{tube((L_z)_{BC_z}),j})^{L_y} \end{aligned} \quad (3.7)$$

where c'_j are coefficients analogous to those in (3.5). Therefore,

$$\begin{aligned} \lim_{L_y \rightarrow \infty} [P(\text{sc}[2_F \times (L_y)_{BC_y} \times (L_z)_{BC_z}], q)]^{1/L_y} &= \\ &= \lambda_{tube((L_z)_{BC_z}),max} . \end{aligned} \quad (3.8)$$

Now let us denote the column sum

$$C_j(T) = \sum_{i=1}^{\mathcal{N}} T_{ij} , \quad (3.9)$$

which is equal to the row sum $\sum_{j=1}^{\mathcal{N}} T_{ij}$, since T is symmetric. We also define the sum of all entries (S_E) of T as

$$S_E(T) = \sum_{i,j=1}^{\mathcal{N}} T_{ij} . \quad (3.10)$$

Note that $S_E(T)/\mathcal{N}$ is the average row (= column) sum. Next, we observe that

$$S_E(T) = P(\text{sc}[2_F \times (L_y)_{BC_y} \times (L_z)_{BC_z}], q) . \quad (3.11)$$

To obtain our lower bound, we then use the $r = 1$ special case of the theorem that for a non-negative symmetric matrix T and $r \in \mathbb{N}_+$ [38]

$$\lambda_{T,max} \geq \left[\frac{S_E(T^r)}{\mathcal{N}} \right]^{1/r} . \quad (3.12)$$

The lower bound is then

$$W(S_{(L_z)_{BC_z}}, q) \geq W(S_{(L_z)_{BC_z}}, q)_\ell \quad (3.13)$$

where

$$\begin{aligned} W(S_{(L_z)_{BC_z}}, q)_\ell &= \lim_{L_y \rightarrow \infty} \left(\frac{S_E(T)}{\mathcal{N}} \right)^{1/(L_y L_z)} \\ &= \lim_{L_y \rightarrow \infty} \left[\frac{P(\text{sc}[2_F \times (L_y)_{BC_y} \times (L_z)_{BC_z}], q)}{P(\text{sq}[(L_y)_{BC_y} \times (L_z)_{BC_z}], q)} \right]^{1/(L_y L_z)} \\ &= \left[\frac{\lambda_{\text{tube}((L_z)_{BC_z}),max}}{\lambda_{\text{ts}((L_z)_{BC_z}),max}} \right]^{1/L_z} . \end{aligned} \quad (3.14)$$

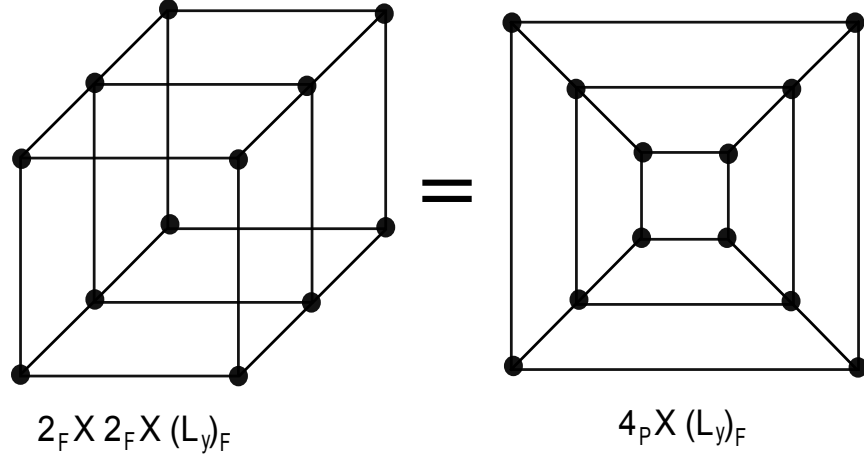


Figure 3.1: Equivalence between simple cubic slab graph $sc[2_F \times 2_F \times (L_y)_F]$ and square lattice strip graph $sq[4_P \times (L_y)_F]$, using $L_y = 3$ as an illustration.

3.2 Results for Slab of Thickness $L_z = 2$ with FBC_z

We now evaluate our general lower bound in Eqs. (3.13) and (3.14) for a slab of the simple cubic lattice with thickness $L_z = 2$ and FBC_z , denoted S_{2F} . In this case the transverse slice is the graph $sq[2_F \times (L_y)_{\text{BC}y}]$. For FBC_y , an elementary calculation yields

$$P(sq[2_F \times (L_y)_F], q) = q(q-1)(q^2 - 3q + 3)^{L_y-1} \quad (3.15)$$

with a single $\lambda_{ts(2F)} = \lambda_{ts(2P)} \equiv \lambda_{ts(2)}$, and this is also the maximal λ for PBC_y [8, 52], so that

$$\lambda_{ts(2),max} = q^2 - 3q + 3. \quad (3.16)$$

We next use the calculation of

$$\begin{aligned}
P(sc[2_F \times (L_y)_F \times 2_F], q) &= P(sc[2_F \times 2_F \times (L_y)_F], q) \\
&= P(sq[4_P \times (L_y)_F], q)
\end{aligned} \quad (3.17)$$

in Ref. [47] (where each of the 2_F BC's is equivalent to 2_P , and for the

equivalence between simple cubic slab graph $sc[2_F \times 2_F \times (L_y)_F]$ and square lattice strip graph $sq[4_P \times (L_y)_F]$, see Fig. (3.1) as an illustration), from which we calculate the maximal $\lambda_{tube(2),max}$ to be

$$\lambda_{tube(2),max} = \frac{1}{2} \left[q^4 - 8q^3 + 29q^2 - 55q + 46 + \sqrt{R_{22}} \right] \quad (3.18)$$

where

$$\begin{aligned} R_{22} &= q^8 - 16q^7 + 118q^6 - 526q^5 + 1569q^4 \\ &- 3250q^3 + 4617q^2 - 4136q + 1776 . \end{aligned} \quad (3.19)$$

We then substitute these results for $\lambda_{ts(2),max}$ and $\lambda_{tube(2),max}$ into the $L_z = 2$ special case of (3.14) to obtain $W(S_2, q)_\ell$, and thus the resultant lower bound on $W(S_{2_F}, q) = W(S_{2_P}, q) \equiv W(S_2, q)$: $W(S_2, q) \geq W(S_2, q)_\ell$.

3.3 Comparison with Large- q Series Expansions

One way to elucidate how this lower bound $W(S_2, q)_\ell$ compares with the exact $W(sq, q)$ and $W(sc, q)$ is to compare the large- q series expansions for these three functions. For this purpose, it is first appropriate to give some relevant background on large- q series expansions for $W(\{G\}, q)$ functions. Since there are q^n possible colorings of the vertices of an n -vertex graph G with q colors if no conditions are imposed, an obvious upper bound on the number of proper q -colorings of the vertices of G is $P(G, q) \leq q^n$. This yields the corresponding upper bound $W(\{G\}, q) < q$. Hence, it is natural to define a reduced function that has a finite limit as $q \rightarrow \infty$,

$$W_r(\{G\}, q) = q^{-1} W(\{G\}, q) . \quad (3.20)$$

For a lattice or, more generally, a graph whose vertices have bounded degree, $W_r(\{G\}, q)$ is analytic about $1/q = 0$. ($W_r(\{G\}, q)$ is non-analytic at $1/q = 0$ for certain families of graphs that contain one or more vertices with unbounded degree as $n \rightarrow \infty$, although the presence of a vertex with unbounded degree in this limit does not necessarily imply non-analyticity of $W_r(\{G\}, q)$ at $1/q = 0$ [56].) It is conventional to express the large- q Taylor series for a function that has some factors removed from W_r , since this function yields a simpler expansion.

A chromatic polynomial has the general form

$$P(G, q) = \sum_{j=0}^{n-k(G)} (-1)^j a_{n-j} q^{n-j} , \quad (3.21)$$

where the $a_{n-j} > 0$ and $k(G)$ is the number of connected components of G (taken here to be $k(G) = 1$ without loss of generality). One has $a_n = 1$, $a_{n-1} = e(G)$, and, provided that the girth¹ $g(G) > 3$, as is the case here, $a_{n-2} = \binom{e(G)}{2}$. A κ -regular graph is a graph such that each vertex has degree (coordination number) κ . For a κ -regular graph, $e(G) = \kappa n/2$. The coefficients of the three terms of highest degree in q in $P(G, q)$ for a κ -regular graph are precisely the terms that would result from the expansion of $[q(1 - q^{-1})^{\kappa/2}]^n$. Hence, for a κ -regular graph or lattice, one usually displays the large- q series expansions for the reduced function

$$\overline{W}(\Lambda, q) = \frac{W(\Lambda, q)}{q(1 - q^{-1})^{\kappa/2}} . \quad (3.22)$$

The large- q Taylor series for this function can be written in the form

$$\overline{W}(\Lambda, q) = 1 + \sum_{j=1}^{\infty} w_{\Lambda, j} y^j , \quad (3.23)$$

where

$$y = \frac{1}{q - 1} . \quad (3.24)$$

The two results that we shall need here are the large- q (i.e., small- y) Taylor series for $\overline{W}(\text{sq}, q)$ and $\overline{W}(\text{sc}, q)$. The large- q series for $\overline{W}(\text{sq}, q)$ was calculated to successively higher orders in [40], [3] and [2]. Here we only quote the terms to $O(y^{11})$:

$$\begin{aligned} \overline{W}(\text{sq}, q) &= 1 + y^3 + y^7 + 3y^8 + 4y^9 + 3y^{10} \\ &+ 3y^{11} + O(y^{12}) . \end{aligned} \quad (3.25)$$

As noted above, lower bounds on $W(\Lambda, q)$ obtained from the inequality (3.12) for two-dimensional lattices Λ were found to be quite close to the actual values of the respective $W(\Lambda, q)$ for a large range of values of q . This can be understood for large values of q from the fact that they coincide with the large-

¹The girth of a graph G , $g(G)$ is defined as the number of edges of a minimal-length closed circuit on G .

q expansions to many orders, and the agreement actually extends to values of q only moderately above $q = 2$. For example, the lower bound on $W(\text{sq}, q)$ in [9] is equivalent to $\overline{W}(\text{sq}, q) \geq (1 + y^3)$. This agrees with the small- y series up to order $O(y^6)$, as is evident from comparison with Eq. (3.25). This lower bound also agrees quite closely with the value of $W(\text{sq}, q)$ determined by Monte Carlo simulations in [52, 53, 55] (see Table 1 of [52] and Table 1 of [53]). We include this comparison here in Table (3.1). For our purposes, it is sufficient to quote the results from Ref. [52] only to three significant figures. Since we are using large- q series for this comparison, we list the results in Table (3.1) for a set of values $q \geq 4$. As another example, the lower bound obtained for the honeycomb lattice in Ref. [55], $\overline{W}(\text{hc}, q) \geq (1 + y^5)^{1/2}$, agreed with the small- y series for $\overline{W}(\text{hc}, q)$ to $O(y^{10})$. Thus, it was found that for all of the cases studied, $W(\Lambda, q)_\ell$ provides not only a lower bound on $W(\Lambda, q)$, but a rather good approximation to the latter function. It is thus reasonable to expect that this will also be true for the lower bounds $W(S_{(L_z)BC_z}, q)_\ell$ for the slabs S_{L_z} of the simple cubic lattice considered here, of infinite extent in the x and y directions and of thickness L_z in the z direction.

From ingredients given in Ref. [3], we have calculated a large- q expansion of the $\overline{W}(\text{sc}, q)$ for the simple cubic (sc) lattice and obtain

$$\overline{W}(\text{sc}, q) = 1 + 3y^3 + 22y^5 + 31y^6 + O(y^7) . \quad (3.26)$$

In Table (3.1) we list the corresponding values of $W(\text{sc}, q)$ obtained from this large- q series, denoted $W(\text{sc}, q)_{\text{ser.}}$, for $q \geq 4$. We also list estimates of $W(\text{sc}, q)$, denoted $W(\text{sc}, q)_{MC}$, for $4 \leq q \leq 6$ from the Monte Carlo calculations in Ref. [28]. One sees that the approximate values obtained from the large- q series are close to the estimates from Monte Carlo simulations even for q values as low as $q = 4$.

The coordination number for the S_{2_F} slab of the simple cubic lattice (of infinite extent in the x and y directions) is $\kappa(S_{2_F}) = 5$. We thus analyze the reduced function $\overline{W}(S_2, q)_\ell = W(S_2, q)_\ell / [q(1 - q^{-1})^{5/2}]$. This has the large- q (small- y) expansion

$$\overline{W}(S_2, q)_\ell = 1 + 2y^3 + 2y^5 + 9y^6 + O(y^7) . \quad (3.27)$$

As this shows, $\overline{W}(S_2, q)_\ell$ provides an interpolation between $\overline{W}(\text{sq}, q)$ and $\overline{W}(\text{sc}, q)$; for example, the coefficient of the y^3 term is 1 for $\Lambda = \text{sq}$, 2 for $\Lambda = S_2$, and 3 for $\Lambda = \text{sc}$. Furthermore, the coefficient of the y^5 term is 0 for $\Lambda = \text{sq}$, 2 for $\Lambda = S_2$, and 22 for $\Lambda = \text{sc}$. This is in agreement with the fact that the exact functions $W(S_{(L_z)_F}, q)$ interpolate between $W(\text{sq}, q)$ and $W(\text{sc}, q)$ as L_z increases from 1 to ∞ [58] and the expectation, as discussed above, that

$W(S_{(L_z)_F}, q)_\ell$ should be close to $W(S_{(L_z)_F}, q)$.

3.4 Results for Slabs of Thickness $L_z = 3, 4$ with FBC_z

For the slab of the simple cubic lattice with thickness $L_z = 3$ and FBC_z , denoted S_{3_F} , the transverse slice is the graph $\text{sq}[3_F \times (L_y)_{\text{BC}y}]$. The chromatic polynomials $P(\text{sq}[3_F \times (L_y)_F], q)$, $P(\text{sq}[3_F \times (L_y)_P], q)$, and $P(\text{sq}[3_F \times (L_y)_{TP}], q)$ (where TP denotes twisted periodic, i.e., Möbius BC) were computed for arbitrary L_y in Refs. [46], [63], [65] and [48], respectively, and the maximal λ was shown to be the same for all of these boundary conditions. The other input that is needed to obtain the lower bound in Eq. (3.14) is the maximal λ for the chromatic polynomial of the $\text{sc}[2_F \times 3_F \times L_y]$ tube graph, i.e., $\lambda_{\text{tube}(3_F), \text{max}}$. The relevant transfer matrix that determines the chromatic polynomial for this tube graph was given with Ref. [47]. Because it is 13×13 dimensional, one cannot solve the corresponding characteristic polynomial analytically to obtain $\lambda_{\text{tube}(3_F), \text{max}}$ for general q . However, one can calculate $\lambda_{\text{tube}(3_F), \text{max}}$ numerically, and we have done this. Combining these results with Eqs. (A2) and (A2) in the Appendix of [68], we then evaluate the lower bound $W(S_{3_F}, q)_\ell$ by evaluating the $L_z = 3$ special case of (3.14).

For the slab of the simple cubic lattice with thickness $L_z = 4$ and FBC_z , S_{4_F} , the transverse slice is the graph $\text{sq}[4_F \times (L_y)_{\text{BC}y}]$. Here the maximal $\lambda_{\text{ts}(4_F), \text{max}}$ is the solution of the cubic equation Eq. (A5) given in the Appendix of [68]. One also needs the maximal λ for the chromatic polynomial of the $\text{sc}[2_F \times 4_F \times L_y]$ tube graph, i.e., $\lambda_{\text{tube}(4_F), \text{max}}$. The relevant (136×136 dimensional) transfer matrix for this tube graph was calculated for Ref. [47], and we have used this to compute $\lambda_{\text{tube}(4_F), \text{max}}$ numerically. We then obtain the lower bound $W(S_{4_F}, q)_\ell$ from the $L_z = 4$ special case of Eq. (3.14). The results for $W(S_{3_F}, q)_\ell$ and $W(S_{4_F}, q)_\ell$ are listed in Table (3.1).

3.5 Result for Slab of Thickness $L_z = 3$ with PBC_z

It is also of interest to obtain a lower bound for W for a slab with periodic boundary conditions in the z direction, since these minimize finite-volume effects. For this purpose we consider the slab of the simple cubic lattice with thickness $L_z = 3$ and PBC_z , S_{3_P} . In this case the transverse slice is the graph $\text{sq}[3_P \times (L_y)_{\text{BC}y}]$. For FBC_y the chromatic polynomial involves only one λ ,

and this is also the maximal λ for PBC_y and TPBC_y [11], viz.,

$$\lambda_{ts(3P),max} = q^3 - 6q^2 + 14q - 13 . \quad (3.28)$$

One then needs $\lambda_{tube(3P),max}$. The relevant (4×4 dimensional) transfer matrix for this tube graph was calculated for Ref. [47], and we have used this to compute $\lambda_{tube(3P),max}$ numerically. The results for $W(S_{3P}, q)$ are given in Table (3.1).

3.6 Discussion

Since the slabs of infinite extent in the x and y directions and of finite thickness L_z geometrically interpolate between the square and simple cubic lattices, it follows that the resultant W functions for these slabs interpolate between $W(\text{sq}, q)$ and $W(\text{sc}, q)$ [58]. Given that it was shown previously that the lower bounds $W(\Lambda, q)_\ell$ obtained by the coloring matrix method are quite close to the actual values of the respective $W(\Lambda, q)$ for a number of two-dimensional lattices, this is also expected to be true for the $W(S_{(L_z)BC_z}, q)_\ell$ bounds. We have shown above how $W(S_2, q)_\ell$ interpolates between $W(\text{sq}, q)$ and $W(\text{sc}, q)$ via a comparison of the large- q series expansions for these three functions. Table (3.1) provides a further numerical comparison for $W(S_{3F}, q)_\ell$, $W(S_{4F}, q)_\ell$, and $W(S_{3P}, q)_\ell$ with $W(\text{sq}, q)$ and $W(\text{sc}, q)$, the latter being determined to reasonably good accuracy from large- q series expansions and, where available, Monte Carlo measurements. As noted, the lower end of the range of q values for the comparison is chosen as $q = 4$ in view of the use of large- q series.

For sections of lattices, and, more generally, graphs that are not κ -regular, one can define an effective vertex degree (coordination number) as [57]

$$\kappa_{eff} = \frac{2e(G)}{n(G)} . \quad (3.29)$$

For $3 \leq L_z < \infty$, the slab of the simple cubic lattice (of infinite extent in the x and y directions) with FBC_z is not κ -regular, but has the effective coordination number

$$\kappa_{eff}(S_{(L_z)F}) = 2 \left(3 - \frac{1}{L_z} \right) . \quad (3.30)$$

We observe that for the q values considered in Table (3.1), $W(\text{sq}, q) > W(S_2, q)_\ell > W(S_{3F}, q)_\ell > W(S_{4F}, q)_\ell > W(\text{sc}, q)$.

The fact that for fixed q , the exact function $W(S_{(L_z)F}, q)$ is a non-increasing function of L_z , and, for $q > 2$, a monotonically decreasing function of L_z ,

follows from a theorem proved in Ref. [58]. To the extent that the lower bounds $W(S_{(L_z)_F}, q)_\ell$ lie close to the actual values of $W(S_{(L_z)_F}, q)$, it is understandable that they also exhibit the same strict monotonicity. As was noted in Ref. [58], the reason for the monotonicity of the exact values is that the number of proper q -colorings per vertex of a lattice graph is more highly constrained as one increases the effective coordination number of the lattice section. (This is also evident in Fig. 5 of [52].) In the present case, the monotonicity can be seen as a result of the fact that the effective coordination number increases monotonically as a function of L_z .

The use of periodic boundary conditions in the z direction minimizes finite-size effects, so that for a given L_z , $W(S_{(L_z)_P}, q)$ would be expected to be closer to $W(\text{sc}, q)$ than $W(S_{(L_z)_F}, q)$ [58]. Again, to the extent that the lower bounds are close to the actual W functions for these respective slabs, one would expect $W(S_{(L_z)_P}, q)_\ell$ to be closer than $W(S_{(L_z)_F}, q)_\ell$ to $W(\text{sc}, q)$. Our results agree with this expectation. In contrast to $W(S_{(L_z)_F}, q)$, $W(S_{(L_z)_P}, q)$ is not, in general, a non-increasing function of L_z , as was discussed in general in [58] (see Fig. 1 therein). Thus, values of $W(S_{(L_z)_P}, q)$, and hence, *a fortiori*, $W(S_{(L_z)_P}, q)_\ell$, may actually lie slightly below those for $W(\text{sc}, q)$, as is evident for the $W(S_{3P}, q)_\ell$ entries in Table (3.1).

Table 3.1: Comparison of lower bounds $W(S_{(L_z)BC_z}, q)_\ell$ for $(L_z)BC_z = 2_F = 2_P, 3_F, 3_P, 4_F, 3_P$ with approximate values of $W(\Lambda, q)$ for the square (sq) and simple cubic (sc) lattices Λ , as determined from large- q series expansions, denoted $W(\Lambda, q)_{ser.}$ and, where available, Monte Carlo simulations, denoted $W(\Lambda, q)_{MC}$. We also list $W(sq, q)_\ell$ for reference. See text for further details.

q	$W(sq, q)_{MC}$	$W(sq, q)_{ser.}$	$W(sq, q)_\ell$	$W(S_{2_F}, q)_\ell$	$W(S_{3_F}, q)_\ell$	$W(S_{4_F}, q)_\ell$	$W(sc, q)_{ser.}$	$W(sc, q)_{MC}$	$W(S_{3_P}, q)_\ell$
4	2.34	2.34	2.33	2.13	2.07	2.04	2.06	1.9	1.78
5	3.25	3.25	3.25	2.96	2.875	2.83	2.75	2.7	2.62
6	4.20	4.20	4.20	3.87	3.765	3.71	3.58	3.6	3.51
7	5.17	5.17	5.17	4.81	4.69	4.64	4.48	—	4.43
8	6.14	6.14	6.14	5.76	5.64	5.58	5.41	—	5.37
9	7.125	7.125	7.125	6.73	6.605	6.54	6.36	—	6.325
10	8.11	8.11	8.11	7.71	7.58	7.51	7.32	—	7.29
100	—	98.0	98.0	97.5	97.4	97.3	97.0	—	97.0

Chapter 4

Ground State Entropy of the Potts Antiferromagnet: II. Exact Calculations of Homeomorphic Expansions of Kagomé Lattice Strips

4.1 Homeomorphic Expansions of Kagomé Lattice Strips

For the ground state degeneracy per site W , a particular question of interest is how W changes when one inserts new vertices on certain bonds of the graph. In mathematical graph theory, this insertion process is called a homeomorphic expansion of the graph (and the opposite process, removing degree-2 vertices from bonds of a graph, is called a homeomorphic reduction). It is useful to answer this question in simple cases such as lattice strips, since one can get exact explicit analytic results for these cases [59],[64].

Continuing the above line of study by Shrock and Tsai [59] and [64], in this chapter we report exact calculations of the chromatic polynomial and resultant ground state degeneracy per site of the q -state Potts antiferromagnet on lattice strips that are homeomorphic expansions of a strip graph of the kagomé lattice. These results were published in Ref. [69]. Our findings and their comparison with analogous exact calculations for the kagomé strips without homeomorphic expansion in [46], [63], [65], and with homeomorphic expansions of square-lattice ladder graphs in [64] add to our understanding of the effect of homeomorphic expansions on the per-site ground state degeneracy

and entropy of the Potts antiferromagnet.

The family of homeomorphically expanded graphs of the kagomé lattice strip that we consider are denoted $[H_k(kag)]_{m,BC}$, where H , kag , and BC stand for homeomorphic expansion, kagomé, and longitudinal boundary conditions, free (f) or cyclic (c). A member of this family is defined as follows. We start with a minimal-width kagomé strip graph, a portion of which is shown in Fig. (4.1), comprised of m subgraphs, each of which consists of a hexagon with its two adjoining triangles. We then insert k vertices on each longitudinal edge of a hexagon in this original kagomé strip graph. Thus, the graph $[H_k(kag)]_{m,BC}$ is a strip of m subgraphs each of which consists of two triangles and a p -gon with

$$p = 6 + 2k . \quad (4.1)$$

The graph $[H_1(kag)]_{m,BC}$ involves subgraphs with two triangles and an octagon, and so forth for higher values of k . The kagomé strip itself is the case $k = 0$. The chromatic number of the free and cyclic kagomé strips is $\chi = 3$, and this remains true for the homeomorphic expansions $[H_k(kag)]_{m,BC}$:

$$\chi([H_k(kag)]_{m,f}) = \chi([H_k(kag)]_{m,c}) = 3 . \quad (4.2)$$

We shall sometimes use the abbreviations $kag_{k,m,BC} \equiv [H_k(kag)]_{m,BC}$ with $BC = f$ or $BC = c$ and, for the family as a whole, suppressing the m index, $kag_{k,BC} \equiv [H_k(kag)]_{BC}$. For the (minimal-width) Kagomé lattice strip with free and periodic boundary conditions, and its $k = 1$ homeomorphic expansion, see Fig. (4.1) as illustrations.

For the relevant range, $q \geq 3$, of interest here, the $W(\{G\}, q)$ functions computed via the infinite-length limits of the $[H_k(kag)]_{m,BC}$ strips with free and cyclic (and Möbius) longitudinal boundary conditions (BC) are all the same. Since the calculation is easiest if one uses strip graphs with free longitudinal boundary conditions, we shall do this. It is also of interest to calculate the chromatic polynomials for the corresponding strip graphs with cyclic boundary conditions and we will do this. The $m \rightarrow \infty$ limits for these families of homeomorphically expanded kagomé strips will be denoted $\{[H_k(kag)]_{BC}\}$ and, for the W function, which is independent of the boundary conditions, $W(\{H_k(kag)\}, q)$.

As noted above, our exact results for the infinite-length homeomorphically expanded kagomé strip graphs complement other methods of studying W functions on lattices, such as rigorous bounds, large- q series, and Monte Carlo measurements [9], [55], [57], [68]. Other homeomorphic expansions of this kagomé strip graph are also of interest, e.g., expansions in which additional vertices are added to edges of the triangles, but here we shall restrict

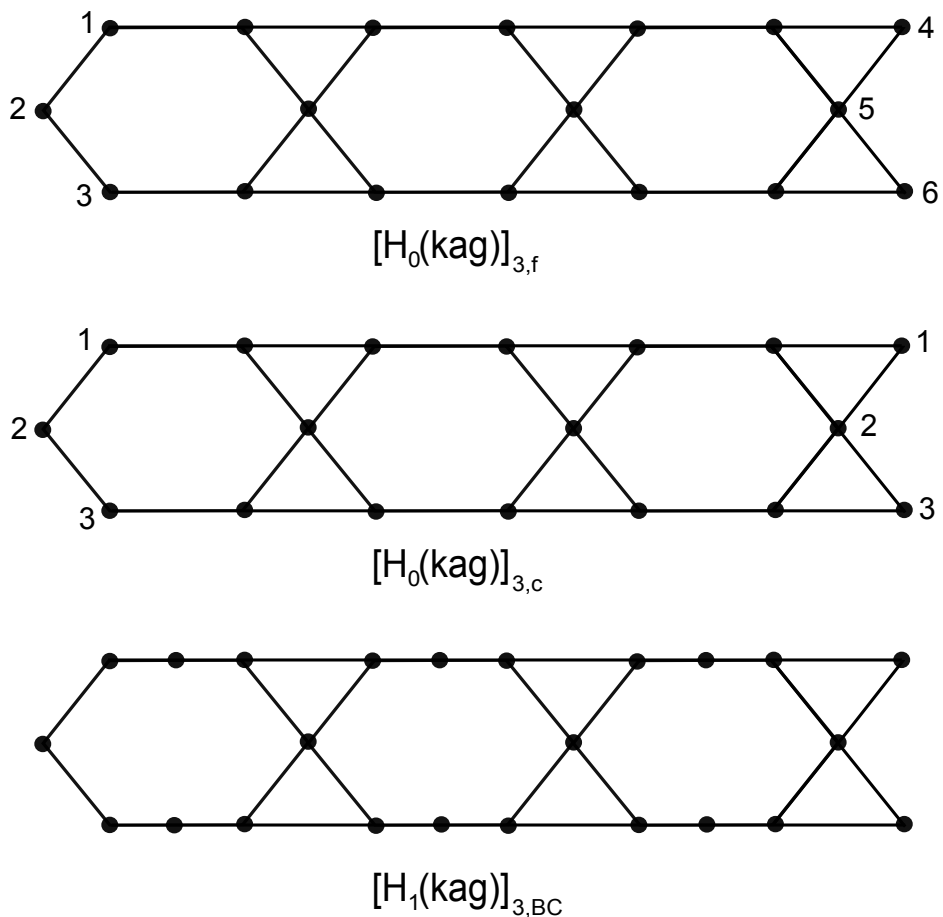


Figure 4.1: The minimal-width Kagomé lattice strip with free ($[H_0(kag)]_{3,f}$) and periodic ($[H_0(kag)]_{3,c}$) boundary conditions, and its $k = 1$ homeomorphic expansion ($[H_1(kag)]_{3,BC}$). All strips illustrated here are comprised of $m = 3$ subgraphs.

ourselves to studying the specific homeomorphic expansion defined above. In passing, we mention that chromatic polynomials of homeomorphic expansions of other types of graphs have been studied in, e.g., Refs. [59], [29].

4.2 Calculational Method

The chromatic polynomial $P(G, q)$ can be calculated in several ways. One is via the deletion-contraction relation (2.32). $P(G, q)$ can also be determined via the cluster formula by setting $v = -1$ in Eq. (1.5):

$$P(G, q) = \sum_{G' \subseteq G} q^{k(G')} (-1)^{e(G')} , \quad (4.3)$$

where we recall from previous chapters that $k(G')$ denotes the number of connected components in G' (not to be confused with the homeomorphic expansion parameter k ; the meaning should be clear from context).

The numbers of vertices and edges on the $[H_k(kag)]_{m,f}$ and $[H_k(kag)]_{m,c}$ graphs are

$$n([H_k(kag)]_{m,c}) = n([H_k(kag)]_{m,f}) - 3 = (5 + 2k)m \quad (4.4)$$

and

$$e([H_k(kag)]_{m,c}) = e([H_k(kag)]_{m,f}) - 2 = (8 + 2k)m . \quad (4.5)$$

(For the cyclic strip with $m = 1$ some of these are double edges; this does not affect the chromatic polynomial.) The graph $[H_k(kag)]_{m,c}$ has vertices with degrees 3, 4, and, for $k \geq 1$, also 2. For reference, the infinite 2D kagomé lattice has vertices of uniform degree 4. Defining, as in Ref. [57], an effective vertex degree,

$$\Delta_{eff} \equiv \lim_{n \rightarrow \infty} \frac{2e(G)}{n(G)} , \quad (4.6)$$

we have

$$\Delta_{eff} = \frac{4(4+k)}{5+2k} \quad \text{for } \{H_k(kag)\} . \quad (4.7)$$

Because $\chi([H_k(kag)]_{m,f}) = 3$, it follows that $P([H_k(kag)]_{m,BC}, q) = 0$ for $q = 0, 1, 2$ for free or cyclic BC. Since $P([H_k(kag)]_{m,BC}, q)$ is a polynomial, this implies that

$$P([H_k(kag)]_{m,BC}, q) \quad \text{contains the factor} \quad q(q-1)(q-2) . \quad (4.8)$$

4.3 Strips with Free Longitudinal Boundary Conditions

For the family $[H_k(kag)]_f$ of strip graphs $[H_k(kag)]_{m,f}$, it is convenient to use a generating function formalism, as before [46], [59]. For arbitrary k , this generating function is

$$\Gamma([H_k(kag)]_f, q, x) = \sum_{m=0}^{\infty} P([H_k(kag)]_{m+1,f}, q) x^m . \quad (4.9)$$

The generating function is a rational function in x and q of the form

$$\Gamma([H_k(kag)]_f, q, x) = \frac{a_{k,0} + a_{k,1}x}{1 + b_{k,1}x + b_{k,2}x^2} . \quad (4.10)$$

We write the denominator as

$$1 + b_{k,1}x + b_{k,2}x^2 = \prod_{j=1}^2 (1 - \lambda_{kag_k,0,j} x) . \quad (4.11)$$

By means of an iterative use of the deletion-contraction relation and induction on the homeomorphic expansion parameter k , we have calculated $\Gamma([H_k(kag)]_f, q, x)$ and hence $P([H_k(kag)]_{m,f}, q)$ for arbitrary k and q .

Recall that the chromatic polynomial of the circuit graph C_n is $P(C_n, q) = (q-1)^n + (q-1)(-1)^n$. Since this has a factor $q(q-1)$, it is convenient to define

$$D_n = \frac{P(C_n, q)}{q(q-1)} = \sum_{s=0}^{n-2} (-1)^s \binom{n-1}{s} q^{n-2-s} \quad (4.12)$$

so that $D_2 = 1$, $D_3 = q-2$, $D_4 = q^2 - 3q + 3$, etc. (Where it appears, we shall write D_3 simply as $q-2$.) We find (with $p = 6 + 2k$ as given in Eq. (4.1))

$$a_{k,0} = q(q-1)(q-2)^2 D_p , \quad (4.13)$$

$$a_{k,1} = -q(q-1)^{5+2k} (q-2)^3 , \quad (4.14)$$

$$b_{k,1} = -(q-2)(D_p - D_{p-1} + 1) , \quad (4.15)$$

and

$$b_{k,2} = (q-1)^{3+2k} (q-2)^3 . \quad (4.16)$$

It is readily checked that for the special case $k = 0$, these results reduce to the generating function for the kagomé strip given in Ref. [46].

Substituting the results for $b_{k,1}$ and $b_{k,2}$ in Eq. (4.11) and solving for $\lambda_{kag_k,0,j}$, we find

$$\lambda_{kag_k,0,j} = \frac{1}{2}(q-2)(D_p - D_{p-1} + 1 \pm \sqrt{R_{kkd0}}), \quad (4.17)$$

where $p = 6 + 2k$ as given in Eq. (4.1), $j = 1, 2$ correspond to the \pm signs, and

$$R_{kkd0} = (D_p - D_{p-1} + 1)^2 - 4(q-1)^{3+2k}(q-2). \quad (4.18)$$

Using the general methods of [59] for expressing the chromatic polynomial in terms of the coefficients in the generating function, we find that $P([H_k(kag)]_{m,f}, q)$ is given by

$$P([H_k(kag)]_{m,f}, q) = \frac{(a_{k,0}\lambda_{kag_k,0,1} + a_{k,1})}{(\lambda_{kag_k,0,1} - \lambda_{kag_k,0,2})} (\lambda_{kag_k,0,1})^{m-1} + \frac{(a_{k,0}\lambda_{kag_k,0,2} + a_{k,1})}{(\lambda_{kag_k,0,2} - \lambda_{kag_k,0,1})} (\lambda_{kag_k,0,2})^{m-1}. \quad (4.19)$$

(Note that this is symmetric under the interchange $\lambda_{kag_k,0,1} \leftrightarrow \lambda_{kag_k,0,2}$.) For the relevant range of q , $\lambda_{kag_k,0,1} > \lambda_{kag_k,0,2}$. Therefore, in the limit $m \rightarrow \infty$, the ground state degeneracy per vertex of this family of lattice strips is

$$W(\{H_k(kag)\}, q) = (\lambda_{kag_k,0,1})^{\frac{1}{5+2k}}, \quad (4.20)$$

where the $\lambda_{kag_k,0,j}$ for $j = 1, 2$ were given in Eq. (4.17). This and Eq. (4.19) are the main results of the present chapter.

From the analytic result (4.20), there follow two monotonicity properties: (i) for a given k , $W(\{H_k(kag)\}, q)$ is a monotonically increasing function of q in the range $q \geq \chi = 3$; and (ii) for a given $q \geq 3$, $W(\{H_k(kag)\}, q)$ is a monotonically increasing function of k for $k \geq 0$. The fact that $W(\{G\}, q)$ is an increasing function of q for $q \geq \chi(G)$ is quite general and is a consequence of the greater freedom in performing proper q -colorings of G for larger q . Property (ii) can be understood as a result of the fact that a proper q -coloring of a graph G involves a constraint on the coloring of adjacent vertices of G , and this, in turn, gives rise to a constraint from circuits in G . Since the minimum length of a circuit is the girth, increasing the girth tends to reduce the severity of this latter constraint. (Here, the girth of a graph G is defined as the number of edges that one traverses in a minimum-length circuit on G .) Although the girth of $[H_k(kag)]_{m,BC}$ (ignoring the double edges that occur for $m = 1$ with cyclic BC) is equal to 3, independent of k , the girth of the polygons with $p = 6 + 2k$ sides in the strip does increase with k . Hence, for a fixed $q \geq \chi(G) = 3$, this increase in the girth of the p -gons increases the possibilities for proper q -colorings, and this, in turn, increases the W function. These monotonicity properties are

Table 4.1: Values of $W(\{kag\}, q) \equiv W(\{H_0(kag)\}, q)$, $W(\{H_1(kag)\}, q)$, and $W(\{H_2(kag)\}, q)$ for $3 \leq q \leq 10$. For comparison, we also show $W(\{sq\}, q) \equiv W(\{H_0(sq)\}, q)$, $W(\{H_1(sq)\}, q)$, and $W(\{H_2(sq)\}, q)$ for the square-lattice ladder strips. To save space, we omit the argument q in these W functions below. See text for further details

q	$W(\{kag\})$	$W(\{H_1(kag)\})$	$W(\{H_2(kag)\})$	$W(\{sq\})$	$W(\{H_1(sq)\})$	$W(\{H_2(sq)\})$
3	1.409	1.550	1.639	1.732	1.821	1.872
4	2.410	2.564	2.655	2.646	2.795	2.860
5	3.410	3.569	3.660	3.606	3.784	3.854
6	4.410	4.571	4.663	4.583	4.778	4.850
7	5.409	5.571	5.664	5.568	5.773	5.848
8	6.408	6.572	6.665	6.557	6.770	6.846
9	7.407	7.572	7.665	7.550	7.768	7.844
10	8.407	8.572	8.665	8.544	8.766	8.843

reflected in the large- q Taylor series expansions of the W functions. As $q \rightarrow \infty$, the leading terms of the large- q series expansions of $q^{-1}W(\{H_k(kag)\}, q)$ are of the form $q^{-1}W(\{H_k(kag)\}, q) = 1 - \alpha_k/q + \dots$, where \dots represents higher order terms in $1/q$, and the coefficients for $k = 0, 1, 2$ are $\alpha_0 = 8/5$, $\alpha_1 = 10/7$, and $\alpha_2 = 4/3$, so that $\alpha_0 > \alpha_1 > \alpha_2$, and so forth for higher k .

In Table (4.1) we list values of $W(\{kag\}, q) \equiv W(\{H_0(kag)\}, q)$, $W(\{H_1(kag)\}, q)$, and $W(\{H_2(kag)\}, q)$ for $3 \leq q \leq 10$. The two general monotonicity properties stated above are evident in the table. As is also evident, $W(\{H_k(kag)\})$ is an approximately linear function of q for values of q moderately above the chromatic number, $\chi = 3$.

It is of interest to compare these results for the ground state degeneracy and entropy on infinite-length limits of homeomorphic expansions of the kagomé strip with those obtained for homeomorphic expansions of the square lattice ladder strip in Ref. [64]. The strip graphs considered in Ref. [64] were constructed by starting with a free or cyclic (or Möbius) square-ladder strip of m squares and adding $k - 2$ vertices to each longitudinal edge, with $k \geq 2$. Thus, the parameter $k - 2$ of Ref. [64] corresponds to the parameter k in our present notation, and the resultant strip is (with our present notational convention for k) $[H_k(sq)]_{m,BC}$. This graph is thus a homopolygonal strip of p' -gons, where $p' = 2k + 4$. We denote the $m \rightarrow \infty$ limit of this strip as $\{[H_k(sq)]_{BC}\}$. For $\{[H_k(sq)]_c\}$, $q_c = 2$ (independent of k) and, for $q \geq q_c$, W is the same for the free and cyclic (and Möbius) longitudinal boundary conditions; $W(\{[H_k(sq)]_f\}, q) = W(\{[H_k(sq)]_c\}, q) \equiv W(\{H_k(sq)\}, q)$. Converting

the result of Ref. [64] to our present notation by the replacement $k - 2 \rightarrow k$, one has

$$W(\{H_k(sq)\}, q) = (D_{2k+4})^{\frac{1}{2k+2}} . \quad (4.21)$$

In general, for even $p' = 2k+4$, (i) $D_{p'} = 1$ if $q = 2$ and hence $W(\{H_k(sq)\}, 2) = 1$; (ii) $D_{p'}$ is a monotonically increasing function of q , and hence so is $W(\{H_k(sq)\}, q)$; (iii) for a given $q > 2$, $W(\{H_k(sq)\}, q)$ is a monotonically increasing function of k . This monotonic increase as a function of the homeomorphic expansion parameter k is understandable in a manner analogous to that explained above, with the difference that whereas the girth of the $[H_k(kag)]_{m,BC}$ strip is 3, independent of k , the girth of $[H_k(sq)]_{m,BC}$ is p' .

The comparison of the exact analytic result (4.21) for $W(\{H_k(sq)\}, q)$ from Ref. [64] for homeomorphic expansions of the square-lattice ladder strip with our result (4.20) for homeomorphic expansions of the kagomé strip yields another inequality, namely that for $q \geq 3$ (so that one can perform a proper q -coloring of the $[H_k(kag)]_{m,BC}$ strip),

$$W(\{H_k(kag)\}, q) < W(\{H_k(sq)\}, q) . \quad (4.22)$$

This inequality can be understood heuristically as follows. As before, it will suffice to use free longitudinal boundary conditions and hence the graphs $[H_k(sq)]_{m,f}$ and $[H_k(kag)]_{m,f}$ for the $m \rightarrow \infty$ limits that define the respective W functions. Roughly speaking, for a given k , the larger $q - \chi(G)$ is for a given graph G , the more freedom there is in performing proper q -colorings of this graph. Now, for any k , the chromatic number χ is larger (namely, 3) for $[H_k(kag)]_{m,f}$ than for $[H_k(sq)]_{m,f}$ (namely, 2). Hence, for q greater than the larger of the two chromatic numbers on these strips, $q - \chi(G)$ is larger for the homeomorphic expansion of the square strip than for the homeomorphic expansion of the kagomé strip. The resultant greater freedom in performing proper q -colorings of $[H_k(sq)]_{m,f}$ than of $[H_k(kag)]_{m,f}$ makes the inequality (4.22) understandable.

4.4 Cyclic Strip $[H_k(kag)]_{m,c}$

Using similar methods, we have calculated the chromatic polynomial for the homeomorphically expanded cyclic kagomé strip, $P([H_k(kag)]_{m,c}, q)$. We find that (using the abbreviation $kag_k = [H_k(kag)]_c$ here)

$$P([H_k(kag)]_{m,c}, q) = \sum_{d=0}^2 c^{(d)} \sum_{j=1}^{n_P(kag_k, d)} (\lambda_{kag_k, d, j})^m \quad (4.23)$$

where $c^{(0)} = 1$, $c^{(1)} = q - 1$, and $c^{(2)} = q^2 - 3q + 1$, and

$$n_P(kag_k, 0) = 2, \quad n_P(kag_k, 1) = 3, \quad n_P(kag_k, 2) = 1, \quad (4.24)$$

independent of k . Hence, the total number of λ terms that enter in Eq. (4.23) is

$$N_{P,[H_k(kag)]_c,\lambda} = 6, \quad (4.25)$$

independent of k . Our structural result (4.23) showing the role that the coefficients $c^{(d)}$ play for these homeomorphic expansions of a cyclic kagomé strip graph generalizes what had been established earlier, namely that they occur for the corresponding homeomorphic expansions of a square-lattice strip graph [64] and for (non-homeomorphically expanded) cyclic strips of the square, triangular [21], and honeycomb [22] strip graphs, with the maximal d corresponding to the width, L_y . Although it is not needed here, we recall the general formula

$$c^{(d)} = \sum_{s=0}^d (-1)^s \binom{2d-s}{s} q^{d-s}. \quad (4.26)$$

We give the λ terms that enter in Eq. (4.23) next. As is true in general for these recursive strip graphs [24], the λ 's that occur for the strip with free longitudinal boundary conditions, $\lambda_{kag_k,0,j}$ (given in Eq. (4.17)), are the same as the λ 's with $d = 0$ in Eq. (4.23) for the cyclic strip. Note that

$$\lambda_{kag_k,0,1} \lambda_{kag_k,0,2} = b_{k,2} = (q-1)^{3+2k} (q-2)^3. \quad (4.27)$$

At $q = 0$,

$$(\lambda_{kag_k,0,j})_{q=0} = -2(p-1 \pm \sqrt{p^2 - 2p - 1}). \quad (4.28)$$

For the λ 's with $d = 1$, we find, first,

$$\lambda_{kag_k,1,1} = (-1)^k (q-1)^{1+k} (q-2)^2. \quad (4.29)$$

Let us define

$$S_{k,1} = q - 4 + (-1)^k (q-2)(D_{k+4} - 2D_{k+3} + D_{k+2}) \quad (4.30)$$

and

$$P_{k,1} = (-1)^k (q-1)^{1+k} (q-2)^3. \quad (4.31)$$

Then

$$\lambda_{kag_k,1,j} = \frac{1}{2} (S_{k,1} \pm \sqrt{S_{k,1}^2 - 4P_{k,1}}), \quad (4.32)$$

where $j = 2, 3$ corresponds to the \pm sign. Thus,

$$\lambda_{kag_k,1,2}\lambda_{kag_k,1,3} = P_{k,1} \quad (4.33)$$

so that

$$\prod_{j=1}^3 \lambda_{kag_k,1,j} = (q-1)^{2(1+k)}(q-2)^5. \quad (4.34)$$

For the λ with $d = 2$, we calculate

$$\lambda_{kag_k,2} = q - 4. \quad (4.35)$$

independent of k . It is easily checked that the $k = 0$ special case of these general results agrees with the calculation of the chromatic polynomial for the cyclic kagomé strip in [63].

4.5 Locus \mathcal{B}

Via relation Eq. (4.3), one can generalize q from positive integers to real and complex numbers, thus it follows that $P(G, q)$ can be written in terms of its zeros (called chromatic zeros) q_{zj} , $j = 1, \dots, n$, as $P(G, q) = \prod_{j=1}^n (q - q_{zj})$. These zeros are a natural topic for study in the context of chromatic polynomials. For a strip graph such as the ones considered here, as $m \rightarrow \infty$, chromatic zeros merge to form an asymptotic accumulation set (locus) consisting of various curves. As in our earlier work, we denote this locus as \mathcal{B} . This locus is the solution to the equation of degeneracy in magnitude of the dominant λ 's (i.e., the λ 's with the largest absolute value in the complex q plane [6]).

4.5.1 Case of Free Longitudinal Boundary Conditions

For the $m \rightarrow \infty$ limit of the free strip $[H_k(kag)]_{m,f}$, the locus \mathcal{B} involves a set of curves forming arcs. For the kagomé strip itself (i.e., the case $k = 0$), these were shown in Fig. 7 of Ref. [46], and we find a similar arc-like structure for $k \geq 1$. The arc endpoints occur at the zeros of the polynomial R_{kkd0} given in Eq. (4.18). For example, for the actual kagomé strip itself, this is a polynomial of degree 8, with zeros at

$$q_1, q_1^* = 0.41 \pm 0.955i,$$

$$q_2, q_2^* = 1.18 \pm 1.14i,$$

$$\begin{aligned}
q_3, q_3^* &= 1.80 \pm 1.19i, \\
q_4, q_4^* &= 2.62 \pm 0.15i .
\end{aligned}
\tag{4.36}$$

In this case \mathcal{B} consists of four arcs, forming two complex-conjugate pairs, namely an arc connecting q_1 and q_2 , an arc connecting q_3 and q_4 , and the complex-conjugate arcs. For general k , R_{kkd0} is a polynomial in q of degree

$$\deg(R_{kkd0}) = 8 + 4k . \tag{4.37}$$

For this case of of $m \rightarrow \infty$ limit of $[H_k(kag)]_{m,f}$ with general k , the locus \mathcal{B} consists of $4 + 2k$ arcs consisting of $2 + k$ complex-conjugate pairs, with endpoints at the $8 + 4k$ zeros of R_{kkd0} .

4.5.2 Case of Cyclic Longitudinal Boundary Conditions

The analysis of the locus \mathcal{B} is more complicated for the $m \rightarrow \infty$ limit of the cyclic $[H_k(kag)]_{m,c}$ strips because of the presence of more λ 's, namely six in all. Again, the locus is determined by the equality in magnitude of two dominant λ 's. For the infinite-length limit of a given family of graphs $\{G\}$, the maximal point at which \mathcal{B} crosses the real axis is denoted $q_c(\{G\})$. As our previous work showed, for families of graphs with free longitudinal boundary conditions, \mathcal{B} does not necessarily cross the real axis. However, for families of graphs with cyclic boundary conditions, \mathcal{B} always crosses the real axis, so a q_c is defined. For the $m \rightarrow \infty$ limit of the $[H_k(kag)]_{m,c}$ graphs, considered here, denoted as $\{[H_k(kag)]_c\}$, q_c is determined by the equality of the dominant λ 's

$$|\lambda_{kagk,0,1}| = |\lambda_{kagk,2}| = |q - 4| . \tag{4.38}$$

For the infinite-length limit of the cyclic kagomé strip, $\{kag_c\}$ [63],

$$q_c(\{kag_c\}) \simeq 2.62 . \tag{4.39}$$

In the thermodynamic limit of the 2D kagomé lattice, previous work suggests that $q_c(kag, 2D) = 3$ [85]. Hence, one sees that the q_c value for this kagomé strip is already within about 13 % of the value for the infinite 2D lattice. For the $[H_k(kag)]_{m,c}$ graphs, as k increases, the effect of the p -gons with $p = 6 + 2k$ becomes greater, so one expects that q_c will decrease as k increases, since $q_c = 2$ for the $m \rightarrow \infty$ limit of the circuit graph C_m . Our exact results confirm this expectation. For example, for the infinite-length limits of the $[H_k(kag)]_{m,c}$

strips with $k = 1$, $k = 2$, and $k = 3$, we find

$$q_c(\{[H_1(kag)]_c\}) \simeq 2.52 , \quad (4.40)$$

$$q_c(\{[H_2(kag)]_c\}) \simeq 2.44 , \quad (4.41)$$

and

$$q_c(\{[H_3(kag)]_c\}) \simeq 2.38 . \quad (4.42)$$

The boundary \mathcal{B} crosses the real q axis at $q = 0$, $q = 2$, and $q = q_c$. The degeneracy of λ magnitudes at q_c was given above in Eq. (4.38). At $q = 0$ there is a degeneracy in magnitude between $\lambda_{kag_k,0,1}$ and the dominant $\lambda_{kag_k,1,j}$, $j = 2, 3$. At $q = 2$, there is a degeneracy in magnitude between this dominant $\lambda_{kag_k,1,j}$ and $\lambda_{kag_k,2}$, with both having magnitude equal to 2. There are thus three regions that include parts of the real axis. Region R_1 includes the two semi-infinite line segments $q > q_c$ and $q < 0$ and extends outward infinitely far from the origin. In region R_1 , $\lambda_{kag_k,0,1}$ is the dominant λ (i.e., the one with the largest magnitude). Region R_2 includes the interval $2 \leq q \leq q_c$. In region R_2 , $\lambda_{kag_k,2} = q - 4$ is the dominant λ . Region R_3 includes the real interval $0 \leq q \leq 2$, and in this region, the dominant term is the maximal-magnitude $\lambda_{kag_k,1,j}$ for $j = 2, 3$. Other complex-conjugate bubble phases are also present, as was found in Ref. [64] and [63]. Indeed, as is evident from Fig. 2 of Ref. [63], for the infinite-length strip of the cyclic kagomé lattice itself, the boundary \mathcal{B} encloses two very small complex conjugate phases centered at approximately $q \simeq 2.53 \pm 0.50i$.

Chapter 5

Chromatic Polynomials of Planar Triangulation Graphs: I. The Tutte Upper Bound and One-Parameter Families

5.1 Chromatic Polynomials of Planar Triangulations and the Tutte Upper Bound

In this chapter and the next we present results on chromatic polynomials of planar triangulations. The results in this chapter were published in Ref. [70] and most of those in the next chapter are in press in Ref. [71]. Planar triangulation graphs (abbreviated *PT* or *pt*), denoted G_{pt} , are defined as graphs that can be drawn in a plane without any intersecting edges and have the property that all of their faces are triangles. These are necessarily connected graphs. Tutte proved an interesting upper bound on the absolute value of the chromatic polynomial of a planar triangulation, $P(G_{pt}, q)$ evaluated at a certain value of q , viz., $q = \tau + 1 = (3 + \sqrt{5})/2 = 2.6180339887\dots$, where $\tau = (1 + \sqrt{5})/2$ is the “golden ratio”, satisfying $\tau + 1 = \tau^2$, or equivalently, $\tau^{-1} = \tau - 1$. Tutte’s upper bound is [76] (see also [44]),

$$0 < |P(G_{pt}, \tau + 1)| \leq U(n(G_{pt})) \quad (5.1)$$

where

$$U(n) = \tau^{5-n} = (\tau - 1)^{n-5} . \quad (5.2)$$

Since $\tau - 1 < 1$, the upper bound $U(n)$ decreases exponentially rapidly as a function of n .

For a planar triangulation graph G_{pt} , we define the ratio of the evaluation of its chromatic polynomial at $q = \tau + 1$ to the Tutte upper bound as

$$r(G_{pt}) \equiv \frac{|P(G_{pt}, \tau + 1)|}{U(n(G_{pt}))} \quad (5.3)$$

It is of interest to study this ratio for various planar triangulation graphs. For this purpose, we shall construct infinite recursive families of planar triangulations G_{pt} and show that if these only involve a single power of a polynomial $f_G(q)$, then $r(G_{pt})$ approaches zero exponentially fast as $n \rightarrow \infty$. We also construct infinite recursive families for which $P(G_{pt}, q)$ is a sum of powers and show that for these $r(G_{pt})$ may approach a finite nonzero constant as $n \rightarrow \infty$. The Tutte upper bound is sharp, since it is saturated by the simplest planar triangulation, namely the triangle, K_3 ¹. For this graph,

$$P(K_3, \tau + 1) = \tau + 1 = U(3), \quad \Rightarrow \quad r(K_3) = 1. \quad (5.4)$$

However, for planar triangulations with higher n , the upper bound is realized as a strict inequality. For example, for K_4 ,

$$P(K_4, \tau + 1) = -1, \quad \Rightarrow \quad r(K_4) = \frac{1}{\tau} = \tau - 1 = 0.6180.. \quad (5.5)$$

In connection with the upper bound (5.1), Tutte reported his empirical observation that chromatic polynomials of plane triangulations typically have a real zero quite close to $q = \tau + 1$ and remarked that this property could be related to the fact that they obey his bound [76]-[44]. Although several decades have passed since Tutte's work on this topic, the nature of this relation between the zero of a chromatic polynomial $P(G_{pt}, q)$ near to $q = \tau + 1$ and the upper bound (5.1) remains to be understood. We shall elucidate this connection and generalize the investigation to the study of complex zeros of $P(G_{pt}, q)$.

The chromatic polynomial of a graph G may be computed via the deletion-contraction relation (2.32) or from the cluster formula (4.3), as we recall from the discussion in Sect. (4.2). For a general graph G or family of graphs G_m , the calculation of the chromatic polynomial takes an exponentially long time. Since a triangulation graph G_t (whether planar or not) contains at least one triangle, $P(G_t, q)$ always contains the factor $P(K_3, q) = q(q - 1)(q - 2)$.

¹For the definition and illustration of the complete graph K_n , refer to the discussion in Sect. (2.5). Here we simply remind the reader that for the complete graph K_n , its chromatic polynomial is $P(K_n, q) = \prod_{s=0}^{n-1} (q - s)$, and its chromatic number is $\chi(K_n) = n$.

5.2 General Properties of One-Parameter Families of Planar Triangulations

5.2.1 General

We have constructed and studied various one-parameter families of planar triangulations $G_{pt,m}$ that can be built up in an iterative (recursive) manner [70],[71]. In this section we derive general properties of the chromatic polynomials of these families of planar triangulations. For our families, the number of vertices is linearly related to m ,

$$n(G_{pt,m}) = \alpha m + \beta , \quad (5.6)$$

where α and β are constants that depend on the type of family. We recall the Euler relation $|V(G)| - |E(G)| + |F(G)| = \chi_E = 2$ for a graph G embedded on a surface of genus 0, such as the plane, where χ_E is the Euler characteristic. In general, for a planar graph each of whose faces has p sides, $n(G)$, $e(G)$, and $f(G)$ satisfy the relations $e(G) = p(n(G) - 2)/(p - 2)$ and $f(G) = 2(n(G) - 2)/(p - 2)$. For the case of interest here, namely planar triangulation graphs, where each face is a triangle, it follows that

$$e(G_{pt}) = 3(n(G_{pt}) - 2) \quad (5.7)$$

and

$$f(G_{pt}) = 2(n(G_{pt}) - 2) , \quad (5.8)$$

so that $e(G_{pt}) = (3/2)f(G_{pt})$.

In our present study we will make use of several results that we derived in [70]. First, since $U(n) \rightarrow 0$ as $n \rightarrow \infty$ and since m is proportional to n , it follows that for these families of planar triangulations,

$$\lim_{m \rightarrow \infty} P(G_{pt,m}, \tau + 1) = 0 . \quad (5.9)$$

Second, given the upper bound (5.1) and the fact that $U(n)$ approaches zero exponentially fast as $n \rightarrow \infty$, it follows that

$$P(G_{pt,m}, \tau + 1) \text{ approaches zero exponentially fast as } m \rightarrow \infty. \quad (5.10)$$

We recall two definitions that apply to any graph: (i) the degree $d(v_i)$ of a vertex $v_i \in V$ is the number of edges that connect to it, and (ii) a k -regular graph is a graph for which all vertices have degree k . Since a triangulation graph G_t is not, in general, k -regular, it is useful to define an effective vertex

degree in the limit $|V| \rightarrow \infty$. For this purpose, we introduce, as in our earlier work, the notation $\{G\}$ for the formal limit $n \rightarrow \infty$ of a family of graphs G . We define

$$\begin{aligned} d_{eff}(\{G\}) &= \lim_{|V| \rightarrow \infty} \frac{2|E|}{|V|} \\ &= \lim_{|V| \rightarrow \infty} \frac{\sum_i n_i d_i}{|V|}, \end{aligned} \quad (5.11)$$

where for a given G , n_i denotes the number of vertices with degree d_i and $n(G) \equiv |V|$. Substituting (5.7) in (5.11), we obtain

$$d_{eff}(\{G_{pt}\}) = 6. \quad (5.12)$$

We will use this below, in Sect. (6.12).

5.2.2 Families with $P(G_{pt,m}, q)$ Consisting of a Power of a Single Polynomial

There are several ways of constructing one-parameter families of planar triangulations. One method that we have used is the following, which produces families for which the chromatic polynomial involves a single power of a polynomial in q . Start with a basic graph $G_{pt,1}$, drawn in the usual explicitly planar manner. The outer edges of this graph clearly form a triangle, K_3 . Next pick an interior triangle in $G_{pt,1}$ and place a copy of $G_{pt,1}$ in this triangle so that the intersection of the resultant graph with the original $G_{pt,1}$ is the triangle chosen. Denote this as $G_{pt,2}$. Continuing in this manner, one constructs $G_{pt,m}$ with $m \geq 3$. The chromatic polynomial $P(G_{pt,2}, q)$ is calculated from $P(G_{pt,1}, q)$ by using the $s = 3$ special case of the complete-graph intersection theorem. This theorem states that if for two graphs G and H (which are not necessarily planar or triangulations), the intersection $G \cap H = K_s$ for some s , then $P(G \cup H, q) = P(G, q)P(H, q)/P(K_s, q)$. (Note that $P(K_s, q) = \prod_{j=0}^{s-1} (q - j)$.)

It follows that for planar triangulations formed in this iterative manner, the chromatic polynomial has the form

$$P(G_{pt,m}, q) = c_{G_{pt}} (\lambda_{G_{pt}})^m. \quad (5.13)$$

where the coefficient $c_{G_{pt}}$ and the term $\lambda_{G_{pt}}$ are polynomials in q that do not depend on m . Here and below, it is implicitly understood that $m \geq m_{min}$, where m_{min} is the minimal value of m for which the family $G_{pt,m}$ is well defined. Since G_{pt} contains at least one triangle, K_3 , the coefficient $c_{G_{pt}}$ contains (and

may be equal to) $P(K_3, q) = q(q-1)(q-2)$. The chromatic number of G_{pt} may be 3 or 4. In the case of a planar triangulation which is a strip of the triangular lattice of length m vertices with cylindrical boundary conditions, to be discussed below, an alternate and equivalent way to construct the $(m+1)$ 'th member of the family is simply to add a layer of vertices to the strip at one end.

5.2.3 Families with $P(G_{pt,m}, q)$ Consisting of Powers of Several Functions

We have also devised methods to obtain families of planar triangulations $G_{pt,m}$ with the property that the chromatic polynomial is a sum of more than one power of a function of q . We begin with the simplest case, $p = 1$, i.e., one-parameter families and then discuss families with $p \geq 2$. For one-parameter families, we find the general structure

$$P(G_{pt,m}, q) = \sum_{j=1}^{j_{max}} c_{G_{pt},j} (\lambda_{G_{pt},j})^m, \quad (5.14)$$

where $m \geq m_{min}$ and the $c_{G_{pt},j}$ and $\lambda_{G_{pt},j}$ are certain coefficients and functions depending on q but not on m . Here we use the label G_{pt} to refer to the general family of planar triangulations $G_{pt,m}$. We will describe these methods below. Parenthetically, we recall that the form (5.14) is a general one for one-parameter recursive families of graphs, whether or not they are planar triangulations [8], [52]. For (5.14) evaluated at a given value $q = q_0$, as $m \rightarrow \infty$, and hence $n \rightarrow \infty$, the behavior of $P(G_{pt,m}, q)$ is controlled by which $\lambda_{G_{pt},j}$ is dominant at $q = q_0$, i.e., which of these has the largest magnitude $|\lambda_{G_{pt},j}(q_0)|$. For our purposes, a q_0 of major interest is $\tau + 1$, since the Tutte upper bound (5.1) applies for this value. We denote the $\lambda_{G_{pt},j}$ that is dominant at $q = \tau + 1$ as $\lambda_{G_{pt},dom}$. Clearly, if $P(G_{pt,m}, q)$ involves only a single power, as in (5.13), then $\lambda_{G_{pt},dom} = \lambda_{G_{pt}}$.

As in earlier works [52] [59], [49], it can be convenient to obtain the chromatic polynomials $P(G_{pt,m}, q)$ via a Taylor series expansion, in an auxiliary variable x , of a generating function $\Gamma(G_{pt}, q, x)$. Below, we will have occasion to use this method for the family F_m (5.95). Both the form (5.14) and the expression via a generating function are equivalent to the property that $P(G_{pt,m}, q)$ satisfies a recursion relation, for $m \geq j_{max} + m_{min}$:

$$P(G_{pt,m}, q) + \sum_{j=1}^{j_{max}} b_{G_{pt},j} P(G_{pt,m-j}, q) = 0, \quad (5.15)$$

where the $b_{G_{pt},j}$, $j = 1, \dots, j_{max}$, are given by

$$1 + \sum_{j=1}^{j_{max}} b_j x^j = \prod_{j=1}^{j_{max}} (1 - \lambda_{G_{pt},j} x) . \quad (5.16)$$

Thus,

$$b_{G_{pt},1} = - \sum_{j=1}^{j_{max}} \lambda_{G_{pt},j} , \quad (5.17)$$

$$b_{G_{pt},2} = \sum_{j=1, k=1, j \neq k}^{j_{max}} \lambda_{G_{pt},j} \lambda_{G_{pt},k} , \quad (5.18)$$

and so forth, up to

$$b_{G_{pt},j_{max}} = (-1)^{j_{max}} \prod_{j=1}^{j_{max}} \lambda_{G_{pt},j} . \quad (5.19)$$

5.2.4 Asymptotic Behavior as $m \rightarrow \infty$

In [70] we discussed the asymptotic behavior of the chromatic polynomials as $m \rightarrow \infty$. In both the cases of Eq. (5.13) and (5.14), a single power $[\lambda_{G_{pt},j}]^m$ dominates the sum as $m \rightarrow \infty$. For a member of a one-parameter family of planar triangulations, $G_{pt,m}$, we use the notation $r(G_{pt,m})$ for the ratio (5.3), and we define

$$r(G_{pt,\infty}) \equiv \lim_{m \rightarrow \infty} r(G_{pt,m}) . \quad (5.20)$$

We define the (real, non-negative) constant $a_{G_{pt}}$ as [70]

$$a_{G_{pt}} = \lim_{n \rightarrow \infty} [r(G_{pt,m})]^{1/n} = \frac{|\lambda_{G_{pt},dom}(\tau + 1)|^{1/\alpha}}{\tau - 1} . \quad (5.21)$$

We showed in [70] that if $j_{max} = 1$, then $a_{G_{pt}} < 1$ and hence for the classes of $G_{pt,m}$ under consideration, (i) $r(G_{pt,\infty}) = 0$ and (ii) $r(G_{pt,m})$ decreases toward zero exponentially rapidly as a function of m and n as $m \rightarrow \infty$. Note that this does not imply that $P(G_{pt,m}, q)$ has a zero that approaches $q = \tau + 1$ as $m, n \rightarrow \infty$.

For one-parameter families of planar triangulation graphs $G_{pt,m}$ where $P(G_{pt,m}, q)$ has the form (5.14) with $j_{max} \geq 2$, a consequence of the Tutte upper bound (5.1) is that as $m \rightarrow \infty$, any contribution $c_{G_{pt},j} (\lambda_{G_{pt},j})^m$ in (5.14), when evaluated at $q = \tau + 1$, must be less than or equal in magnitude to

$(\tau - 1)^{n-5}$. Therefore, for a given j in this case, either the coefficient $c_{G_{pt},j}$ vanishes for $q = \tau + 1$ or, if this coefficient does not vanish at $q = \tau + 1$, then, taking into account the relation (5.6), it follows that

$$\frac{|\lambda_{G_{pt},j}|^{1/\alpha}}{\tau - 1} \leq 1 \quad \text{at } q = \tau + 1 \quad \forall j . \quad (5.22)$$

If this inequality is realized as an equality, then $r(G_{pt,\infty})$ is a nonzero constant, which necessarily lies in the interval $(0, 1)$, so that $a_{G_{pt}} = 1$. For the families $G_{pt,m}$ for which m and n are linearly related, as specified in (5.6), this type of behavior occurs if and only if, when $P(G_{pt,m}, q)$ is evaluated at $q = \tau + 1$, the (necessarily) dominant $\lambda_{G_{pt},j}$ (with nonvanishing coefficient $c_{G_{pt},j}$), is equal to $\tau - 1$ in magnitude, i.e., $|\lambda_{G_{pt},dom}| = \tau - 1$ at $q = \tau + 1$. This is true, in particular, if this $\lambda_{G_{pt},j} = q - 2$. In the structural form (5.38) below, we shall label this as the $j = 1$ term.

It is a general property that if a graph G contains a complete graph K_p as a subgraph, then $P(G, q)$ contains the factor $P(K_p, q)$. In particular, a triangulation graph, whether planar or not, has the factor $P(K_3, q)$ and a planar triangulation may also contain a K_4 . (However, by Kuratowski's Theorem, a planar graph may not contain a K_p with $p \geq 5$.) Thus, for a planar triangulation G_{pt} , $P(G_{pt}, q) = 0$ for $q = 0, 1, 2$. If $G_{pt} \supseteq K_4$, then $P(G_{pt}, q)$ also vanishes at $q = 3$. If $P(G_{pt}, q)$ has the form of a single power, given as Eq. (5.13), then these factors are explicit. If, however, $P(G_{pt}, q)$ has the form of a sum of $j_{max} \geq 2$ powers $[\lambda_{G_{pt},j}]^m$, then the conditions that $P(G_{pt}, q)$ vanish at $q = 0, 1, 2$ imply relations between the various terms. Moreover, the condition that $P(G_{pt,m}, \tau + 1)$ obeys the Tutte upper bound (5.1) also implies conditions on the structure of this chromatic polynomial. We derive these next.

5.3 Properties of a Class of $G_{pt,m}$ with $P(G_{pt,m}, q)$ Having $j_{max} = 3$ and Certain $\lambda_{G_{pt},j}$

5.3.1 Structure of Coefficients $c_{G_{pt},j}$ in $P(G_{pt,m}, q)$

For a large class of one-parameter families of planar triangulations that we have constructed and studied, for which $P(G_{pt,m}, q)$ has the form (5.14), we find that (i) $j_{max} = 3$ and (ii) the $\lambda_{G_{pt},j} \equiv \lambda_j$ with $j = 1, 2, 3$ have the form

$$\lambda_1 = q - 2, \quad \lambda_2 = q - 3, \quad \lambda_3 = -1 . \quad (5.23)$$

For this class of planar triangulations, we can derive some general results concerning the functional form of the coefficients $c_{G_{pt},j}$ (where we will often suppress the subscript pt on G_{pt} where the meaning is obvious). Using the general form (5.14) with $j_{max} = 3$ and these λ_j 's, we can derive the following identities. The fact that $P(G_{pt}, 0) = 0$ implies that

$$c_{G,1}(-2)^m + c_{G,2}(-3)^m + c_{G,3}(-1)^m = 0 . \quad (5.24)$$

where for ease of notation we suppress the subscript pt on G_{pt} here and in related equations. Since this equation must hold for arbitrary m (understood implicitly to be an integer in the range $m \geq m_{min}$, where m_{min} is the minimal value for which the family $G_{pt,m}$ is well defined), it implies that $c_{G,j} = 0$ for all j . Hence, for these families,

$$c_{G,j} \text{ contains the factor } q \text{ for } j = 1, 2, 3 . \quad (5.25)$$

The evaluation $P(G_{pt}, 1) = 0$ reads

$$c_{G,1}(-1)^m + c_{G,2}(-2)^m + c_{G,3}(-1)^m = 0 \quad \text{at } q = 1 . \quad (5.26)$$

Since this equation must hold for arbitrary $m \geq m_{min}$, it implies two conditions on the evaluation of the coefficients at $q = 1$, namely

$$c_{G,2} = 0 \quad \text{and} \quad c_{G,1} + c_{G,3} = 0 \quad \text{at } q = 1 . \quad (5.27)$$

In particular, (5.27) implies that

$$c_{G,2} \text{ contains the factor } q - 1 . \quad (5.28)$$

The evaluation $P(G_{pt}, 2) = 0$ reads

$$c_{G,1}0^m + [c_{G,2} + c_{G,3}](-1)^m = 0 \quad \text{at } q = 2 . \quad (5.29)$$

Since this equation holds for arbitrary $m \geq m_{min}$, it implies that

$$c_{G,2} + c_{G,3} = 0 \quad \text{at } q = 2 . \quad (5.30)$$

If a family $G_{pt,m}$ which has $m_{min} = 0$, (5.29) and (5.30) together would also imply that $c_{G,1} = 0$ at $q = 2$.

Continuing with $P(G_{pt,m}, q)$ of the form (5.14) with (5.23), we next analyze the evaluation of $P(G_{pt,m}, q)$ at $q = \tau + 1$, viz., $P(G_{pt,m}, \tau + 1)$. Since $\tau - 1 = 0.61803\dots$ and $\tau - 2 = -0.381966$ are smaller than unity in magnitude, the first two terms in $P(G_{pt,m}, \tau + 1)$ vanish exponentially rapidly as m increases. As

regards the ratio $r(G_{pt,m})$, as m increases, the contribution of the first term to this upper bound approaches a constant, while the contribution of the second term vanishes exponentially rapidly. Given the relation (5.6), the Tutte upper bound also vanishes exponentially rapidly as a function of m . Therefore, in order for $P(G_{pt,m}, \tau + 1)$ to satisfy the Tutte upper bound (5.1), it is necessary and sufficient that

$$c_{G,3} = 0 \quad \text{at } q = \tau + 1 . \quad (5.31)$$

This means that

$$c_{G,3} \quad \text{contains the factor } q - \left(\frac{3 + \sqrt{5}}{2} \right) . \quad (5.32)$$

Given that a chromatic polynomial has rational (actually integer) coefficients as a polynomial in q , this means that $c_{G,3}$ must also contain a factor involving the algebraically conjugate root, i.e.,

$$c_{G,3} \quad \text{contains the factor } q - \left(\frac{3 - \sqrt{5}}{2} \right) . \quad (5.33)$$

Combining these, we derive the result that

$$c_{G,3} \quad \text{contains the factor } q^2 - 3q + 1 . \quad (5.34)$$

Having proved these results, it is thus convenient to extract the factors explicitly and define

$$\kappa_{G,1} \equiv \frac{c_{G,1}}{q} , \quad (5.35)$$

$$\kappa_{G,2} \equiv \frac{c_{G,2}}{q(q-1)} , \quad (5.36)$$

and

$$\kappa_{G,3} \equiv \frac{c_{G,3}}{q(q^2 - 3q + 1)} . \quad (5.37)$$

For this class of planar triangulation graphs $G_{pt,m}$, we thus have the general structural formula

$$\begin{aligned} P(G_{pt,m}, q) = & q \left[\kappa_{G,1}(q-2)^m + \kappa_{G,2}(q-1)(q-3)^m \right. \\ & \left. + \kappa_{G,3}(q^2 - 3q + 1)(-1)^m \right] , \end{aligned} \quad (5.38)$$

where m and n are related by (5.6). We observe that the form (5.38) satisfies

the general results that we derived above for the evaluation at $q = \tau + 1$. Thus, if $P(G_{pt,m}, q)$ has this form (5.38) with (5.6) and $\alpha = 1$, then

$$r(G_{pt,\infty}) = [q \kappa_{G,1}] \Big|_{q=\tau+1} \quad (5.39)$$

and hence

$$a(G_{pt}) = 1 . \quad (5.40)$$

The conditions on the coefficients $c_{G,j}$'s evaluated at $q = 1$ and $q = 2$ that we have derived, (5.27), together with the definitions (5.35)-(5.37), are equivalent to the following relations:

$$\kappa_{G,1} = \kappa_{G,3} \quad \text{at } q = 1 \quad (5.41)$$

and

$$\kappa_{G,2} = \kappa_{G,3} \quad \text{at } q = 2 . \quad (5.42)$$

For certain families of planar triangulations $G_{pt,m} \equiv G_m$, the chromatic number $\chi(G_m)$ is 3 for even m and 4 for odd m or vice versa. In these cases, we can also derive another relation between the coefficients. Thus, if $\chi(G_m) = 3$ for even m and $\chi(G_m) = 4$ for odd m , then $\kappa_{G,1} = \kappa_{G,3}$ at $q = 3$. On the other hand, if $\chi(G_m) = 3$ for odd m and $\chi(G_m) = 4$ for even m , then $\kappa_{G,1} = -\kappa_{G,3}$ at $q = 3$. In the case of families G_m for which $\chi(G_m) = 4$ for all m , we have

$$\kappa_{G,1} + \kappa_{G,3} (-1)^m = 0 \quad \text{at } q = 3 \quad \text{if } \chi(G_m) = 4 , \quad (5.43)$$

which implies

$$\kappa_{G,1} = \kappa_{G,3} = 0 \quad \text{at } q = 3 \quad \text{if } \chi(G_m) = 4 . \quad (5.44)$$

5.3.2 Properties of Real Chromatic Zeros

Here we derive some properties of chromatic zeros of planar triangulation graphs $G_{pt,m}$ for which the chromatic polynomial has the form (5.14). It is appropriate first to review some relevant properties of chromatic zeros of general graphs and planar triangulation graphs. For a general graph G , it is elementary that there are no negative chromatic zeros and that there are no chromatic zeros in the intervals $(0,1)$ [79]. The property that $(0,1)$ is a zero-free interval for the chromatic polynomial implies that $q = \tau + 1$ cannot be a chromatic zero for any graph G , as noted above (independent of whether it is a planar triangulation or not). Another interval that has been proved to be

free of chromatic zeros is $(1, 32/27]$ [35] [73].

Specializing now to planar triangulation graphs, it has been proved that G_{pt} has no chromatic zeros in the interval $(2, q_w)$ [80] [83], where q_w is the unique real zero of

$$\lambda_{TC} = q^3 - 9q^2 + 29q - 32 , \quad (5.45)$$

i.e.,

$$q_w = 3 - \frac{[12(9 + \sqrt{177})]^{1/3}}{6} + 4[12(9 + \sqrt{177})]^{-1/3} = 2.546602.. \quad (5.46)$$

We remark that q_w occurs as a chromatic zero of some planar triangulation graphs, in particular, the family comprised of cylindrical sections of the triangulation lattice with $L_y = 3$, or equivalently iterated octahedra. In 1992 Woodall conjectured that a planar triangulation has no chromatic zeros in the interval $(q_m, 3)$, where $q_m = 2.6778146..$ is the unique real zero of $q^3 - 9q^2 + 30q - 35$, [80], but later he gave counterexamples to his conjecture involving one-parameter families of planar triangulations each of which has a real zero that approaches 3 from below as this parameter goes to infinity [81].

Here we present some further results on chromatic zeros of planar triangulations. First, if $P(G_{pt,m}, q)$ has the form (5.13) involving only a single power of a $\lambda_{G_{pt}}$, then its zeros are fixed, independent of m , and hence although it typically has a zero close to $\tau + 1$, this zero does not move as a function of m . However, if $P(G_{pt,m}, q)$ has the multi-term form (5.38) with $j_{max} = 3$ and the λ_j 's in (5.23), then it necessarily has a zero in the interval $[q_w, 3)$ that approaches $\tau + 1$ as $m \rightarrow \infty$. The proof of this is as follows. Let us assume that q is a real number in this interval $[q_w, 3)$. In the limit as $m \rightarrow \infty$, the first two terms, which are proportional to $(q - 2)^m$ and $(q - 3)^m$, respectively, vanish (exponentially fast), so that

$$P(G_{pt,m}, q) \sim \epsilon_m + q(q^2 - 3q + 1)\kappa_{G_{pt},3}(-1)^m , \quad (5.47)$$

where ϵ_m denotes the contribution of these first two terms. If $\kappa_{G_{pt},3}$ happens to vanish at $q = \tau + 1$, then the result follows, since $\epsilon_m \rightarrow 0$ as $m \rightarrow \infty$. If $\kappa_{G_{pt},3} \neq 0$ at $q = \tau + 1$, then consider the limit as $q \rightarrow \tau + 1$, where we can write

$$\begin{aligned} \frac{(-1)^m P(G_{pt,m}, q)}{(\tau + 1)\kappa_{G_{pt},3}|_{q=\tau+1}} &= \frac{(-1)^m \epsilon_m}{(\tau + 1)\kappa_{G_{pt},3}|_{q=\tau+1}} + q^2 - 3q + 1 \\ &\equiv \delta_m + q^2 - 3q + 1 . \end{aligned} \quad (5.48)$$

To show that $P(G_{pt}, q)$ has a zero that approaches $q = \tau + 1$ as $m \rightarrow \infty$, we

use the fact that $P(G_{pt,m}, q)$ is a continuous function of q and solve (5.48) for q , subject to the condition that $q \in [q_w, 3)$, obtaining a consistent result with

$$q = \frac{1}{2} \left[3 + \sqrt{5 - 4\delta_m} \right], \quad (5.49)$$

which approaches $q = \tau + 1$ as $m \rightarrow \infty$. Note that the other zero at $q = (1/2)(3 - \sqrt{5 - 4\delta_m})$, is irrelevant because we assumed at the outset that q is in the interval $[q_w, 3)$ and this other zero is outside this interval; in the vicinity of this other zero, the analysis does not apply because the terms proportional to $(q - 2)^m$ and $(q - 3)^m$ do not vanish as $m \rightarrow \infty$.

In 5.1 we have exhibited two one-parameter families of planar triangulation graphs with this property, namely B_m and H_m . We construct and analyze several more families of this type here. Thus, for these families, we have provided an understanding of why $P(G_{pt,m}, q)$ has a chromatic zero near to $\tau + 1$ and, furthermore, have proved that this zero approaches $\tau + 1$ as $m \rightarrow \infty$. From the derivation above, it is evident that our result requires, for a given family $G_{pt,m}$, that m be sufficiently large. As is illustrated from numerical results presented below, for specific families of planar triangulations that we have studied, $P(G_{pt,m}, q)$ has a real zero reasonably close to $\tau + 1$ even for moderate values of m .

Our second result follows immediately from this analysis. With the same assumptions, we have observed that in the limit $m \rightarrow \infty$, $P(G_{pt,m}, q)$ has a real zero in the interval $q \in [q_w, 3)$ if and only if $c_{G_{pt},3}$ has a real zero in this interval, $q \in [q_w, 3)$. We know that there is at least one such zero, namely the one arising from the factor $q^2 - 3q + 1$ in $c_{G_{pt},3}$. Therefore, in the limit $m \rightarrow \infty$, $P(G_{pt,m}, q)$ has another real zero in the interval $q \in [q_w, 3)$ in addition to the one approaching $\tau + 1$ if and only if $\kappa_{G,3}$ has a real zero in this interval $q \in [q_w, 3)$. We will present several applications of these results below.

We remark that, with the same assumptions as above,

$$\lim_{m \rightarrow \infty} |P(G_{pt,m}, q)| = c_{G_{pt},3}. \quad (5.50)$$

Note that the limit $\lim_{m \rightarrow \infty} P(G_{pt,m}, q)$ itself does not exist, because the term $\lambda_3^m = (-1)^m$ factor has no limit as $m \rightarrow \infty$.

In [70], we investigated the question of whether for a planar triangulation graph G_{pt} it is true that the chromatic zero of G_{pt} nearest to $\tau + 1$ is always real. We exhibited an example, with a graph we denoted $G_{CM,1}$, which is, to our knowledge, the first case for which the zero closest to $\tau + 1$ is not real but instead the zeros closest to $\tau + 1$ form a complex-conjugate pair. Our result is in agreement with a previous observation by Woodall that this graph has no

real zero near to $\tau + 1$ [82]. Since $P(G_{CM,m}, q)$ has the form of (5.13) with a single λ , as m increases, its zeros are fixed and just increase in multiplicity, in contrast to the motion of chromatic zeros for families $G_{pt,m}$ whose chromatic polynomials are of the form (5.14) with $j_{max} > 1$.

The value of q where the Tutte upper bound applies, namely $q = \tau + 1 = (3 + \sqrt{5})/2$ is also a member of a sequence of numbers related to roots of unity, namely the Tutte-Beraha numbers, q_r . Thus, for a root of unity of the form $z_r = e^{\pi i/r}$, one defines $q_r = (z_r + z_r^*)^2 = 4 \cos^2(\pi/r)$. One has $\tau + 1 = q_5$. Parenthetically, we note that chromatic zeros have been studied for sections of triangular lattices with various boundary conditions that are not planar triangulations, either because they have at least one face that is not a triangle or because they are not planar (e.g., have toroidal or Klein-bottle boundary conditions). We refer the reader to [70] for references to some of these papers; here, in view of our focus on the Tutte upper bound (5.1) we restrict to planar triangulations.

5.3.3 Properties of Complex Chromatic Zeros

As before, we consider a one-parameter of planar triangulation graphs $G_{pt,m}$ such that $P(G_{pt,m}, q)$ has the form (5.38). Here we give a general determination of the continuous accumulation set \mathcal{B} of chromatic zeros of $P(G_{pt,m}, q)$ in the complex q plane in the limit $m \rightarrow \infty$ (and, hence, owing to (5.6), $n \rightarrow \infty$). If the zeros form a discrete set (some with multiplicities that go to infinity as $n \rightarrow \infty$), then this locus is null. As in earlier work, we denote the formal limit of the family G_m as $m \rightarrow \infty$ as $\{G\}$. In general, the locus \mathcal{B} may or may not intersect the real q axis. If it does, the maximal point where it intersects the real axis is denoted $q_c(\{G\})$. For a $P(G, q)$ of the form (5.14), the curves comprising the locus \mathcal{B} are determined as the solutions of the equality in magnitude of the dominant $\lambda_{G_{pt,j}}$, in accordance with general results for recursive functions [6]. These curves extend infinitely far from the origin if and only if such an equality can be satisfied as $|q| \rightarrow \infty$, as was discussed in [52],[56], [60], [62].

We now consider families of planar triangulations $G_{pt,m}$ whose chromatic polynomials have the form (5.38). For these families, first, because $\lambda_1 = q - 2$ is dominant for large q and is equal in magnitude to $\lambda_3 = -1$ at $q = 3$, it follows that $q_c(\{G_{pt}\}) = 3$. Second, as a consequence of the fact that the equality $|q - 2| = |q - 3|$ holds for the infinite line $\text{Re}(q) = 5/2$, part of the boundary \mathcal{B} extends infinitely far away from the origin in the q plane, i.e., passes through the origin of the $1/q$ plane. As is evident for specific families $G_{pt,m}$, as m and hence n go to infinity, the degree of one or more vertices also goes to infinity, so the fact that the magnitudes of zeros diverge is in accord with the upper

bound $|q| < b\Delta(G)$ obtained in [72] (with $b \simeq 7.96$) and strengthened slightly in [30] (with $b \simeq 6.91$), where $\Delta(G)$ is the maximal degree of any vertex in G . Note, however, that the property that the degree of a vertex diverges as $n \rightarrow \infty$ does not, by itself, imply that \mathcal{B} passes through the origin of the $1/q$ plane. This is clear from the $n \rightarrow \infty$ limit of wheel graphs, for which the central vertex $v_{cent.}$ has degree $d(v_{cent.}) \rightarrow \infty$, but the locus \mathcal{B} has bounded support in the q plane [52]. Continuing with our analysis of families of planar triangulations $G_{pt,m}$ whose chromatic polynomials have the form (5.38), the \mathcal{B} separates the q plane into three regions, which we denote as R_j , $j = 1, 2, 3$. These are defined as follows:

$$R_1 : \operatorname{Re}(q) > \frac{5}{2} \quad \text{and} \quad |q - 2| > 1, \quad (5.51)$$

$$R_2 : \operatorname{Re}(q) < \frac{5}{2} \quad \text{and} \quad |q - 3| > 1, \quad (5.52)$$

and

$$R_3 : |q - 2| < 1 \quad \text{and} \quad |q - 3| < 1. \quad (5.53)$$

The boundaries between these regions are thus the two circular arcs

$$\mathcal{B}(R_1, R_3) : q = 2 + e^{i\theta}, \quad -\frac{\pi}{3} < \theta < \frac{\pi}{3} \quad (5.54)$$

and

$$\mathcal{B}(R_2, R_3) : q = 3 + e^{i\phi}, \quad \frac{2\pi}{3} < \phi < \frac{4\pi}{3}, \quad (5.55)$$

together with the semi-infinite vertical line segments

$$\mathcal{B}(R_1, R_2) = \{q\} : \operatorname{Re}(q) = \frac{5}{2} \quad \text{and} \quad |\operatorname{Im}(q)| > \frac{\sqrt{3}}{2}. \quad (5.56)$$

These meet at the triple points

$$q_t, q_t^* = \frac{5 \pm i\sqrt{3}}{2}. \quad (5.57)$$

A specific example of a locus \mathcal{B} that extends infinitely far from the origin in the q plane was studied in [52], for the family B_m . Here we have generalized the result to all families of planar triangulations whose chromatic polynomials have the form (5.38).

We have constructed and studied a two-parameter family of planar triangulations D_{m_1, m_2} (see the next chapter). By keeping one of the two indices m_1 or m_2 fixed, we have obtained a number of one-parameter families and

have analyzed the chromatic polynomials for these. We have also considered the special cases where one allows both m_1 and m_2 to vary, such that one is a linear function of the other. We have, in particular, analyzed the diagonal case where $m_1 = m_2$, $D_{m,m}$, to be discussed below. For this family the chromatic polynomial $P(D_{m,m}, q)$ has the form (5.14) with $j_{max} = 6$ and a set of λ 's that are squares and cross products of those in (5.38). Since the equations defining the equality of magnitude of dominant λ 's can again be satisfied as $1/q \rightarrow 0$, it again follows, by the criteria of [52], [55], [56] that the locus \mathcal{B} extends infinitely far from the origin of the complex q plane.

In a different direction, we have also studied a family F_m (see below) for which the chromatic polynomial $P(F_m, q)$ is of the form (5.38) with $j_{max} = 3$, but with terms $\lambda_{F,j}$, $j = 1, 2, 3$, that are not simple polynomials, but instead are roots of a cubic equation, (5.107). In the $m \rightarrow \infty$ limit, the continuous accumulation set \mathcal{B} for this family has bounded magnitude (does not extend infinitely far away from the origin in the q plane), as can be seen because the condition that defines \mathcal{B} , namely the equality in magnitude of two dominant $\lambda_{F,j}$'s, cannot be satisfied for arbitrarily great $|q|$.

5.4 The Family $R_m = P_m + P_2$

In this section we illustrate the general results derived in the previous section for recursive families of planar triangulations whose chromatic polynomials have the form (5.13). For this purpose, we consider a family whose m 'th member, denoted R_m , is the join² of the path graph P_m with $P_2 = K_2$,

$$R_m = P_m + P_2 . \quad (5.58)$$

Thus, $R_1 = K_3$, $R_2 = K_4$, etc. The graph R_4 is shown in Fig. (5.1). We have $n(R_m) = m + 2$, so $\alpha = 1$ and $\beta = 2$ for this family. An elementary calculation yields $P(R_m, q) = q(q-1)(q-2)[\lambda_R(q)]^{m-1}$, where $\lambda_R(q) = q - 3$. Evaluating $P(R_m, q)$ at $q = \tau + 1$, we obtain

$$P(R_m, \tau + 1) = (\tau + 1)(\tau - 2)^{m-1} = \left(\frac{3 + \sqrt{5}}{2} \right) \left(\frac{-3 + \sqrt{5}}{2} \right)^{m-1} \quad (5.59)$$

²The join $G + H$ of two graphs $G = (V_G, E_G)$ and $H = (V_H, E_H)$ is defined as the graph with vertex set $V_{G+H} = V_G \cup V_H$ and edge set E_{G+H} comprised of the union of $E_G \cup E_H$ with the set of edges obtained by connecting each vertex of G with each vertex of H .

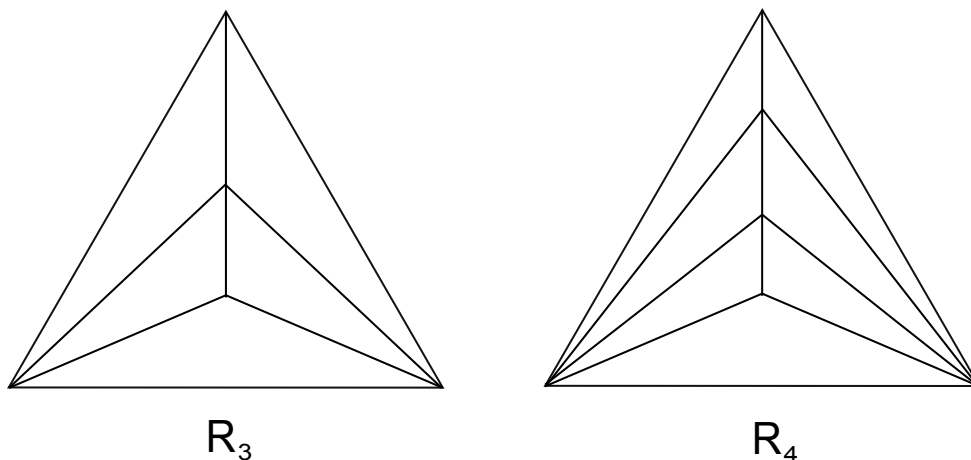


Figure 5.1: Graphs R_3 and R_4 .

The ratio of $|P(R_m, \tau + 1)|$ to the Tutte upper bound is

$$r(R_m) = (\tau - 1)^{m-1} = \left(\frac{-1 + \sqrt{5}}{2}\right)^{m-1} \quad (5.60)$$

so that

$$a_R = \frac{-1 + \sqrt{5}}{2} = 0.61803.. \quad (5.61)$$

for this family.

5.5 The Cylindrical Strip of the Triangular Lattice with $L_y = 3$

Another illustration of recursive families of planar triangulations whose chromatic polynomials have the form (5.13) is provided by the family of cylindrical strips of the triangular (*tri*) lattice. Consider a strip in this family of variable length $L_x = m$ vertices in the x (longitudinal) direction and L_y vertices in the y (transverse) direction. Denote the boundary conditions in the x and y directions as (BC_x, BC_y) , where free and periodic boundary conditions are abbreviated as *FBC* and *PBC*. We take the boundary conditions to be (FBC_x, PBC_y) , denoted as cylindrical. The cylindrical strip of the triangular lattice with $L_y = 3$, i.e., transverse cross sections consisting of triangles, and arbitrary length $L_x = m$, denoted TC_m , is a planar triangulation, with $n(TC_m) = 3m$ vertices. In this family, TC_1 is a degenerate case of a triangle,

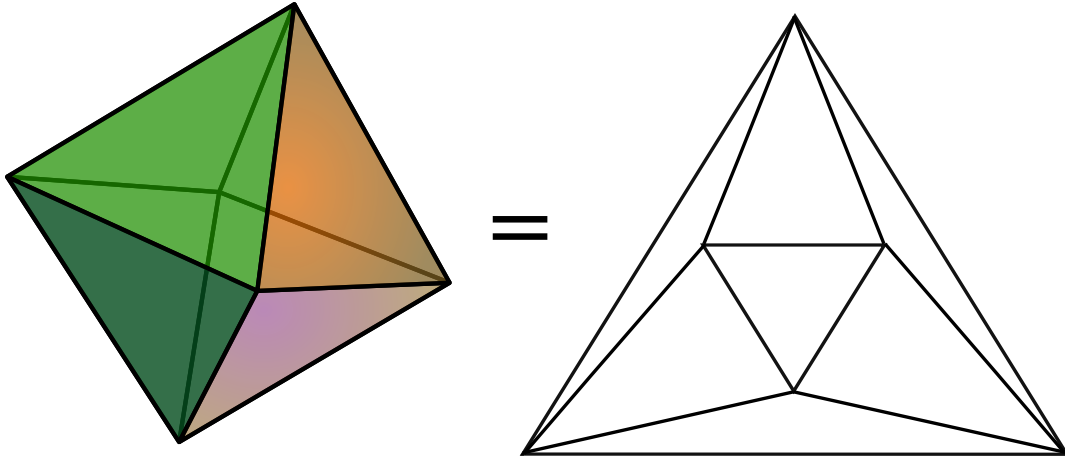


Figure 5.2: Octahedron as planar triangulation graph, TC_2 .

K_3 , while TC_2 is the graph of the octahedron, as shown in Fig. (5.2). TC_m may also be constructed in the recursive manner described in Sect. (5.2) by starting with TC_2 , choosing an interior triangle, and placing a copy of TC_2 onto this triangle to get TC_3 , and so forth for $m \geq 4$. Thus, TC_m may also be considered as a recursively iterated octahedron graph, see Fig. (5.2). An elementary calculation yields $P(TC_m, q) = q(q-1)(q-2) [\lambda_{TC}(q)]^{m-1}$, where $\lambda_{TC}(q) = q^3 - 9q^2 + 29q - 32$. Evaluating $P(TC_m, q)$ at $q = \tau + 1$ gives

$$P(TC_m, \tau + 1) = \left(\frac{3 + \sqrt{5}}{2} \right) (-11 + 5\sqrt{5})^{m-1}. \quad (5.62)$$

Hence,

$$r(TC_m) = \frac{(3 + \sqrt{5})}{4} (3 - \sqrt{5})^m, \quad (5.63)$$

so that

$$a_{TC} = (3 - \sqrt{5})^{1/3} = 0.91415... \quad (5.64)$$

$P(TC_m, q)$ has a real zero near to $\tau + 1$, at $q \simeq 2.546602$.

5.6 Iterated Icosahedron Graphs

A more complicated family of planar triangulations yielding chromatic polynomials of the form (5.13) is provided by recursive iterates of the icosahedron graph I_1 , shown in Fig. (5.3). We construct these recursive iterates I_m with $m \geq 2$ by the procedure given in Sect. (5.2). The graph I_m has

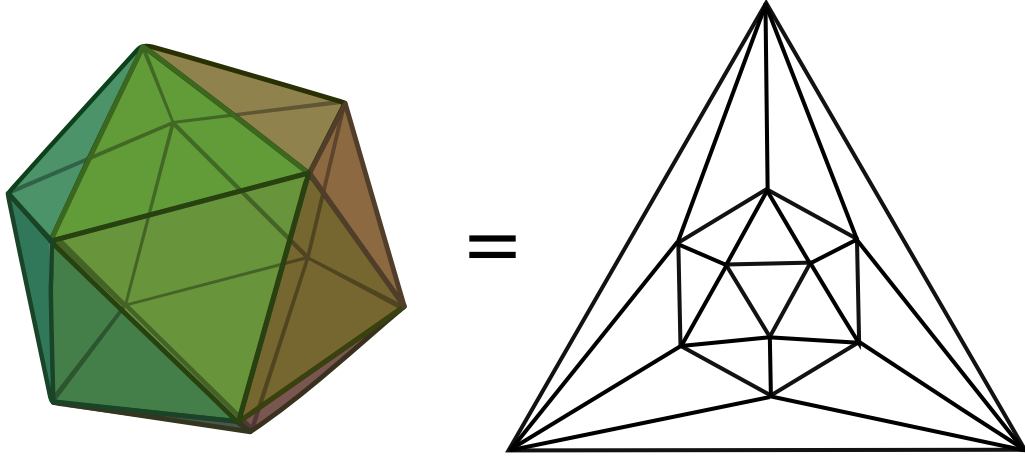


Figure 5.3: Icosahedron as planar triangulation graph, I_1 .

$n(I_m) = 3 + 9m$ vertices. The chromatic polynomial is

$$P(I_m, q) = q(q-1)(q-2) [\lambda_I(q)]^m \quad (5.65)$$

where

$$\begin{aligned} \lambda_I(q) = & (q-3)(q^8 - 24q^7 + 260q^6 - 1670q^5 + 6999q^4 - 19698q^3 \\ & + 36408q^2 - 40240q + 20170) . \end{aligned} \quad (5.66)$$

We calculate

$$P(I_m, \tau + 1) = \left(\frac{3 + \sqrt{5}}{2} \right) \left(\frac{-23955 + 10713\sqrt{5}}{2} \right)^m . \quad (5.67)$$

Hence,

$$r(I_m) = \frac{(3 + \sqrt{5})}{4} \left(\frac{-315 + 141\sqrt{5}}{2} \right)^m , \quad (5.68)$$

so that

$$a_I = \left(\frac{-315 + 141\sqrt{5}}{2} \right)^{1/9} = 0.80552... \quad (5.69)$$

$P(I_m, q)$ has a real zero quite close to $\tau + 1$, at $q \simeq 2.6181973$ and another real zero near to q_7 , at $q \simeq 3.222458$.

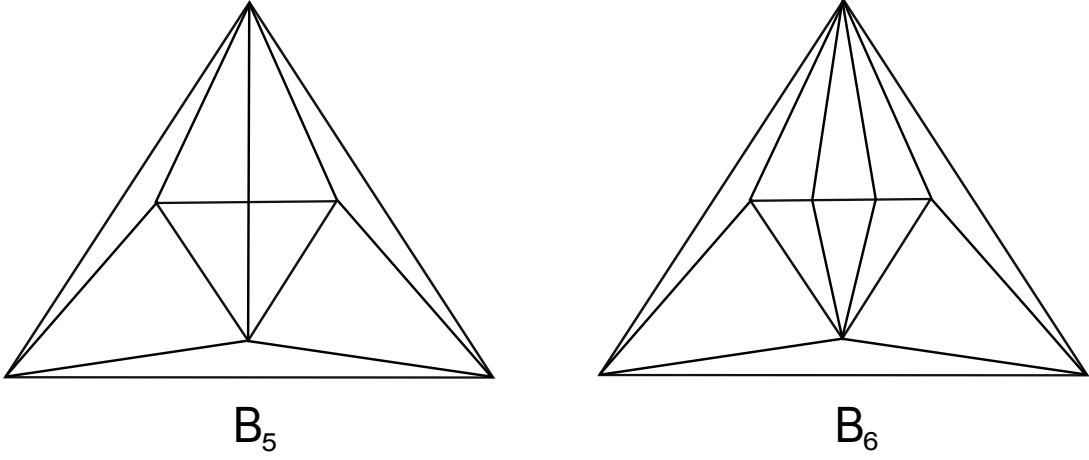


Figure 5.4: Graphs B_5 and B_6 .

5.7 The Bipyramid Family B_m

In this section we consider a recursive family of planar triangulations whose chromatic polynomials have the form (5.14) with $j_{max} = 3$. This is the bipyramid family, which is the join

$$B_m = \bar{K}_2 + C_m. \quad (5.70)$$

for $m \geq 3$, where \bar{K}_p , the complement of K_p , is the graph of p disjoint vertices with no edges. Clearly, $n(B_m) = m + 2$. B_4 is the octahedron graph (Fig. (5.2)). B_5 and B_6 are shown in Fig. (5.4).

In Fig. (5.4), the uppermost and the lower middle vertices of B_m have degree m , so that the degrees of these two vertices go to infinity as $m \rightarrow \infty$. All of the other vertices have degree 4. The chromatic polynomial for this family is of the form (5.14) with three λ s:

$$P(B_m, q) = \sum_{j=1}^3 c_{B,j}(q) [\lambda_{B,j}(q)]^m, \quad (5.71)$$

where

$$c_{B,1}(q) = q, \quad c_{B,2}(q) = q(q-1), \quad c_{B,3}(q) = q(q^2 - 3q + 1) \quad (5.72)$$

and

$$\lambda_{B,1}(q) = q - 2, \quad \lambda_{B,2}(q) = q - 3, \quad \lambda_{B,3}(q) = -1. \quad (5.73)$$

$P(B_m, q)$ contains the factor $P(K_3, q)$ if m is even and $P(K_4, q)$ if m is odd; related to this, $\chi(B_m) = 3$ if m is even and $\chi(B_m) = 4$ if m is odd.

In view of the general factorizations for the coefficients $c_{G_{pt,m},j}$ that we have proved here, it is useful to express the results in terms of the reduced coefficients $\kappa_{G,j}$:

$$\kappa_{B,1} = \kappa_{B,2} = \kappa_{B,3} = 1 . \quad (5.74)$$

Evaluating $P(B_m, q)$ at $q = \tau + 1$, we find

$$P(B_m, \tau + 1) = (\tau + 1) \left[(\tau - 1)^m + \tau(\tau - 2)^m \right] . \quad (5.75)$$

In accordance with the general discussion in Sect. (5.3.1), $c_{B,3}(q)$ vanishes for $q = \tau + 1$ (see the related Eq. (2.8) of [21]), so that the $j = 3$ term does not contribute for this value of q . Hence,

$$r(B_m) = (\tau - 1) \left[1 + \tau(1 - \tau)^m \right] \quad (5.76)$$

Since $|1 - \tau| < 1$, the second term, $\tau(1 - \tau)^m$, vanishes as $m \rightarrow \infty$, so

$$\lim_{m \rightarrow \infty} r(B_m) = \tau - 1 = \frac{-1 + \sqrt{5}}{2} = 0.61803.. \quad (5.77)$$

and

$$a_B = 1 . \quad (5.78)$$

Because $1 - \tau$ is negative, the ratios $r(B_m)$ form a sequence such that for increasing even (odd) m , $r(B_m)$ approaches the $n \rightarrow \infty$ limit $\tau - 1$ from above (below). For $m \geq 4$, $P(B_m, q)$ has real zeros that are close to $q = \tau + 1$. These form a sequence such that for even (odd) m the nearby zero is slightly less than (greater than) $q = \tau + 1$, respectively. These are listed in Table (5.1) for m from 4 to 18.

The continuous accumulation set of zeros of $P(B_m, q)$ in the complex q plane as $m \rightarrow \infty$ was studied in [52], as the most simple example of the $j_{max} = 3$ one parameter family of planar triangulations, which was fully discussed in Sect.(5.3.3) of this chapter.

5.8 The Family H_m

Here we remark on another family of planar triangulations H_m [70], which is well-defined for $m \geq m_{min} = 3$ and has $n(H_m) = m + 5$. In Fig. (5.5) we

Table 5.1: Location of zeros q_z of $P(B_m, q)$ closest to $\tau + 1 = 2.6180339887..$ for m from 4 to 18. Notation $ae-n$ means $a \times 10^{-n}$.

m	q_z	$q_z - (\tau + 1)$
4	2.546602	-0.07143
5	2.677815	0.05978
6	2.594829	-0.02321
7	2.636118	0.01808
8	2.609130	-0.8904e-2
9	2.624356	0.6322e-2
10	2.614541	-3.493e-3
11	2.620356	2.322e-3
12	2.616673	-1.361e-3
13	2.618905	0.8713e-3
14	2.617509	-0.5254e-3
15	2.618364	3.301e-4
16	2.617832	-2.017e-4
17	2.618160	1.256e-4
18	2.617957	-0.7725e-4

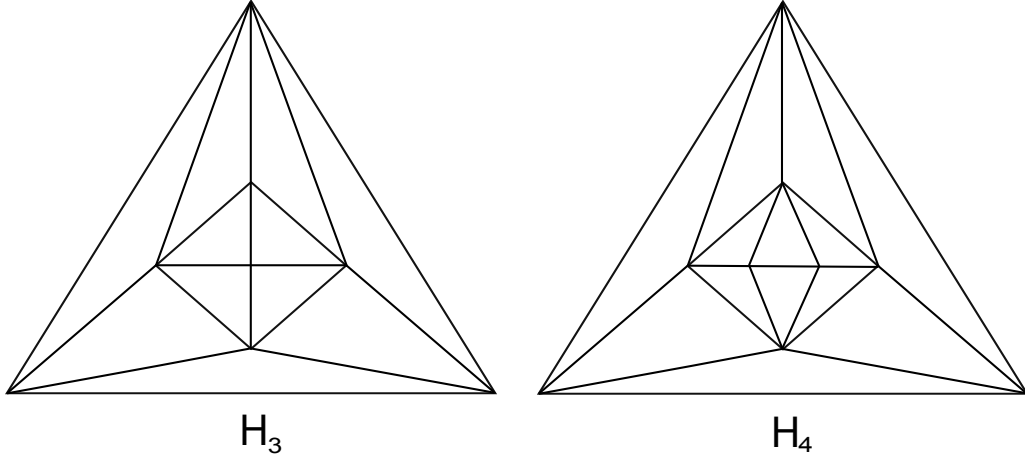


Figure 5.5: Graphs H_3 and H_4 .

show the lowest member of the family, H_3 . The next higher member, H_4 , is constructed by adding a vertex and associated edges in the central diamond-like subgraph, as shown in Fig. (5.5), and so forth for higher members.

We have given the chromatic polynomial for this family in Ref. [70] and have analyzed its properties there. In our present notation, $P(H_m, q)$ has the form (5.38) with

$$\kappa_{H,1} = (q - 3)^3, \quad (5.79)$$

$$\kappa_{H,2} = q^3 - 9q^2 + 30q - 35, \quad (5.80)$$

and

$$\kappa_{H,3} = -(q - 3)(q - 5). \quad (5.81)$$

Evaluating $P(H_m, q)$ at $q = \tau + 1$, we find

$$P(H_m, \tau + 1) = \left(\frac{-7 + 3\sqrt{5}}{2} \right) (\tau - 1)^m + \left(\frac{5 - 3\sqrt{5}}{2} \right) (\tau - 2)^m. \quad (5.82)$$

Consequently,

$$r(H_m) = \frac{-7 + 3\sqrt{5}}{2} + \left(\frac{5 - 3\sqrt{5}}{2} \right) \left(\frac{1 - \sqrt{5}}{2} \right)^m. \quad (5.83)$$

Since $|(1 - \sqrt{5})/2| < 1$, the second term in Eq. (5.83) vanishes as $m \rightarrow \infty$, so for this family

$$\lim_{m \rightarrow \infty} r(H_m) = \frac{7 - 3\sqrt{5}}{2} = 0.145898.. \quad (5.84)$$

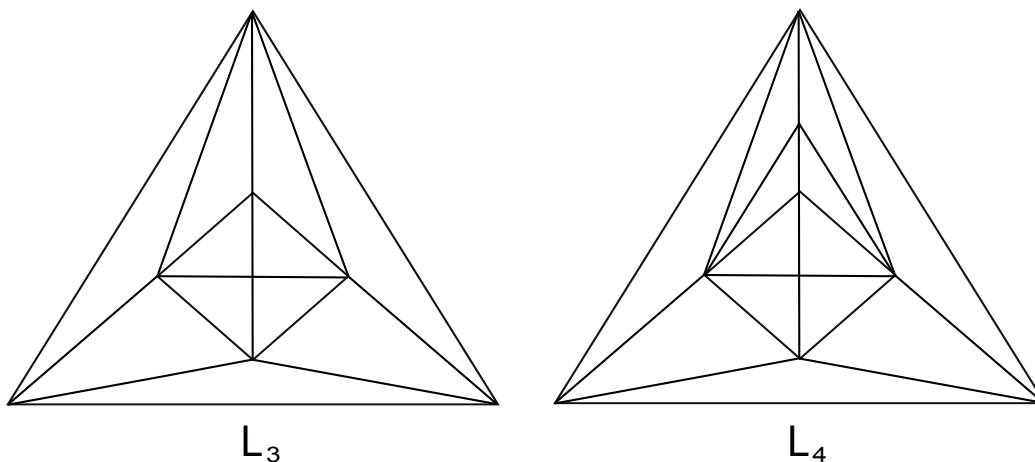


Figure 5.6: Graphs L_3 and L_4 .

and

$$a_H = 1 . \tag{5.85}$$

5.9 The Family L_m

For comparative purposes, it is useful to study another family of planar triangulations with chromatic polynomials of the multi-term form (5.14). Here we denote this family as L_m . It is well-defined for $m \geq m_{min} = 3$ and has $n(L_m) = m + 5$. The lowest member of this family, L_3 , is the same as H_3 . The next higher member, L_4 , is constructed by adding a vertex and associated edges in the central “diamond”, as shown in Fig. (5.6), and so forth for higher members.

For this family of planar triangulations we calculate the chromatic polynomial $P(L_m, q)$ to be of the form (5.38) with

$$\kappa_{L,1} = (q - 2)(q - 3)^2 , \tag{5.86}$$

$$\kappa_{L,2} = q^3 - 9q^2 + 29q - 32 , \tag{5.87}$$

(equal to λ_{TC}) and

$$\kappa_{L,3} = 2(q - 3) . \tag{5.88}$$

$P(L_m, q)$ contains the factor $P(K_4, q)$ and has $\chi(L_m) = 4$.

Evaluating $P(L_m, q)$ at $q = \tau + 1$, we find

$$P(L_m, \tau + 1) = (-2 + \sqrt{5}) \left[(\tau - 1)^m + 2(\tau - 2)^m \right]. \quad (5.89)$$

Consequently,

$$r(L_m) = (-2 + \sqrt{5}) \left[1 + 2 \left(\frac{1 - \sqrt{5}}{2} \right)^m \right]. \quad (5.90)$$

As before, since $|(1 - \sqrt{5})/2| < 1$, the second term in Eq. (5.90) vanishes (exponentially fast) as $m \rightarrow \infty$, so

$$r(L_\infty) = -2 + \sqrt{5} = 0.236068 \quad (5.91)$$

(to the indicated accuracy) and, as a special case of Eq. (5.40), $a_L = 1$.

We proved in general above that for any family of planar triangulations $G_{pt,m}$ with chromatic polynomials $P(G_{pt,m}, q)$ of the form (5.38), $P(G_{pt,m}, q)$ has a zero that approaches $\tau + 1$ as $m \rightarrow \infty$. The families B_m , H_m , and L_m (as well as others to be discussed below) illustrate this general result. In the present case, for odd m and hence even $n = m + 5$, this zero of $P(L_m, q)$ is slightly less than $q = \tau + 1$, while for even m and hence odd n , the nearby zero is slightly greater than $\tau + 1$. If and only if m is odd, i.e., n is even, $P(L_m, q)$ has another real zero somewhat larger than 3, which decreases monotonically toward 3 from above as $m \rightarrow \infty$. As examples, for $n = 8, 12, 16, 20$, and 24, this zero occurs at approximately $q = 3.61, 3.37, 3.25, 3.19$, and 3.16, respectively.

5.10 The Family F_m

In this section we construct and study a family of planar triangulations, denoted F_m , with the property that $P(F_m, q)$ has the form (5.14) with $j_{max} = 3$, but the $\lambda_{F,j}$ are not given by (5.23), but instead are roots of a certain cubic equation. The number of vertices is $n(F_m) = m + 4$. This family is useful as a contrast to the other one-parameter families of planar triangulations with chromatic polynomials of the form (5.14) that we have constructed. The construction of members of this family is somewhat more complicated than that of the other families analyzed in this chapter, and accordingly, for illustration we include several graphs, namely F_m with $m = 3, 4, 5, 6$, are shown in Figs. (5.7) and (5.8). As these show, starting from a given member F_m , one constructs the next higher member F_{m+1} in an interleaved manner, first adding

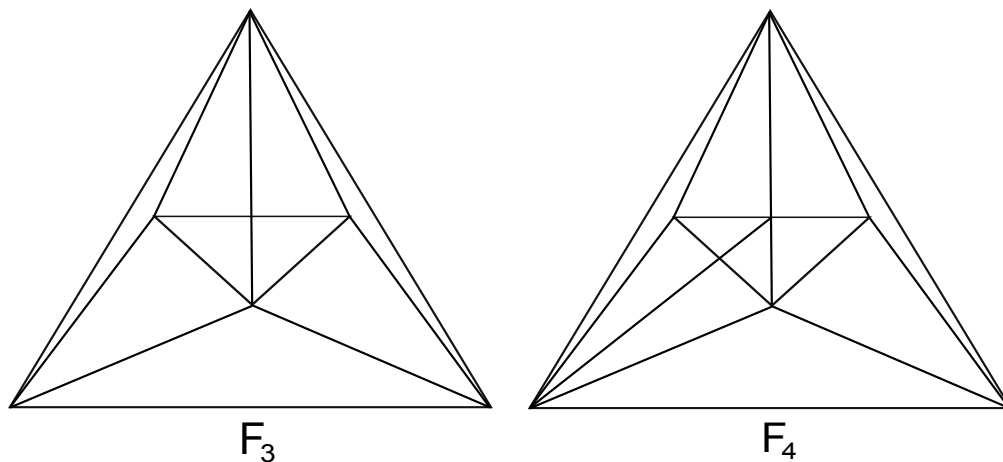


Figure 5.7: Graphs F_3 and F_4 .

a new set of edges one of which emanates from the lower left-hand vertex of the graph, and then a new set of edges one of which emanates from the uppermost vertex, and so forth. We note that in contrast to the previous planar triangulations with chromatic polynomials of the form (5.38), the degrees of the vertices remain bounded as $m \rightarrow \infty$ for this family.

As in earlier works [52], [59], [49], it is most convenient to express the $P(F_m, q)$ via a generating function, $\Gamma(F, q, x)$, which is a rational function in q and an auxiliary expansion variable x , of the form

$$\Gamma(F, q, x) = \frac{\mathcal{N}(F, q, x)}{\mathcal{D}(F, q, x)}, \quad (5.92)$$

where the numerator and denominator are

$$\mathcal{N}(F, q, x) = a_{F,0} + a_{F,1} x + a_{F,2} x^2 \quad (5.93)$$

and

$$\mathcal{D}(F, q, x) = 1 + b_{F,1} x + b_{F,2} x^2 + b_{F,3} x^3. \quad (5.94)$$

with $a_{F,j}$ and $b_{F,j}$ being polynomials in q . The chromatic polynomial $P(F_m, q)$ is then given as the coefficient in the Taylor series expansion of this generating function:

$$\Gamma(F, q, x) = \sum_{m=0}^{\infty} P(F_{m+1}, q) x^m \quad (5.95)$$

Using an iterative deletion-contraction method, we have determined this

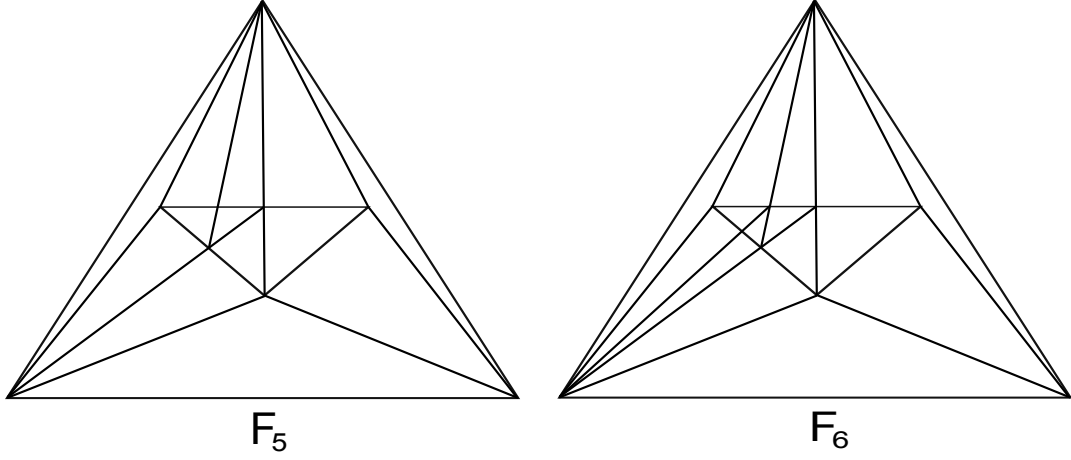


Figure 5.8: Graphs F_5 and F_6 .

generating function. We find

$$a_{F,0} = q(q-1)(q-2)(q-3)^2 \quad (5.96)$$

$$a_{F,1} = q(q-1)(q-2)(2q-5) \quad (5.97)$$

$$a_{F,2} = q(q-1)(q-2)^2(q-3)^2 \quad (5.98)$$

$$b_{F,1} = -(q-3) \quad (5.99)$$

$$b_{F,2} = q-3 \quad (5.100)$$

and

$$b_{F,3} = -(q-2)(q-3) . \quad (5.101)$$

The chromatic polynomial may also be expressed in the form of Eq. (5.14), with $j_{max} = 3$, namely

$$P(F_m, q) = \sum_{j=1}^3 c_{F,j} (\lambda_{F,j})^m . \quad (5.102)$$

Using Eq (2.13) (or (2.15)) of Ref. [59], one can calculate the coefficients $c_{F,j}$ for $j = 1, 2, 3$ from the generating function. Specifically, we have

$$c_{F,1} = \frac{(a_{F,0}\lambda_{F,1}^2 + a_{F,1}\lambda_{F,1} + a_{F,2})}{(\lambda_{F,1} - \lambda_{F,2})(\lambda_{F,1} - \lambda_{F,3})} \quad (5.103)$$

$$c_{F,2} = \frac{(a_{F,0}\lambda_{F,2}^2 + a_{F,1}\lambda_{F,2} + a_{F,2})}{(\lambda_{F,2} - \lambda_{F,1})(\lambda_{F,2} - \lambda_{F,3})} \quad (5.104)$$

and

$$c_{F,3} = \frac{(a_{F,0}\lambda_{F,3}^2 + a_{F,1}\lambda_{F,3} + a_{F,2})}{(\lambda_{F,3} - \lambda_{F,1})(\lambda_{F,3} - \lambda_{F,2})} . \quad (5.105)$$

As discussed before [52], [59], [49], the $\lambda_{F,j}$ s appear via the factorized form of the denominator of the generating function,

$$\mathcal{D}(F, q, x) = \prod_{j=1}^3 (1 - \lambda_{F,j}x) . \quad (5.106)$$

Equivalently, the $\lambda_{F,j}$ s are determined from the equation $\xi^3 + b_{F,1}\xi^2 + b_{F,2}\xi + b_{F,3} = 0$, i.e.,

$$\xi^3 + (3 - q)\xi^2 + (q - 3)\xi - (q - 2)(q - 3) = 0 . \quad (5.107)$$

Let us define

$$R_F = 3(4q^3 - 24q^2 + 76q - 93) \quad (5.108)$$

and

$$S_F = \left[4(q - 3) \left(2q^2 + 6q - 9 + 3\sqrt{R_F} \right) \right]^{1/3} . \quad (5.109)$$

With appropriate choices of branch cuts for the various fractional powers in (5.109), we have

$$\lambda_{F,1} = \frac{S_F}{6} + \frac{2(q - 3)(q - 6)}{3S_F} + \frac{q - 3}{3} . \quad (5.110)$$

The other $\lambda_{F,j}$, $j = 2, 3$ can be written explicitly in a similar manner. Thus, this family is valuable as an illustration of a family of planar triangulation graphs with a chromatic polynomial of the form (5.14) and with λ terms that are different from those in (5.23) and, indeed, are nonpolynomial, in contrast to the families with chromatic polynomials of the form (5.13) or (5.38).

With regard to the evaluation of $P(F_m, q)$ at $q = \tau + 1$ (with an appropriate choice of branch cuts for the square and cube roots), $\lambda_{F,1}$ and one of the other two roots of (5.107) comprise the complex-conjugate pair

$$\frac{1}{4} \left[-1 + \sqrt{5} \pm (-38 + 18\sqrt{5})^{1/2} i \right] \quad (5.111)$$

with magnitude 0.485867..., while the third root of (5.107) is equal to -1 . Since

0.485867.. is less than $\tau - 1 = 0.6180\dots$, the corresponding two coefficients do not have to, and do not, vanish at $q = \tau + 1$. Since the third root has magnitude greater than $\tau - 1$, its coefficient must vanish at $q = \tau + 1$ in order for $|P(F_m, \tau + 1)|$ to obey the Tutte upper bound (5.1). With these values of the $\lambda_{F,j}$'s at $q = \tau + 1$, the ratio $r(F_m)$ vanishes (exponentially rapidly) as $m \rightarrow \infty$ and $r(F_\infty) = 0$. This illustrates the general property that if $G_{pt,m}$ is a family of planar triangulations with $P(G_{pt,m}, q)$ of the form (5.14) and $\alpha = 1$ in (5.6), and if none of the $\lambda_{G_{pt,j}}$ has magnitude equal to $\tau - 1$ when evaluated at $q = \tau + 1$, then, since (i) the $\lambda_{G_{pt,j}}$ with $|\lambda_{G_{pt,j}}| > \tau - 1$ have coefficients that must vanish, and (ii) the $\lambda_{G_{pt,j}}$ with $|\lambda_{G_{pt,j}}| < \tau - 1$ give zero contribution in the limit $m \rightarrow \infty$, it follows that $r(G_{pt}) = 0$. We calculate

$$a_F = 0.786151\dots \quad (5.112)$$

The term $\lambda_{F,1}$ is real and positive and is dominant for $q > \tau + 2 = 3.618\dots$. In this interval, the other two roots, $\lambda_{F,j}$, $j = 2, 3$ are complex, with smaller magnitudes. At $q = \tau + 2$, $\lambda_{F,1} = -1$ and $|\lambda_{F,2}| = |\lambda_{F,3}| = 1$, so all $\lambda_{F,j}$ are degenerate in magnitude. Hence, in the notation of [52], $q_c = \tau + 2$ for this family. At $q = 3$, all $\lambda_{F,j} = 0$, $j = 1, 2, 3$, as is obvious from Eq. (5.107).

We exhibit the first few $P(F_m, q)$. For $m = 1$, $P(F_1, q) = a_{F,0}$, as given above in (5.96). For $m = 2$ to $m = 6$,

$$P(F_2, q) = q(q-1)(q-2)(q^3 - 9q^2 + 29q - 32) \quad (5.113)$$

$$P(F_3, q) = q(q-1)(q-2)(q-3)(q^3 - 9q^2 + 30q - 35) \quad (5.114)$$

$$P(F_4, q) = q(q-1)(q-2)(q-3)(q^4 - 12q^3 + 58q^2 - 133q + 119) \quad (5.115)$$

$$P(F_5, q) = q(q-1)(q-2)(q-3)(q^5 - 15q^4 + 95q^3 - 317q^2 + 553q - 398) \quad (5.116)$$

$$P(F_6, q) = q(q-1)(q-2)(q-3)^2(q^5 - 15q^4 + 96q^3 - 327q^2 + 591q - 447) \quad (5.117)$$

As m increases further, $P(F_m, q)$ has increasingly high powers of the factor $(q - 3)$.

As with the other planar triangulation families, the F_m family has chromatic zeros near to $\tau + 1$. We find that these approach $\tau + 1$ as m gets large. Depending on the value of m , $P(F_m, q)$ also may have real zeros in the interval

$[q_w, 3)$. The complex zeros of $P(F_m, q)$ form a complex-conjugate arc, with arc endpoints at the complex zeros of R_F , namely $q, q^* \simeq 1.9111 \pm 2.6502i$.

Chapter 6

Chromatic Polynomials of Planar Triangulation Graphs: II. Multi-Parameter Families and Implications for Statistical Physics

6.1 Two-Parameter Families of Planar Triangulations, G_{pt,m_1,m_2}

In this section we introduce a substantial generalization [71], to a two-parameter family G_{pt,m_1,m_2} of planar triangulations involving the three λ_j 's in (5.23) [71], with a chromatic polynomial of the form

$$P(G_{pt,m_1,m_2}, q) = \sum_{i_1=1}^3 \sum_{i_2=1}^3 c_{G,i_1 i_2} \lambda_{i_1}^{m_1} \lambda_{i_2}^{m_2} . \quad (6.1)$$

Explicitly,

$$\begin{aligned} P(G_{pt,m_1,m_2}, q) &= c_{G,11}(q-2)^{m_1+m_2} + c_{G,22}(q-3)^{m_1+m_2} + c_{G,33}(-1)^{m_1+m_2} \\ &+ c_{G,12}(q-2)^{m_1}(q-3)^{m_2} + c_{G,21}(q-3)^{m_1}(q-2)^{m_2} \\ &+ c_{G,13}(q-2)^{m_1}(-1)^{m_2} + c_{G,31}(-1)^{m_1}(q-2)^{m_2} \\ &+ c_{G,23}(q-3)^{m_1}(-1)^{m_2} + c_{G,32}(-1)^{m_1}(q-3)^{m_2} . \end{aligned} \quad (6.2)$$

(Below we shall often take $i_1 = i$, $i_2 = j$ to simplify the notation.) Clearly, if one keeps one of the indices m_1 or m_2 fixed and varies the other, this defines an infinite set of one-parameter families of planar triangulations. For specific families G_{pt,m_1,m_2} we will show how the general structure (6.1) reduces, in such cases, to the form (5.38) considered above for a class of one-parameter planar triangulations, with m being equal to the variable index, up to an appropriate integer shift.

As before for the one-parameter families, an equivalent way to obtain the $P(G_{pt,m_1,m_2}, q)$ is via a Taylor series expansion, in the auxiliary variables x_1 and x_2 , of a generating function $\Gamma(G_{pt}, q, x_1, x_2)$. Equivalent to both of these is the property that $P(G_{pt,m_1,m_2}, q)$ satisfies a two-dimensional recursion relation, for $m_1 \geq (m_1)_{min} + 3$ and $m_2 \geq (m_2)_{min} + 3$,

$$P(G_{pt,m_1,m_2}, q) + \sum_{i_1=1}^3 \sum_{i_2=1}^3 b_{G_{pt},i_1 i_2} P(G_{pt,m_1-i_1,m_2-i_2}, q) = 0 . \quad (6.3)$$

The coefficients in this recursion relation are given by

$$1 + \sum_{i_1=1}^3 \sum_{i_2=1}^3 b_{G_{pt},i_1 i_2} x_1^{i_1} x_2^{i_2} = \left[\prod_{i_1=1}^3 (1 - \lambda_{i_1} x_1) \right] \left[\prod_{i_2=1}^3 (1 - \lambda_{i_2} x_2) \right] . \quad (6.4)$$

Note that they satisfy the symmetry property

$$b_{G_{pt},i_1 i_2} = b_{G_{pt},i_2 i_1} . \quad (6.5)$$

We first derive a number of restrictions on the coefficients $c_{G,i_1 i_2}$. As is true of any triangulation, $P(G_{pt,m_1,m_2}, q) = 0$ for $q = 0$, $q = 1$, and $q = 2$. The evaluation $P(G_{pt,m_1,m_2}, 0) = 0$ reads

$$\begin{aligned} & c_{G,11}(-2)^{m_1+m_2} + c_{G,22}(-3)^{m_1+m_2} + c_{G,33}(-1)^{m_1+m_2} \\ & + c_{G,12}(-2)^{m_1}(-3)^{m_2} + c_{G,21}(-3)^{m_1}(-2)^{m_2} \\ & + c_{G,13}(-2)^{m_1}(-1)^{m_2} + c_{G,31}(-1)^{m_1}(-2)^{m_2} \\ & + c_{G,23}(-3)^{m_1}(-1)^{m_2} + c_{G,32}(-1)^{m_1}(-3)^{m_2} = 0 \quad \text{at } q = 0 . \end{aligned} \quad (6.6)$$

Since this equation applies for arbitrary m_1 and m_2 in their respective ranges, it implies that $c_{G,i_1 i_2} = 0$ for all i_1, i_2 at $q = 0$ and hence that

$$c_{G,i_1 i_2} \quad \text{contains the factor } q \quad \forall i_1, i_2 . \quad (6.7)$$

It will often be convenient to extract this common factor, via the definition

$$\bar{c}_{G,i_1 i_2} = \frac{c_{G,i_1 i_2}}{q} . \quad (6.8)$$

The evaluation $P(G_{pt,m_1,m_2}, 1) = 0$ reads

$$\begin{aligned} & [c_{G,11} + c_{G,33} + c_{G,13} + c_{G,31}](-1)^{m_1+m_2} + c_{G,22}(-2)^{m_1+m_2} \\ & + [c_{G,12} + c_{G,32}](-1)^{m_1}(-2)^{m_2} \\ & + [c_{G,21} + c_{G,23}](-2)^{m_1}(-1)^{m_2} = 0 \quad \text{at } q = 1 . \end{aligned} \quad (6.9)$$

Since this equation applies for arbitrary m_1 and m_2 , it implies the conditions

$$\begin{aligned} c_{G,11} + c_{G,33} + c_{G,13} + c_{G,31} &= 0, \quad c_{G,22} = 0, \\ c_{G,12} + c_{G,32} &= 0, \quad c_{G,21} + c_{G,23} = 0 \quad \text{at } q = 1 . \end{aligned} \quad (6.10)$$

In particular, this implies that

$$c_{G,22} \quad \text{contains the factor } q - 1 . \quad (6.11)$$

The evaluation $P(G_{pt,m_1,m_2}, 2) = 0$ reads

$$\begin{aligned} & c_{G,11}0^{m_1+m_2} + [c_{G,22} + c_{G,33} + c_{G,23} + c_{G,32}](-1)^{m_1+m_2} \\ & + [c_{G,12} + c_{G,13}]0^{m_1}(-1)^{m_2} + [c_{G,21} + c_{G,31}](-1)^{m_1}0^{m_2} = 0 \quad \text{at } q = 2 . \end{aligned} \quad (6.12)$$

Since this equation applies for arbitrary m_1 and m_2 , including $m_1 = m_2 = 0$, it implies the conditions

$$\begin{aligned} c_{G,11} &= 0, \quad c_{G,22} + c_{G,33} + c_{G,23} + c_{G,32} = 0, \\ c_{G,12} + c_{G,13} &= 0, \quad c_{G,21} + c_{G,31} = 0 \quad \text{at } q = 2 . \end{aligned} \quad (6.13)$$

In particular, this implies that

$$c_{G,11} \quad \text{contains the factor } q - 2 . \quad (6.14)$$

For families G_{pt,m_1,m_2} with $\chi(G_{pt,m_1,m_2}) = 4$ for certain values of m_1 and m_2 , further conditions hold, as we shall discuss below.

We next derive some further restrictions on the coefficients $c_{G,i_1 i_2}$ from

the condition that $P(G_{pt,m_1,m_2}, q)$ must obey the Tutte upper bound when evaluated at $q = \tau + 1$. We consider families such that

$$n(G_{pt,m_1,m_2}) = m_1 + m_2 + \beta \quad (6.15)$$

Carrying out this evaluation and calculating the ratio $r(G_{pt,m_1,m_2})$, we have

$$\begin{aligned} r(G_{pt,m_1,m_2}) &= (\tau - 1)^{5-\beta} \left| c_{G,11} + c_{G,22} \left(\frac{\tau - 2}{\tau - 1} \right)^{m_1+m_2} + c_{G,33} \left(\frac{-1}{\tau - 1} \right)^{m_1+m_2} \right. \\ &+ c_{G,12} \left(\frac{\tau - 2}{\tau - 1} \right)^{m_2} + c_{G,21} \left(\frac{\tau - 2}{\tau - 1} \right)^{m_1} \\ &+ c_{G,13} \left(\frac{-1}{\tau - 1} \right)^{m_2} + c_{G,31} \left(\frac{-1}{\tau - 1} \right)^{m_1} \\ &\left. + c_{G,23} \frac{(\tau - 2)^{m_1} (-1)^{m_2}}{(\tau - 1)^{m_1+m_2}} + c_{G,32} \frac{(-1)^{m_1} (\tau - 2)^{m_2}}{(\tau - 1)^{m_1+m_2}} \right|. \end{aligned} \quad (6.16)$$

The condition that $r(G_{pt,m_1,m_2}) \leq 1$ for arbitrary m_1 and m_2 implies that

$$c_{G,33} = c_{G,13} = c_{G,31} = c_{G,23} = c_{G,32} = 0 \quad \text{at } q = \tau + 1. \quad (6.17)$$

By the same argument that we used above for the analysis of the coefficients of chromatic polynomials of one-parameter planar triangulation graphs, (6.17) implies that

$$c_{G,i_1 i_2} \quad \text{contains the factor } q^2 - 3q + 1 \quad \text{if } i_1 = 3 \text{ or } i_2 = 3. \quad (6.18)$$

By taking either $m_1 \rightarrow \infty$ or $m_2 \rightarrow \infty$, and requiring that the resultant ratio $r(G_{pt,\infty,m_2})$ or $r(G_{pt,m_1,\infty})$ must obey the Tutte upper bound, one deduces the inequality

$$(\tau - 1)^{5-\beta} |c_{G,11}| < 1 \quad \text{at } q = \tau + 1. \quad (6.19)$$

We next generalize our result on a real chromatic zero that approaches $q = \tau + 1$ for one-parameter planar triangulations to these two-parameter planar triangulations with $P(G_{pt,m_1,m_2}, q)$ of the form (6.1). As in the $p = 1$ case, we assume that q is a real number in the interval $[q_w, 3)$. We will actually obtain two results, corresponding to $m_1 \rightarrow \infty$ for fixed m_2 and $m_2 \rightarrow \infty$ for fixed m_1 . For the first of these limits, the six terms proportional to $c_{G,11}$, $c_{G,22}$, $c_{G,12}$, $c_{G,21}$, $c_{G,13}$, and $c_{G,23}$ all vanish (exponentially rapidly), so that

$$P(G_{pt,m_1,m_2}, q) \sim c_{G,33} (-1)^{m_1+m_2} + c_{G,31} (-1)^{m_1} (q-2)^{m_2} + c_{G,32} (-1)^{m_1} (q-3)^{m_2} \quad \text{for } m_1 \rightarrow \infty \quad (6.20)$$

But we have shown above in (6.18) that $c_{G,i_1 i_2}$ contains the factor $q^2 - 3q + 1$

if $i_1 = 3$ or $i_2 = 3$. Since this factor vanishes at $q = \tau + 1$ in this interval $[q_w, 3)$, it follows that for sufficiently large m_1 , $P(G_{pt,m_1,m_2}, q)$ has a real zero that approaches $\tau + 1$. With obvious changes, a corresponding argument shows that for sufficiently large m_2 and fixed m_1 , $P(G_{pt,m_1,m_2}, q)$ has a real zero that approaches $\tau + 1$. Clearly, the result also holds if both m_1 and m_2 get large.

6.2 General Form of $P(G_{pt,\mathbf{m}}, q)$

The generalization of our structural results for two-parameter families of planar triangulations, G_{pt,m_1,m_2} to p -parameter families is as follows. Let $G_{pt,\mathbf{m}}$ be a family of planar triangulation graphs involving the three λ_j 's in (5.23) and depending on the p parameters $\mathbf{m} = (m_1, \dots, m_p)$ taking on integer values in the ranges $m_i \geq (m_i)_{min}$, $i = 1, \dots, p$. Then

$$P(G_{pt,m_1,\dots,m_p}, q) = \sum_{i_1=1}^3 \cdots \sum_{i_p=1}^3 c_{G_{pt,i_1\dots i_p}} \left[\prod_{\ell=1}^p \lambda_{i_\ell}^{m_\ell} \right]. \quad (6.21)$$

In general, there are 3^p terms involving products of the λ 's (multiplied by respective coefficients) in this sum.

This general form is of considerable interest. It shows that one can carry out a p -fold sequence of edge proliferations, each of which involves arbitrarily many additional edges, as indexed by the parameters m_1, \dots, m_p , with the chromatic polynomial $P(G_{pt,\mathbf{m}}, q)$ still retaining the rather simple form (6.21) with the same set of three λ_i 's given in (5.23). This is a much simpler situation than that in previous calculations of chromatic polynomials for multiparameter families of graphs. For example, in [61], Shrock and Tsai calculated the chromatic polynomial $P(G_{e_1,e_2,e_g,m}, q)$ for a certain four-parameter family of cyclic chain graphs in which each subgraph on the chain has e_1 edges above, and e_2 edges below, the main line, with e_g edges between the subgraphs, and m subgraphs in all. Although the number N_λ of $\lambda_{G,j}$'s for this family has the fixed value of 2, the $\lambda_{G,j}$'s have functional forms that depend on the parameters e_1 , e_2 , and e_g (as is the case for the full Potts model partition function [51]). This property was also found to be true for (i) the chromatic polynomials $P((Ch)_{k,m,cyc}, q)$ and $P((Ch)_{k,m,Mb}, q)$ of cyclic (*cyc.*) and Möbius (*Mb.*) strips depending on a homeomorphic expansion parameter k and the strip length, m , where $N_\lambda = 4$ and three of the $\lambda_{Ch,j}$'s depended on k [64]; and (ii) $P(H_{k,r}, q)$ for a family of “hammock” graphs $H_{k,r}$ with r “ropes” (linear sets of edges) joining two end vertices, with each rope having k “knots” (vertices), where again the $N_\lambda = 2$ terms $\lambda_{H,j}$ depended on k and r [60] [62]. The remarkable simplicity of the form (6.21) is a result of the restrictive property that $G_{pt,\mathbf{m}}$ is a planar tri-

angulation. We know that this simple behavior does not obtain even for the lowest case of one-parameter families for planar near-triangulations, from the explicit calculation the chromatic polynomials for free strips of the triangular lattice of length m and width $L_y = 2, 3$ [46] (which are near-triangulations), where it was found that the λ 's changed with increasing width [46]. (Here a near-triangulation is defined as a graph such that all faces except one are triangles.) We also know that it does not hold for nonplanar triangulations, from explicit calculations of chromatic polynomials for the $L_y = 2$ [17], $L_y = 3$ [18], and $L_y = 4$ [20] strips of the triangular lattice with doubly periodic (toroidal) boundary conditions. Thus, chromatic polynomials of multiparameter families of planar triangulation are especially amenable to exact analytic treatment.

The $P(G_{pt,m_1,\dots,m_p}, q)$ satisfy a p -dimensional recursion relation, for $m_\ell \geq (m_\ell)_{min} + 3$, $\ell = 1, \dots, p$, namely

$$P(G_{pt,m_1,\dots,m_p}, q) + \sum_{i_1=1}^3 \cdots \sum_{i_p=1}^3 b_{G_{pt,i_1\dots i_p}} P(G_{pt,m_1-i_1,\dots,m_p-i_p}, q) = 0 \quad (6.22)$$

where the $b_{G_{pt,i_1\dots i_p}}$ are given by

$$1 + \sum_{i_1=1}^3 \cdots \sum_{i_p=1}^3 b_{G_{pt,i_1\dots i_p}} \left(\prod_{s=1}^p x_s^{i_s} \right) = \prod_{\ell=1}^p \left[\prod_{i=1}^3 (1 - \lambda_i x_\ell) \right]. \quad (6.23)$$

Using the same methods as for $p = 2$, it is straightforward to generalize our results to this case, including (i) the conditions on the coefficients $c_{G_{pt},\mathbf{i}}$ (where $\mathbf{i} \equiv (i_1\dots i_p)$) derived from the evaluations $P(G_{pt,m}, q) = 0$ for $q = 0, 1, 2$ and the Tutte upper bound at $q = \tau + 1$, and (ii) the results for $r(G_{pt,m})$ and its limits as one or more of the $m_i \rightarrow \infty$. Clearly, our result on a real zero in the interval $[q_w, 3)$ that approaches $\tau + 1$ also generalizes to this case of families $G_{pt,m}$ with $p \geq 3$.

As in the $p = 2$ case, if one holds all but one of the m_1, \dots, m_p fixed and allows one to vary, then the general form (6.21) reduces to (5.38) with m being equal to the variable parameter, up to an appropriate integer shift.

6.3 The Two-Parameter Family D_{m_1,m_2}

We proceed to analyze our first explicit two-parameter family of planar triangulations, denoted D_{m_1,m_2} (where D stands for the proliferation of a double set of edges). To explain the general method of construction of this family, we

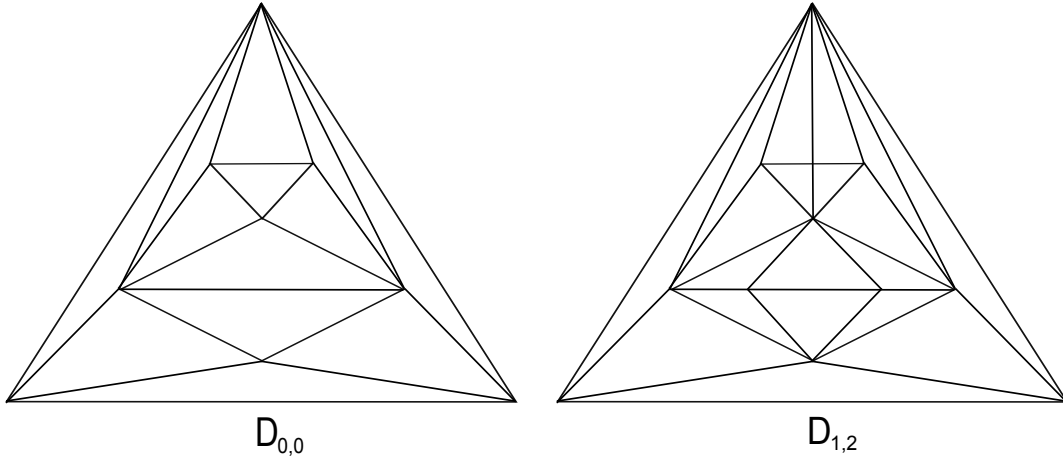


Figure 6.1: Graphs $D_{0,0}$ and $D_{1,2}$.

show in Fig. (6.1) the lowest member of the series, namely the graph $D_{0,0}$. We now add m_1 inner edges joining the uppermost vertex to the upper horizontal edge (thereby producing several such upper horizontal edges) and, separately, add m_2 inner edges joining the central vertex to the lower horizontal edge (thereby producing several such lower horizontal edges), with corresponding edges connecting to the lower central vertex. Thus, in the D_{m_1,m_2} graph, the uppermost vertex has degree $6 + m_1$, the central vertex has degree $m_1 + m_2 + 4$, and the lower central vertex has degree $4 + m_2$. To illustrate this, we show the graphs $D_{1,2}$, $D_{2,2}$ in Figs.(6.1) and (6.2).

From inspection of these graphs, it is evident how to construct D_{m_1,m_2} graphs with higher values of m_1 and m_2 . The number of vertices in the graph D_{m_1,m_2} is

$$n(D_{m_1,m_2}) = m_1 + m_2 + 9 . \quad (6.24)$$

For the chromatic number, we find that (i) if m_2 is odd, then $\chi(D_{m_1,m_2}) = 4$, and (ii) if m_2 is even, then $\chi(D_{m_1,m_2}) = 3$ if m_1 is even and $\chi(D_{m_1,m_2}) = 4$ if m_1 is odd. That is, denoting even as e and odd as o , $\chi(D_{m_1,m_2}) = 3$ for $(m_1, m_2) = (e, e)$ and $\chi(D_{m_1,m_2}) = 4$ for $(m_1, m_2) = (e, o)$, (o, o) , and (o, e) . The chromatic polynomials for the D_{m_1,m_2} with $\chi = 4$ contain a factor $P(K_4, q) = q(q-1)(q-2)(q-3)$ (and some contain an additional factor of $(q-3)$). Of course, all chromatic polynomials of triangulations have the factor $P(K_3, q) = q(q-1)(q-2)$.

By means of an iterative use of the deletion-contraction relation, we have calculated the chromatic polynomial $P(D_{m_1,m_2}, q)$ for an arbitrary graph in this general two-parameter D_{m_1,m_2} family. We find that $P(D_{m_1,m_2}, q)$ has the

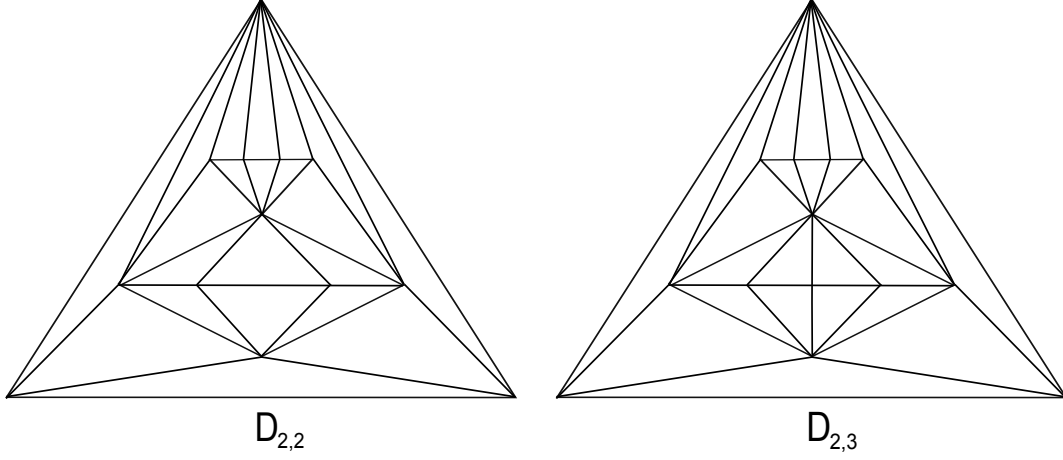


Figure 6.2: Graphs $D_{2,2}$ and $D_{2,3}$.

form (6.1) with coefficients $c_{D,ij}$ that are rational functions of q . With the definition (6.8), we calculate

$$\bar{c}_{D,11} = \frac{(q-2)^7}{q-1}, \quad (6.25)$$

$$\bar{c}_{D,22} = \frac{(q-1)(q-3)^5(q^3 - 9q^2 + 30q - 35)}{q-2}, \quad (6.26)$$

$$\bar{c}_{D,33} = \frac{(q^5 - 11q^4 + 46q^3 - 88q^2 + 74q - 23)(q^2 - 3q + 1)}{(q-1)(q-2)}, \quad (6.27)$$

$$\bar{c}_{D,12} = (q-2)^3(q-3)^4, \quad (6.28)$$

$$\bar{c}_{D,21} = (q-2)(q-3)^6, \quad (6.29)$$

$$\bar{c}_{D,13} = \frac{(q-2)^3(q^2 - 3q + 1)}{q-1}, \quad (6.30)$$

$$\bar{c}_{D,31} = \frac{(q-2)(q^2 - 3q + 1)}{q-1}, \quad (6.31)$$

$$\bar{c}_{D,23} = -\frac{(q-3)^4(q-5)(q^2 - 3q + 1)}{q-2}, \quad (6.32)$$

and

$$\bar{c}_{D,32} = -\frac{(q-3)^2(q-5)(q^2 - 3q + 1)}{q-2}. \quad (6.33)$$

It should be noted that the poles at $q = 1$ and $q = 2$ in certain of these $c_{D,ij}$

coefficients are cancelled in the actual evaluation of $P(D_{m_1, m_2}, q)$, which is, as it must be, a polynomial in q . Furthermore, not only are these poles cancelled, but also the resultant $P(D_{m_1, m_2}, q)$ vanishes at $q = 0$, $q = 1$, and $q = 2$. It is easily verified that the coefficients $c_{D, ij}$ satisfy the requisite conditions (6.10) and (6.13) for these zeros to occur.

Furthermore, since $c_{D, 11} = c_{D, 33} = c_{D, 13} = c_{D, 31} = 3/2$ with the other $c_{D, ij} = 0$ at $q = 3$, it follows that

$$P(D_{m_1, m_2}, 3) = \frac{3}{2} \left[1 + (-1)^{m_1+m_2} + (-1)^{m_2} + (-1)^{m_1} \right]. \quad (6.34)$$

This vanishes for $(m_1, m_2) = (e, o)$, (o, o) , and (o, e) , and is nonvanishing for $(m_1, m_2) = (e, e)$ in our notation above, in agreement with our result on the chromatic number $\chi(D_{m_1, m_2})$.

We proceed to discuss the evaluation of the chromatic polynomial $P(D_{m_1, m_2}, q)$ at $q = \tau + 1$ and the comparison with the Tutte upper bound. We have

$$\begin{aligned} P(D_{m_1, m_2}, \tau + 1) &= (9 - 4\sqrt{5})(\tau - 1)^{m_1+m_2} + \left(\frac{445 - 199\sqrt{5}}{2} \right) (\tau - 2)^{m_1+m_2} \\ &+ \left(\frac{-38 + 17\sqrt{5}}{2} \right) (\tau - 1)^{m_1} (\tau - 2)^{m_2} \\ &+ \left(\frac{-199 + 89\sqrt{5}}{2} \right) (\tau - 2)^{m_1} (\tau - 1)^{m_2} \end{aligned} \quad (6.35)$$

Comparing this with the Tutte upper bound $(\tau - 1)^{m_1+m_2+4}$, we have

$$\begin{aligned} r(D_{m_1, m_2}) &= \frac{3 - \sqrt{5}}{2} + \left(\frac{65 - 29\sqrt{5}}{2} \right) \left(\frac{1 - \sqrt{5}}{2} \right)^{m_1+m_2} \\ &+ \left(\frac{-11 + 5\sqrt{5}}{2} \right) \left(\frac{1 - \sqrt{5}}{2} \right)^{m_2} \\ &+ \left(\frac{-29 + 13\sqrt{5}}{2} \right) \left(\frac{1 - \sqrt{5}}{2} \right)^{m_1}. \end{aligned} \quad (6.36)$$

We list a number of values of $r(D_{m_1, m_2})$ in Table (6.1). One may investigate the behavior of $r(D_{m_1, m_2})$ as $m_1 \rightarrow \infty$ for fixed m_2 and as $m_2 \rightarrow \infty$ for fixed m_1 . Because the quantity $(1 - \sqrt{5})/2$ that is raised to the powers indicated in (6.36) is negative, it follows that, if one keeps m_2 fixed and increases m_1 , then $r(D_{m_1, m_2})$ does not approach $r(D_{\infty, m_2})$ monotonically, although the members of the subsequences $r(D_{m_1, m_2})$ with even (odd) m_1 approach $r(D_{\infty, m_2})$ monotonically from above (below), respectively. Similarly, if one keeps m_1 fixed

and increases m_2 , then $r(D_{m_1, m_2})$ does not approach $r(D_{m_1, \infty})$ monotonically, although the members of the subsequences $r(D_{m_1, m_2})$ with even (odd) m_2 approach $r(D_{m_1, \infty})$ monotonically from above (below), respectively. The results are

$$r(D_{\infty, m_2}) \equiv \lim_{m_1 \rightarrow \infty} r(D_{m_1, m_2}) = \frac{3 - \sqrt{5}}{2} + \left(\frac{-11 + 5\sqrt{5}}{2} \right) \left(\frac{1 - \sqrt{5}}{2} \right)^{m_2} \quad (6.37)$$

$$r(D_{m_1, \infty}) \equiv \lim_{m_2 \rightarrow \infty} r(D_{m_1, m_2}) = \frac{3 - \sqrt{5}}{2} + \left(\frac{-29 + 13\sqrt{5}}{2} \right) \left(\frac{1 - \sqrt{5}}{2} \right)^{m_1} \quad (6.38)$$

In the limit where one takes both m_1 and m_2 to ∞ , one has

$$\begin{aligned} r(D_{\infty, \infty}) &= \lim_{m_1 \rightarrow \infty} \lim_{m_2 \rightarrow \infty} r(D_{m_1, m_2}) = \lim_{m_2 \rightarrow \infty} \lim_{m_1 \rightarrow \infty} r(D_{m_1, m_2}) \\ &= \frac{3 - \sqrt{5}}{2} = 2 - \tau = 0.381966... \end{aligned} \quad (6.39)$$

As m_2 increases from 0 to ∞ , $r(D_{\infty, m_2})$ decreases (non-monotonically) from the value

$$r(D_{\infty, 0}) = -4 + 2\sqrt{5} = 0.4721359... \quad (6.40)$$

to the value in (6.39), and as m_1 increases from 0 to ∞ , $r(D_{m_1, \infty})$ decreases (non-monotonically) from the value

$$r(D_{0, \infty}) = -13 + 6\sqrt{5} = 0.4164078... \quad (6.41)$$

to the value in (6.39). As a consequence of the relation (6.57) (see below), it follows that

$$r(D_{\infty, k+2}) = r(D_{k, \infty}) \quad (6.42)$$

In general, the maximal value of $r(D_{m_1, m_2})$ occurs for the member of the D_{m_1, m_2} family with the minimal values of m_1 and m_2 , namely for $D_{0,0}$. This property is similar to the property that the maximum value of $r(G_{pt})$ for all planar triangulations G_{pt} occurs for the G_{pt} with the minimum number of vertices, namely the single triangle, K_3 .

We next show that our general form for $P(D_{m_1, m_2}, q)$ reduces to (5.38) when either m_2 is held fixed and m_1 varies, or vice versa. If we keep m_2 fixed and vary m_1 , then we can write $P(D_{m_1, m_2}, q)$ as

$$P(D_{m_1, m_2}, q) = \sum_{i=1}^3 \left[\sum_{j=1}^3 c_{D, ij} \lambda_j^{m_2} \right] \lambda_i^{m_1}. \quad (6.43)$$

Table 6.1: Values of the ratio $r(D_{m_1, m_2})$. The rows and columns list m_1 and m_2 , respectively, so that, for example, $r(D_{1,2})$ is the entry 0.3769.

m_1, m_2	0	1	2	3	4	5	6	∞
0	0.5836	0.3131	0.4803	0.3769	0.4408	0.4013	0.4257	0.4164
1	0.4033	0.3344	0.3769	0.3506	0.3669	0.3568	0.3631	0.3607
2	0.5147	0.3212	0.4408	0.3669	0.4126	0.3843	0.4018	0.3951
3	0.4458	0.3293	0.4013	0.3568	0.3843	0.3673	0.3778	0.3738
4	0.4884	0.3243	0.4257	0.36305	0.4018	0.3778	0.3926	0.3870
5	0.4621	0.3274	0.4106	0.3592	0.3910	0.3714	0.3835	0.3789
6	0.4783	0.3255	0.4200	0.3616	0.3977	0.3754	0.38915	0.3839
∞	0.4721	0.3262	0.4164	0.3607	0.3951	0.3738	0.3870	0.3820

The sum $\sum_{j=1}^3 c_{D,ij} \lambda_j^{m_2}$ contains a factor λ_i^4 , which we combine with the $\lambda_i^{m_1}$, to make λ_i^m , where

$$m = m_1 + 4 . \quad (6.44)$$

This shows that $P(D_{m_1, m_2}, q)$ has the form (5.38) with m given by (6.44); explicitly,

$$P(D_{m-4, m_2}, q) = \sum_{i=1}^3 c_{D_{m_2(\ell)}, i} \lambda_i^m , \quad (6.45)$$

where

$$c_{D_{m_2(\ell)}, i} = \lambda_i^{-4} \sum_{j=1}^3 c_{D,ij} \lambda_j^{m_2} . \quad (6.46)$$

Here, since these coefficients depend only on m_2 , and not on m_1 , we have introduced the notation $D_{m_2(\ell)}$ to refer to the entire family D_{m_1, m_2} with fixed m_2 and variable m_1 , where ℓ indicates that m_2 describes the edge proliferation in the lower part of the graph. Expressing (5.35)-(5.37) in our notation (and suppressing the q arguments), we have

$$c_{D_{m_2(\ell)}, 1} = q \kappa_{D_{m_2(\ell)}, 1} , \quad (6.47)$$

$$c_{D_{m_2(\ell)}, 2} = q(q-1) \kappa_{D_{m_2(\ell)}, 2} , \quad (6.48)$$

and

$$c_{D_{m_2(\ell)}, 3} = q(q^2 - 3q + 1) \kappa_{D_{m_2(\ell)}, 3} . \quad (6.49)$$

Similarly, if we keep m_1 fixed and vary m_2 , then we can write $P(D_{m_1, m_2}, q)$

as

$$P(D_{m_1, m_2}, q) = \sum_{j=1}^3 \left[\sum_{i=1}^3 c_{D, ij} \lambda_i^{m_1} \right] \lambda_j^{m_2} . \quad (6.50)$$

The sum $\sum_{i=1}^3 c_{D, ij} \lambda_i^{m_1}$ contains a factor λ_j^2 , which we combine with the $\lambda_j^{m_2}$, to make λ_j^m , where, for this one-parameter reduction,

$$m = m_2 + 2 . \quad (6.51)$$

This shows that $P(D_{m_1, m_2}, q)$ has the form (5.38) with m given by (6.51); explicitly,

$$P(D_{m_1, m-2}, q) = \sum_{j=1}^3 c_{D_{m_1(u), j}} \lambda_j^m , \quad (6.52)$$

where

$$c_{D_{m_1(u), j}} = \lambda_j^{-2} \sum_{i=1}^3 c_{D, ij} \lambda_i^{m_1} . \quad (6.53)$$

Here again, since these coefficients depend only on m_1 , and not on m_2 , we have introduced the notation $D_{m_1(u)}$ to refer to the entire family D_{m_1, m_2} with fixed m_1 and variable m_2 , where u indicates that m_1 describes the edge proliferation in the upper part of the graph. As before, we write

$$c_{D_{m_1(u), 1}} = q \kappa_{D_{m_1(u), 1}} , \quad (6.54)$$

$$c_{D_{m_1(u), 2}} = q(q-1) \kappa_{D_{m_1(u), 2}} , \quad (6.55)$$

and

$$c_{D_{m_1(u), 3}} = q(q^2 - 3q + 1) \kappa_{D_{m_1(u), 3}} . \quad (6.56)$$

We find that

$$c_{D_{k+2(\ell), i}} = c_{D_{k(u), i}} \quad \text{for } i = 1, 2, 3 \quad (6.57)$$

and thus

$$\kappa_{D_{k+2(\ell), i}} = \kappa_{D_{k(u), i}} \quad \text{for } i = 1, 2, 3 . \quad (6.58)$$

However, we note that for arbitrary q ,

$$P(D_{m_1, m_2}, q) \neq P(D_{m_2, m_1}, q) \quad \text{unless } m_1 = m_2 . \quad (6.59)$$

Table 6.2: Values of the ratios $r(D_{m_1,\infty})$ and $r(D_{\infty,m_2})$. Note that $r(D_{k,\infty}) = r(D_{\infty,k-2})$ for $k \geq 2$.

$r(D_{\infty,m_2}), r(D_{m_1,\infty})$	analytic	numerical
$r(D_{\infty,0})$	$-4 + 2\sqrt{5}$	0.472136
$r(D_{\infty,1})$	$(-15 + 7\sqrt{5})/2$	0.326238
$r(D_{\infty,2}) = r(D_{0,\infty})$	$-13 + 6\sqrt{5}$	0.416408
$r(D_{\infty,3}) = r(D_{1,\infty})$	$-22 + 10\sqrt{5}$	0.360680
$r(D_{\infty,4}) = r(D_{2,\infty})$	$(-73 + 33\sqrt{5})/2$	0.395122
$r(D_{\infty,5}) = r(D_{3,\infty})$	$-60 + 27\sqrt{5}$	0.373835
$r(D_{\infty,6}) = r(D_{4,\infty})$	$-98 + 44\sqrt{5}$	0.386991
$r(D_{\infty,7}) = r(D_{5,\infty})$	$(-319 + 143\sqrt{5})/2$	0.378860
$r(D_{\infty,8}) = r(D_{6,\infty})$	$-259 + 116\sqrt{5}$	0.383885
$r(D_{\infty,9}) = r(D_{7,\infty})$	$-420 + 188\sqrt{5}$	0.380780
$r(D_{\infty,10}) = r(D_{8,\infty})$	$(-1361 + 609\sqrt{5})/2$	0.382700
$r(D_{\infty,\infty})$	$(3 - \sqrt{5})/2$	0.381966

6.4 The Family $D_{m-4,0}$

We proceed to examine a number of different D_{m_1,m_2} families of planar triangulations, with m_2 held fixed. Then, we will analyze analogous families with m_1 held fixed, and finally, we will investigate families in which both m_1 and m_2 vary together, and are related in a linear manner. For a given graph D_{m_1,m_2} , one can use either our general result for $P(D_{m_1,m_2}, q)$ above or either of the one-parameter reductions, (6.45) or (6.52). However, we shall be interested in the limits $m_1 \rightarrow \infty$ with m_2 fixed, and $m_2 \rightarrow \infty$ with m_1 fixed, and, to study these, it is convenient to use the one-parameter reductions of our general formula.

We begin with a study of the family $D_{m_1,0} \equiv D_{m-4,0}$ with $m_1 \geq 0$, i.e., $m \geq 4$. From (6.24), we have $n(D_{m-4,0}) = m + 5$. For the coefficients that enter into the equation (5.38), our general formulas (6.46)-(6.49) yield

$$\kappa_{D_{0(\ell),1}} = \kappa_{D_{0(\ell),2}} = \kappa_{D_{0(\ell),3}} = q^3 - 9q^2 + 29q - 32 \quad (6.60)$$

(equal to λ_{TC}). Because these coefficients $\kappa_{D_{0(\ell),j}}$ are all the same, λ_{TC} is a common factor, so for all m , the three zeros of λ_{TC} are zeros of $P(D_{m-4,0}, q)$. Of these, one is real, namely q_w , given in (5.46). In accordance with our general analysis above, $P(D_{m-4,0}, q)$ also has a zero, denoted q_z , that approaches $\tau + 1$

as m increases.

For the evaluation at $q = \tau + 1$, we have

$$P(D_{m-4,0}, \tau + 1) = (-4 + 2\sqrt{5})(\tau - 1)^m + (3 - \sqrt{5})(\tau - 2)^m, \quad (6.61)$$

so that

$$r(D_{m-4,0}) = -4 + 2\sqrt{5} + (3 - \sqrt{5}) \left(\frac{1 - \sqrt{5}}{2} \right)^m. \quad (6.62)$$

Hence,

$$r(D_{\infty,0}) = -4 + 2\sqrt{5} = 0.4721359\dots \quad (6.63)$$

with $a_{D_0(\ell)} = 1$.

6.5 The Family $D_{m-4,1}$

We continue with a study of the family $D_{m,1} \equiv D_{m-4,1}$. From (6.24), we have $n(D_{m-4,1}) = m + 6$. Our general formulas (6.46)-(6.49) give the coefficients $\kappa_{D_{1(\ell)},j}$ as

$$\kappa_{D_{1(\ell)},1} = (q - 3)(q^3 - 9q^2 + 30q - 35), \quad (6.64)$$

$$\kappa_{D_{1(\ell)},2} = q^4 - 12q^3 + 58q^2 - 133q + 119, \quad (6.65)$$

and

$$\kappa_{D_{1(\ell)},3} = -(q - 3)(2q^2 - 14q + 25). \quad (6.66)$$

If m is even, then $P(D_{m-4,1}, q)$ has not only the factor $q(q - 1)(q - 2)(q - 3)$, but also an additional factor of $(q - 3)$. According to our general analysis above, $P(D_{m-4,1}, q)$ has a real zero that approaches $\tau + 1$ as $m \rightarrow \infty$. We also derived the result that for sufficiently large m , a chromatic polynomial of the form (5.38) has another real zero in the interval $[q_w, 3)$ if and only if $\kappa_{G_{pt},3}$ has a zero in this interval. For the present family, $\kappa_{D_{1(\ell)},3}$ has zeros at $q = 3$ and the complex-conjugate pair $q = (7 \pm i)/2$, but does not have a zero in the interval $[q_w, 3)$, in accordance with the fact that $P(D_{m-4,1}, q)$ also does not have a zero in this interval.

For the evaluation at $\tau + 1$, we compute

$$P(D_{m-4,1}, \tau + 1) = \left(\frac{25 + 11\sqrt{5}}{2} \right) (\tau - 1)^m + (-9 + 4\sqrt{5})(\tau - 2)^m, \quad (6.67)$$

so that

$$r(D_{m-4,1}) = \frac{-15 + 7\sqrt{5}}{2} + \left(\frac{11 - 5\sqrt{5}}{2} \right) \left(\frac{1 - \sqrt{5}}{2} \right)^m . \quad (6.68)$$

and

$$r(D_{\infty,1}) = \frac{-15 + 7\sqrt{5}}{2} = 0.3226238 \quad (6.69)$$

with $a_{D_{1(\ell)}} = 1$.

6.6 The Family $D_{m-4,2}$

We next study the family $D_{m_1,2} \equiv D_{m-4,2}$ with $m_1 \geq 0$, i.e., $m \geq 4$. Note that $D_{1,2}$ is the same as the graph denoted G_{ce12} in Fig. 8 of [70]. From (6.24), we have $n(D_{m-4,2}) = m + 7$. For this family our general results give

$$\kappa_{D_{2(\ell),1}} = q^5 - 15q^4 + 94q^3 - 303q^2 + 498q - 332 , \quad (6.70)$$

$$\kappa_{D_{2(\ell),2}} = q^5 - 15q^4 + 95q^3 - 317q^2 + 553q - 398 , \quad (6.71)$$

and

$$\kappa_{D_{2(\ell),3}} = -(q^4 - 16q^3 + 91q^2 - 225q + 206) . \quad (6.72)$$

In Table (6.3) we list (real) zeros of $P(D_{m-4,2}, q)$ in the interval $q \in [q_w, 3)$ as a function of n . As proved above, one zero approaches $\tau + 1$ as $m \rightarrow \infty$. In the same limit, our general analysis above shows that $P(D_{m-4,2}, q)$ has real zero(s) in the interval $[q_w, 3)$ corresponding to the zeros of $\kappa_{D_{2(\ell),3}}$ in this interval. This quartic polynomial has a zero at

$$q = 2.7227000945... \quad (6.73)$$

together with one more real zero at $q = 6.955106...$, outside the interval $[q_w, 3)$, and a complex-conjugate pair. Hence, $P(D_{m-4,2}, q)$ has another zero in the interval $[q_w, 3)$, which is present for $m \geq 5$, and this approaches the zero of $\kappa_{D_{2(\ell),3}}$ given in (6.73) as $m \rightarrow \infty$. For even $m \geq 6$, i.e., odd $n \geq 13$, the real zero near to this asymptotic value (6.73) increases toward it, while for odd $m \geq 5$, i.e., even $n \geq 12$, the nearby real decreases toward the asymptotic value. As noted above, the graph $D_{0,2}$ coincides with the graph $G_{CM,1}$ of [70], for which there is no real zero close to $\tau + 1$; instead, the zeros closest to $\tau + 1$ comprise a complex-conjugate pair at $q = 2.641998 \pm 0.014795i$. Correspondingly, for $D_{0,2}$ there is no zero q'_z in the interval $[q_w, 3)$. For all of the $D_{m-4,2}$ with $m \geq 5$ in Table (6.3), the first real zero q_z in the interval

$[q_w, 3)$ is, in fact, the closest to $\tau + 1$.

The evaluation at $q = \tau + 1$ yields

$$P(D_{m-4,2}, \tau + 1) = \left(\frac{-69 + 31\sqrt{5}}{2} \right) (\tau - 1)^m + (27 - 12\sqrt{5}) (\tau - 2)^m, \quad (6.74)$$

so that

$$r(D_{m-4,2}) = -13 + 6\sqrt{5} + \left(\frac{21 - 9\sqrt{5}}{2} \right) \left(\frac{1 - \sqrt{5}}{2} \right)^m. \quad (6.75)$$

Hence,

$$r(D_{\infty,2}) = -13 + 6\sqrt{5} = 0.41640786... \quad (6.76)$$

with $a_{D_{2(\ell)}} = 1$.

Table 6.3: Location of real zeros of $P(D_{m-4,2}, q)$ in the interval $q \in [q_w, 3)$, as a function of the number of vertices, $n = m + 7$. Here the notation nz means that there is no second real zero in the interval $[q_w, 3)$.

n	q_z	q'_z
11	c.c. pair	nz
12	2.614614	2.818897
13	2.621801	2.689610
14	2.616506	2.762806
15	2.619226	2.705035
16	2.6174035	2.741044
17	2.618462	2.713055
18	2.617785	2.731543
19	2.618194	2.717464
20	2.617938	2.727100
21	2.618094	2.719886
22	2.617997	2.724931
23	2.618057	2.721202
24	2.618020	2.723845

6.7 The Family $D_{m-4,3}$

The final family that we study in this series is $D_{m_1,3} \equiv D_{m-4,3}$, with $m_1 \geq 0$, i.e., $m \geq 4$. From (6.24), it follows that the graph $D_{m-4,3}$ has $n(D_{m-4,3}) = m + 8$. A representative graph of this family is $D_{2,3}$ shown in Fig. (6.2).

For the coefficients $\kappa_{D_{3(\ell)},j}$ we have

$$\kappa_{D_{3(\ell)},1} = (q-3)(q^2 - 5q + 7)(q^3 - 10q^2 + 38q - 49) , \quad (6.77)$$

$$\kappa_{D_{3(\ell)},2} = q^6 - 18q^5 + 141q^4 - 613q^3 + 1551q^2 - 2152q + 1271 , \quad (6.78)$$

and

$$\kappa_{D_{3(\ell)},3} = -(q-3)^2(q^3 - 12q^2 + 48q - 67) . \quad (6.79)$$

In Table (6.4) we list real zeros of $P(D_{m-4,3}, q)$ in the interval $q \in [q_w, 3)$. As is evident in this table, in addition to the zero that approaches $\tau + 1$, there is a second real zero in this interval if and only if m (and hence n) is even. We can prove that, for the subset of $D_{m-4,3}$ with even m where this second zero is present, it approaches $q = 3$ from below as $m \rightarrow \infty$. The proof is as follows. According to our little theorem above on real chromatic zeros besides the one (or complex pair) that approach $\tau + 1$ as $m \rightarrow \infty$, there is a second zero in the interval $q \in [q_w, 3)$ if and only if $\kappa_{G_{pt},3}$ has a real zero in this interval. Now for the $D_{m-4,3}$ family, $\kappa_{D_{3(\ell)},3}$ has no real zero in the interval $[q_w, 3)$. (Its zeros are at $q = 3$, with multiplicity 2, at $q = 5.44224957\dots$ and at $q \simeq 3.278875 \pm 1.249025$.) Hence, according to our little theorem, as $m \rightarrow \infty$ on even integers, in addition to the real zero that is near to $\tau + 1$, the other zero must approach 3, so that in this limit, there is no other zero in the interval $[q_w, 3)$. This family may thus be added to the two known families given (in his Theorem 4) by Woodall in Ref. [81] as examples of one-parameter families of graphs, each of which has a chromatic zero that approaches 3 from below as the parameter (m here) goes to infinity.

The evaluation at $q = \tau + 1$ yields

$$P(D_{m-4,3}, \tau + 1) = (94 - 42\sqrt{5})(\tau - 1)^m + (-76 + 34\sqrt{5})(\tau - 2)^m , \quad (6.80)$$

so that

$$r(D_{m-4,3}) = -22 + 10\sqrt{5} + (18 - 8\sqrt{5}) \left(\frac{1 - \sqrt{5}}{2} \right)^m . \quad (6.81)$$

Hence,

$$r(D_{\infty,3}) = -22 + 10\sqrt{5} = 0.36067977\dots \quad (6.82)$$

Table 6.4: Location of real zeros of $P(D_{m-4,3}, q)$ in the interval $q \in [q_w, 3)$, as a function of the number of vertices, $n = m + 8$. Notation nz means that there is no second zero in this interval.

n	q_z	q'_z
12	2.614614	2.818897
13	2.619530	nz
14	2.616973	2.847527
15	2.618625	nz
16	2.617649	2.866268
17	2.618264	nz
18	2.617889	2.880165
19	2.618122	nz
20	2.617979	2.890985
21	2.618068	nz
22	2.618013	2.899700
23	2.618057	nz
24	2.618020	2.906905
25	2.618039	nz
26	2.618031	2.912980

with $a_{D_{3(\ell)}} = 1$.

6.8 The Family $D_{0,m-2}$

As an example of families with m_1 fixed and variable m_2 we discuss the family $D_{0,m_2} \equiv D_{0,m-2}$. A graph in this family has $n(D_{0,m-2}) = m + 7$. In accord with our result (6.58),

$$\kappa_{D_{0(u)},i} = \kappa_{D_{2(u)},i} \quad \text{for } i = 1, 2, 3 . \quad (6.83)$$

$P(D_{0,m-2}, q)$ has a real zero near to $\tau + 1$, which approaches this point as $m \rightarrow \infty$. Furthermore, since the coefficient $\kappa_{D_{0(u)},3}$ has a real zero in the interval $[q_w, 3)$, at the value in (6.73), it follows from our general analysis above that for sufficiently large m , $P(D_{0,m-2}, q)$ has a real zero that approaches this value. These zeros approach their respective values in a manner similar to that discussed for the family $D_{m-4,2}$.

6.9 A Symmetric Two-Parameter Family S_{m_1,m_2}

In this section we study a two-parameter family of planar triangulations S_{m_1,m_2} which are symmetric under interchange of the parameters:

$$S_{m_1,m_2} = S_{m_2,m_1} . \quad (6.84)$$

We show the lowest member of this family, $S_{0,0}$ and another member, $S_{1,2} = S_{2,1}$ in Fig. (6.3). From these it is clear how to construct the general graph S_{m_1,m_2} in this family. We have $n(S_{m_1,m_2}) = m_1 + m_2 + 7$. The chromatic number is $\chi(S_{m_1,m_2}) = 4$, and $P(S_{m_1,m_2}, q)$ contains the factor $P(K_4, q) = q(q-1)(q-2)(q-3)$.

We have calculated $P(S_{m_1,m_2}, q)$ and find that it involves the same three λ 's as in (5.23), but with an interestingly different form than $P(D_{m_1,m_2}, q)$. Given the symmetry (6.84), it follows that the coefficients in $P(S_{m_1,m_2}, q)$ satisfy

$$c_{S,ij} = c_{S,ji} . \quad (6.85)$$

Consequently, although there are nine terms of the form $\lambda_i^{m_1} \lambda_j^{m_2}$ in $P(S_{m_1,m_2}, q)$, there are only six independent coefficients $c_{S,ij}$ to begin with, and we find that two of these vanish, so that there are only four independent, nonvanishing coefficients $c_{S,ij}$. Explicitly, we calculate

$$c_{S,ij} = q \bar{c}_{S,ij} , \quad (6.86)$$

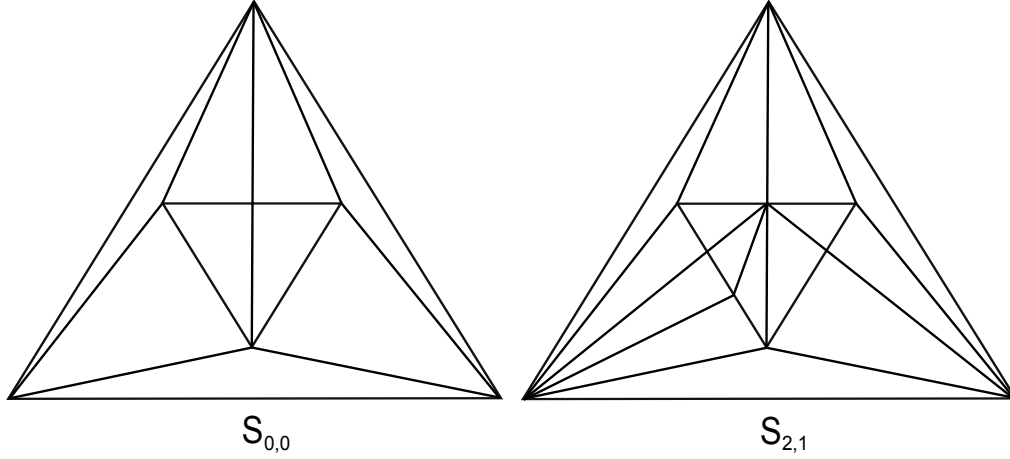


Figure 6.3: Graphs $S_{0,0}$ and $S_{2,1}$.

with

$$c_{S,11} = c_{S,13} = c_{S,31} = 0 , \quad (6.87)$$

$$\bar{c}_{S,22} = \frac{(q-1)(q-3)^6}{q-2} , \quad (6.88)$$

$$\bar{c}_{S,12} = \bar{c}_{S,21} = (q-2)^3(q-3)^2 , \quad (6.89)$$

$$\bar{c}_{S,23} = \bar{c}_{S,32} = \frac{(q-3)^2(q^2-3q+1)}{q-2} , \quad (6.90)$$

and

$$\bar{c}_{S,33} = \frac{(q-1)(q-3)(q^2-3q+1)}{q-2} . \quad (6.91)$$

so that

$$\begin{aligned} P(S_{m_1, m_2}, q) &= c_{S,22} \lambda_2^{m_1+m_2} + c_{S,33} \lambda_3^{m_1+m_2} \\ &+ c_{S,12} (\lambda_1^{m_1} \lambda_2^{m_2} + \lambda_2^{m_1} \lambda_1^{m_2}) + c_{S,23} (\lambda_2^{m_1} \lambda_3^{m_2} + \lambda_3^{m_1} \lambda_2^{m_2}) \end{aligned} \quad (6.92)$$

As before, the poles cancel in the calculation of $P(S_{m_1, m_2}, q)$ and, furthermore, these coefficients satisfy the requisite identities so that $P(S_{m_1, m_2}, q) = 0$ for $q = 1, 2, 3$. These are special cases of (6.10) and (6.13) that incorporate the properties that $c_{S,ij} = c_{S,ji}$ and $c_{S,11} = c_{S,13} = c_{S,31} = 0$, namely,

$$c_{S,22} = 0, \quad c_{S,33} = 0, \quad c_{S,12} + c_{S,23} = 0 \quad \text{at } q = 1 \quad (6.93)$$

and

$$c_{S,22} + 2c_{S,12} + c_{S,33} = 0, \quad c_{S,12} = 0 \quad \text{at } q = 2. \quad (6.94)$$

As a special case of (6.17) we also have

$$c_{S,23} = c_{S,32} = c_{S,33} = 0 \quad \text{at } q = \tau + 1. \quad (6.95)$$

Finally, the condition $P(S_{m_1, m_2}, 3) = 0$ is equivalent to

$$c_{S,33} = 0 \quad \text{at } q = 3 \quad (6.96)$$

For the comparison of $P(S_{m_1, m_2}, q)$ at $q = \tau + 1$ with the Tutte upper bound $(\tau - 1)^{m_1 + m_2 + 2}$, we have

$$\begin{aligned} r(S_{m_1, m_2}) = & \left| (9 - 4\sqrt{5}) \left(\frac{1 - \sqrt{5}}{2} \right)^{m_1 + m_2} \right. \\ & \left. + (-2 + \sqrt{5}) \left[\left(\frac{1 - \sqrt{5}}{2} \right)^{m_1} + \left(\frac{1 - \sqrt{5}}{2} \right)^{m_2} \right] \right| \end{aligned} \quad (6.97)$$

This decreases (non-monotonically) in magnitude as m_1 increases for fixed m_2 and as m_2 increases for fixed m_1 , approaching zero exponentially rapidly as either of these parameters goes to infinity. Thus,

$$\lim_{m_1 \rightarrow \infty} r(S_{m_1, m_2}) = \lim_{m_2 \rightarrow \infty} r(S_{m_1, m_2}) = 0. \quad (6.98)$$

It is also of interest to analyze the one-parameter reductions of $P(S_{m_1, m_2}, q)$ for variable m_1 and fixed m_2 and vice versa. These yield identical results, because of the symmetry (6.84). Hence, without loss of generality we consider variable m_1 and fixed m_2 and find that in this case $P(S_{m_1, m_2}, q)$ reduces to (5.38) with $m = m_1 + 2$, which we write as $P(S_{m-2, m_2}, q)$. Since the coefficients only depend on m_2 and not m , we denote them by $c_{S_{m_2}, i}$. They are given by

$$c_{S_{m_2}, i} = \lambda_i^{-2} \sum_{j=1}^3 c_{S, ij} \lambda_j^{m_2} \quad (6.99)$$

Thus, in terms of the corresponding $\kappa_{S_{m_2}, i}$,

$$\kappa_{S_{0,1}} = (q - 2)(q - 3)^2, \quad (6.100)$$

$$\kappa_{S_{0,2}} = \lambda_{TC} = q^3 - 9q^2 + 29q - 32, \quad (6.101)$$

$$\kappa_{S_{0,3}} = 2(q - 3). \quad (6.102)$$

and so forth for higher values of m_2 .

This family exhibits a number of interesting properties. Among these is the fact that out of the possible 3^2 terms in (6.21) for $p = 2$, some may be absent because of vanishing coefficients $c_{G,i,j}$. In particular, the term $c_{G,11}\lambda_1^{m_1+m_2}$ that would be dominant in the limit where the parameters $m_1 \rightarrow \infty$ and $m_2 \rightarrow \infty$, may be absent, so that in this limit, $r(G_{\infty,\infty})$ may be zero.

6.10 Families of the form G_{pt,m_1,m_2} with $m_1 = m_2$

In previous sections we have analyzed the chromatic polynomials of special cases of two-parameter families of planar triangulations G_{pt,m_1,m_2} as a function of m_1 with m_2 held fixed, and vice versa and shown how they reduce to (5.14) with $j_{max} = 3$. A different type of special case in which G_{pt,m_1,m_2} reduces to a one-parameter family is obtained by requiring that m_1 and m_2 be linearly related to each other. The simplest such example of this type of reduction is the diagonal case obtained by requiring that $m_1 = m_2$. For general families G_{pt,m_1,m_2} that satisfy (6.15) and for which $P(G_{pt,m_1,m_2}, q)$ is of the form (6.1), it follows that $n(G_{pt,k,k}) = 2k + \beta$ and that $P(G_{pt,m_1,m_1}, q)$ reduces, to the form (5.14) with $j_{max} = 6$. We use the shorthand G_d to denote a generic G_{pt,m_1,m_1} . We have

$$P(G_{d,m_1,m_1}, q) = \sum_{j=1}^6 c_{G_d,j} (\lambda_{G_d,j})^m \quad (6.103)$$

where $m = m_1 + \delta m$, with δm depending on the family, and

$$\lambda_{G_d,1} = \lambda_1^2 = (q-2)^2, \quad (6.104)$$

$$\lambda_{G_d,2} = \lambda_2^2 = (q-3)^2, \quad (6.105)$$

$$\lambda_{G_d,3} = \lambda_3^2 = 1, \quad (6.106)$$

$$\lambda_{G_d,4} = \lambda_1 \lambda_2 = (q-2)(q-3), \quad (6.107)$$

$$\lambda_{G_d,5} = \lambda_1 \lambda_3 = -(q-2), \quad (6.108)$$

and

$$\lambda_{G_d,6} = \lambda_2 \lambda_3 = -(q-3). \quad (6.109)$$

The corresponding coefficients are

$$c_{G_d,j} = q \bar{c}_{G_d,j} \quad \text{for } j = 1, \dots, 6, \quad (6.110)$$

with

$$c_{G_d,1} = c_{G,11}, \quad (6.111)$$

$$c_{G_d,2} = c_{G,22} , \quad (6.112)$$

$$c_{G_d,3} = c_{G,33} , \quad (6.113)$$

$$c_{G_d,4} = c_{G,12} + c_{G,21} , \quad (6.114)$$

$$c_{G_d,5} = c_{G,13} + c_{G,31} , \quad (6.115)$$

and

$$c_{G_d,6} = c_{G,23} + c_{G,32} . \quad (6.116)$$

The coefficients $c_{G_d,i}$, $i = 1, \dots, 6$ satisfy various conditions that follow from those that we have derived for the coefficients $c_{G,ij}$ in (6.7), (6.10), (6.13), and (6.17). These are

$$\begin{aligned} c_{G_d,1} + c_{G_d,3} + c_{G_d,5} &= 0, & c_{G_d,2} &= 0, \\ c_{G_d,4} + c_{G_d,6} &= 0 \quad \text{at } q = 1 , \end{aligned} \quad (6.117)$$

$$\begin{aligned} c_{G_d,1} &= 0, & c_{G_d,2} + c_{G_d,3} + c_{G_d,6} &= 0, \\ c_{G_d,4} + c_{G_d,6} &= 0 \quad \text{at } q = 2 , \end{aligned} \quad (6.118)$$

and

$$c_{G_d,3} = c_{G_d,5} = c_{G_d,6} = 0 \quad \text{at } q = \tau + 1 . \quad (6.119)$$

Hence,

$$c_{G_d,2} \quad \text{contains the factor } q - 1 , \quad (6.120)$$

$$c_{G_d,1} \quad \text{contains the factor } q - 2 , \quad (6.121)$$

and

$$c_{G_d,i} \quad \text{contains the factor } q^2 - 3q + 1 \quad \text{if } i = 3, 5, 6 . \quad (6.122)$$

6.11 The Families D_{m_1, m_2} and S_{m_1, m_2} with $m_1 = m_2$

We now discuss two explicit examples of the diagonal special case of a two-parameter planar triangulation family, namely D_{m_1, m_2} and S_{m_1, m_2} with $m_1 = m_2$. We shall use the shorthand notation D_d and S_d to refer to these entire respective families. From (6.24), we have $n(D_{m_1, m_1}) = 2m_1 + 9$ and $n(S_{m_1, m_1}) = 2m_1 + 7$.

The chromatic polynomial $P(D_{m_1, m_1}, q)$ has the form (6.103) with $j_{max} = 6$

and $\delta m = 0$, i.e., $m = m_1$. The lowest member of this family, the graph $D_{0,0}$, and $D_{2,2}$ were shown in Fig. (6.2). The chromatic number $\chi(D_{m,m})$ is 3 if m is even and 4 if m is odd. The coefficients are

$$\bar{c}_{D_d,i} = \bar{c}_{D,ii} \quad \text{for } i = 1, 2, 3, \quad (6.123)$$

$$\bar{c}_{D_d,4} = \bar{c}_{12} + \bar{c}_{21} = (q-2)(q-3)^4(2q^2 - 10q + 13), \quad (6.124)$$

$$\bar{c}_{D_d,5} = \bar{c}_{13} + \bar{c}_{31} = \frac{(q-2)(q^2 - 4q + 5)(q^2 - 3q + 1)}{q-1}, \quad (6.125)$$

and

$$\bar{c}_{D_d,6} = \bar{c}_{23} + \bar{c}_{32} = -\frac{(q-3)^2(q-5)(q^2 - 6q + 10)(q^2 - 3q + 1)}{q-2}, \quad (6.126)$$

Since $\chi(D_{m,m}) = 4$ for odd m , it follows that

$$c_{D_d,1} - c_{D_d,3} + c_{D_d,5} = 0 \quad \text{for } q = 3. \quad (6.127)$$

We calculate

$$\begin{aligned} P(D_{m,m}, \tau + 1) &= (\tau + 1) \left[\left(\frac{47 - 21\sqrt{5}}{2} \right) (\tau - 1)^{2m} \right. \\ &+ \left. \left(\frac{1165 - 521\sqrt{5}}{2} \right) (\tau - 2)^{2m} + (-360 + 161\sqrt{5}) [(\tau - 1)(\tau - 2)]^m \right] \end{aligned} \quad (6.128)$$

The ratio $r(D_{m,m})$ is

$$r(D_{m,m}) = \frac{3 - \sqrt{5}}{2} + \left(\frac{65 - 29\sqrt{5}}{2} \right) \left(\frac{1 - \sqrt{5}}{2} \right)^{2m} + (-20 + 9\sqrt{5}) \left(\frac{1 - \sqrt{5}}{2} \right)^m. \quad (6.129)$$

Hence, defining $r(D_d, \infty) = \lim_{m \rightarrow \infty} r(D_{m,m})$, we have

$$r(D_d, \infty) = \frac{3 - \sqrt{5}}{2} = 0.381966... \quad (6.130)$$

and $a_{D_d} = 1$.

In contrast, the chromatic polynomial $P(S_{m_1, m_1}, q)$ has the form (5.14) with $j_{max} = 4$. The lowest member of this family, the graph $S_{0,0}$, was shown in Fig.

(6.3). The chromatic number $\chi(S_{m,m}) = 4$. The expression for $P(S_{m,m}, q)$ follows immediately from (6.92) and has $j_{max} = 4$,

$$P(S_{m,m}, q) = c_{S,22}(\lambda_2)^{2m} + c_{S,33} + 2c_{S,12}(\lambda_1\lambda_2)^m + 2c_{S,23}(\lambda_2\lambda_3)^m, \quad (6.131)$$

where we used the fact that $(\lambda_3)^{2m} = 1$. The ratio $r(S_{m,m})$ follows from (6.97), with the result that $r(S_{\infty,\infty}) = 0$.

6.12 Some Implications for Statistical Physics

One of the interesting aspects of the present work is its implications for nonzero ground state entropy of the Potts antiferromagnet. (For background on the Potts model, see Refs. [85], [5], [52].) This stems from the identity noted above, $P(G, q) = Z(G, q, T = 0)_{PAF} = W_{tot}(G, q)$. As above, we denote the formal limit of a family of graphs G as $n(G) \rightarrow \infty$ by the symbol $\{G\}$. We recall that the entropy per vertex is given by $S_0 = k_B \ln W$, where W is the degeneracy per vertex, related to the total degeneracy of spin configurations of the zero-temperature Potts antiferromagnet (or equivalently the number of proper q -colorings of the graph) by W_{tot} by $W(\{G\}, q) = \lim_{n \rightarrow \infty} [W_{tot}(G, q)]^{1/n}$. We refer the reader to Ref. [52] for a discussion of a subtlety in this definition resulting from a certain noncommutativity that occurs for a special set of values of q , denoted as $\{q_s\}$, namely

$$\lim_{q \rightarrow q_s} \lim_{n \rightarrow \infty} [P(G, q)]^{1/n} \neq \lim_{n \rightarrow \infty} \lim_{q \rightarrow q_s} [P(G, q)]^{1/n}. \quad (6.132)$$

For the one-parameter families of planar triangulations considered here, this set of special values $\{q_s\}$ includes $q = 0, 1, 2, \tau + 1$ and, for cases where the chromatic number is 4, also $q = 3$. Because of this noncommutativity, it is necessary to specify the order of limits taken in defining W . For a particular value $q = q_s$, we thus define

$$W_{qn}(\{G\}, q_s) = \lim_{q \rightarrow q_s} \lim_{n \rightarrow \infty} [P(G, q)]^{1/n} \quad (6.133)$$

and

$$W_{nq}(\{G\}, q_s) = \lim_{n \rightarrow \infty} \lim_{q \rightarrow q_s} [P(G, q)]^{1/n}. \quad (6.134)$$

For real $q \geq \chi(G_{pt,m})$, both of these definitions are equivalent, and in this case we shall write $W_{qn}(\{G\}, q_s) = W_{nq}(\{G\}, q_s) \equiv W(\{G\}, q_s)$.

We generalize our calculations in [70] as follows. First, for a family of planar triangulations $G_{pt,m}$ with $P(G_{pt,m}, q)$ having the form (5.14) with $j_{max} = 1$,

$W = [\lambda_{G_{pt}}]^{1/\alpha}$. As an example, consider the family R_m with $n(R_m) = m + 2$ considered in Chapter 5 of this dissertation [70].

The W function for the $m \rightarrow \infty$ limit of this family is $W(\{R\}, q) = q - 3$, and $S_0 > 0$ for $q > 4$. For the family TC_m

$$W(\{TC\}, q) = (\lambda_{TC})^{1/3} . \quad (6.135)$$

where λ_{TC} was given in (5.45). The function λ_{TC} is a monotonically increasing function of q , which passes through zero at $q = 2.54660\dots$ and increases through unity at $q = 3$ so that (for the $m \rightarrow \infty$ limit of this family) $S_0 > 0$ for $q > 3$. For the family I_m of iterated icosahedra,

$$W(\{I\}, q) = (\lambda_I)^{1/9} , \quad (6.136)$$

where λ_I was obtained in Eq. (5.66). The function λ_I vanishes at three real values of q , namely $q = 2.618197\dots$ (i.e., slightly above $\tau + 1$), at $q = 3$, and at $q = 3.222458\dots$. This function is positive for $q > 3.222458\dots$ (as well as in an interval $2.618\dots < q < 3$) and increases through unity as q increases through the value $3.5133658\dots$, so that in this latter interval, $S_0 > 0$.

A second general result is that for a family of planar triangulations $G_{pt,m}$ with $P(G_{pt,m}, q)$ having the form (5.38), it follows that (i) $W_{qn}(\{G_{pt}\}, q) = q - 2$ for $q > 3$; (ii) even in the presence of noncommutativity, $W(\{G_{pt}\}, q) = q - 2$ for $q \geq 4$, so that $S_0 > 0$ in this interval (and also in the interval $q > 3$ if one uses $W_{qn}(\{G_{pt}\}, q)$). This result applies, in particular, to the families B_m , H_m , L_m , $D_{m-4,2}$, and $D_{m-4,3}$. Although the family $P(D_{m,m}, q)$ is of the form (5.14) with $j_{max} = 6$, the dominant term for $q > \chi(D_{m,m})$ is again $q - 2$, so that in this interval $W(\{D_d\}, q) = q - 2$ for this family also. In contrast, $P(S_{m_1, m_2}, q)$ has $c_{S,11} = 0$ and hence lacks the term that would normally be dominant as m_1 or m_2 goes to infinity. In this case, for $q \geq 4$ where there is no noncommutativity in limits, we find $W(\{S\}, q) = \sqrt{(q-2)(q-3)}$.

For the family F_m , we find that λ_1 in Eq. (5.110) is dominant for $q > q_c = \tau + 2 = 3.618\dots$, so that in this region,

$$W(\{F\}, q) = \lambda_{F,1} \quad (6.137)$$

Furthermore, since $\lambda_{F,1} > 1$ for real $q > \tau + 2$, it follows that $S_0 > 0$ for (the $m \rightarrow \infty$ limit of this family of graphs) for this range $q > \tau + 2$.

For a regular lattice graph G it is of interest to investigate the dependence of $W(\{G\}, q)$ on the vertex degree (coordination number) d . This study was carried out in [52] [55] [57], and it was shown that $W(\{G\}, q)$ is a non-increasing function of d . This is understood as being a consequence of the

fact that (except for tree graphs, which are not relevant here), roughly speaking, increasing the vertex degree tends to increase the constraints on a proper q -coloring of the vertices and therefore tends to decrease $W(\{G\}, q)$. One is also motivated to investigate the same question with the families of planar triangulations under study here. However, since $d_{eff} = 6$ for a family of planar triangulation graphs one is limited to a fixed $d_{eff} = 6$ and hence cannot carry out the type of comparative study involving a variation in d_{eff} that was performed in [52] [55] [57]. In [70] and the present work, we have found that families of planar triangulations can have different $W(\{G\}, q)$ functions. This is consistent with the results in [52] [57]. Indeed, one has already encountered examples of this. For example, the square and kagomé ($3 \cdot 6 \cdot 3 \cdot 6$) lattices both have the same vertex degree, namely 4, but they have different W functions, and similarly, the honeycomb, ($3 \cdot 12^2$), and ($4 \cdot 8^2$) lattices have the same vertex degree, namely 3, but they have different W functions [52] [55] [57].

6.13 Comparative Discussion

In this section we give a comparative discussion of some limiting quantities for the various families of planar triangulations that we have studied so far. For one-parameter families of planar triangulations $G_{pt,m}$ for which $P(G_{pt,m}, q)$ is of the form (5.13) we have proved that $r(G_{pt,\infty}) = 0$ and have investigated the various values of $a_{G_{pt}}$ defined in (5.40). This constant is strictly less than unity, and it is of interest to see which families yield larger and smaller values of $a_{G_{pt}}$. We display the values that we have obtained in Table (6.5). As is evident, in the set of $j_{max} = 1$ families of planar triangulations, the family of cylindrical strips of the triangular lattice, TC_m (equivalently, iterated octahedra) yields the largest value of $a_{G_{pt}}$, which is within 9 % of its upper bound of 1. In the $j_{max} = 3$ families, the one that yields the largest value of the limiting ratio $r(G_{pt,\infty})$ is the family, B_m , with $r(B_\infty) = 0.6180..$ A second type of asymptotic limiting function is $W(\{G\}, q)$. We have given a comparative analysis of this in the previous section.

We have also investigated the values of $P(G_{pt,m}, q)$ at $q = \chi(G_{pt,m})$ for the families of planar triangulations that we have studied. Recall the definition that a graph G is k -critical iff $\chi(G) = k$ and $P(G, k) = k!$. We find a variety of behavior. For example, (i) $\chi(R_m) = 4$ and $P(R_m, 4) = 4!$, so R_m is 4-critical; (ii) $\chi(TC_m) = 3$ and $P(TC_m, 3) = 3!$, so TC_m is 3-critical; but (iii) $\chi = 4$ for $I_m, H_m, L_m, D_{m-4,3}$, and $F_{m \geq 3}$ but none of these families is 4-critical. For other families $G_{pt,m}$, the chromatic number depends on whether m is even or odd. For example, for even m , $\chi = 3$ for B_m and $D_{m-4,2}$, and these graphs are 3-critical, while for odd m , $\chi = 4$ for B_m and $D_{m-4,2}$, but neither of these

graphs is 4-critical.

6.14 Summary of Chapter

In this chapter, generalizing the results in Chapter 5, we have presented an analysis of the structure and properties of chromatic polynomials $P(G_{pt,\mathbf{m}}, q)$ of families of planar triangulation graphs $G_{pt,\mathbf{m}}$, where $\mathbf{m} = (m_1, \dots, m_p)$ is a vector of integer parameters. We have discussed a number of specific families with $p = 1$ and $p = 2$. These planar triangulation graphs form a particularly attractive class of graphs for the analysis of chromatic polynomials because of their special properties. One of these is the fact that when evaluated at $q = \tau + 1$, the chromatic polynomial of a planar triangulation graph satisfies the Tutte upper bound (5.1). We have studied the ratio of $|P(G_{pt,\mathbf{m}}, \tau + 1)|$ to the Tutte upper bound $(\tau - 1)^{n-5}$ and have calculated limiting values of this ratio as $n \rightarrow \infty$ for various families of planar triangulations. We also have used our calculations to study zeros of these chromatic polynomials. Among our results, we have shown that if $G_{pt,\mathbf{m}}$ is a planar triangulation graph with a chromatic polynomial $P(G_{pt,\mathbf{m}}, q)$ of the form (6.21), then (i) the coefficients $c_{G_{pt},i}$ must satisfy a number of properties, which we have derived; and (ii) $P(G_{pt,\mathbf{m}}, q)$ has a real chromatic zero that approaches $(1/2)(3 + \sqrt{5})$ as one or more $m_i \rightarrow \infty$. We have constructed a $p = 1$ family of planar triangulations with real zeros that approach 3 from below as $m \rightarrow \infty$. A one-parameter family F_m with $j_{max} = 3$ and nonpolynomial $\lambda_{F,j}$ has been studied. We have also presented results for a number of results for chromatic polynomials of various two-parameter families of planar triangulations. Implications for the ground-state entropy of the Potts antiferromagnet are discussed. Our results are of interest both from the point of view of mathematical graph theory and statistical physics and further show the fruitful connections between these fields.

Table 6.5: Some asymptotic limiting quantities for one-parameter families of planar triangulations. The shorthand notation $3me, 4mo$ means $\chi = 3$ if m is even and $\chi = 4$ if m is odd. Additional information for χ values is $\chi(R_3) = 3$, $\chi(F_1) = 4$, and $\chi(F_2) = 3$. Numerical values are quoted to three significant figures.

$G_{pt,m}$	$n(G_{pt,m})$	$\chi(G_{pt,m})$	j_{max}	$r(G_{pt,\infty})$	$a_{G_{pt}}$
R_m	$m + 2$	4 if $m \geq 2$	1	0	$(-1 + \sqrt{5})/2 = 0.618$
TC_m	$3m$	3	1	0	$(3 - \sqrt{5})^{1/3} = 0.914$
I_m	$9m + 3$	4	1	0	$[(-315 + 141\sqrt{5})/2]^{1/9} = 0.8055$
$G_{C,M,m}$	$8m + 3$	3	1	0	$[(115 - 51\sqrt{5})/2]^{1/8} = 0.885$
F_m	$m + 4$	4 if $m \geq 3$	3	0	0.786
B_m	$m + 2$	$3me, 4mo$	3	$(-1 + \sqrt{5})/2 = 0.618$	1
H_m	$m + 5$	4	3	$(7 - 3\sqrt{5})/2 = 0.146$	1
L_m	$m + 5$	4	3	$-2 + \sqrt{5} = 0.236$	1
$D_{m-4,0}$	$m + 5$	$3me, 4mo$	3	$-4 + 2\sqrt{5} = 0.472$	1
$D_{m-4,1}$	$m + 6$	4	3	$(-15 + 7\sqrt{5})/2 = 0.326$	1
$D_{0,m-2}$	$m + 7$	$3me, 4mo$	3	$-13 + 6\sqrt{5} = 0.416$	1
$D_{1,m-2}$	$m + 8$	4	3	$-22 + 10\sqrt{5} = 0.361$	1
$D_{m,m}$	$2m + 9$	$3me, 4mo$	6	$(3 - \sqrt{5})/2 = 0.382$	1
$S_{m,m}$	$m + 7$	4	4	0	$(-1 + \sqrt{5})/2 = 0.618$

Bibliography

- [1] P. W. Atkins and J. De Paula (2006) *Physical Chemistry*, 8th edition, W. H. Freeman and Company, New York.
- [2] A. V. Bakaev and V. I. Kabanovich (1994) Series Expansions for the q -colour Problem on the Square and Cubic Lattices. *J. Phys. A* **27**, 6731.
- [3] G. A. Baker, Jr. (1971) Linked-Cluster Expansion for the Graph-Vertex Coloration Problem. *J. Combinatorial Theory, Series B* **10**, 217.
- [4] R. J. Baxter (1982) *Exactly Solved Models in Statistical Mechanics*, Academic Press, London (2007 Dover Publications).
- [5] R. J. Baxter (1987) Chromatic Polynomials of Large Triangular Lattices. *J. Phys. A* **20**, 5241.
- [6] S. Beraha, J. Kahane, N. Weiss (1980) Limits of Chromatic Zeros of Some Families of Maps. *J. Combinatorial Theory, Series B* **28**, 52.
- [7] B. A. Berg, C. Muguruma, Y. Okamoto (2007) Residual Entropy of Ordinary Ice from Multicanonical Simulations. *Phys. Rev. E* **75**, 092202.
- [8] N. L. Biggs, R. M. Damerell, D. A. Sands (1972) Recursive Families of Graphs. *J. Combinatorial Theory, Series B* **12**, 123.
- [9] N. L. Biggs (1977) Colouring Square Lattice Graphs. *Bull. London Math. Soc.* **9**, 54.
- [10] N. L. Biggs (1993) *Algebraic Graph Theory*, Cambridge University, Cambridge.
- [11] N. L. Biggs and R. Shrock (1999) $T = 0$ Partition Functions for Potts Antiferromagnets on Square Lattice Strips with (Twisted) Periodic Boundary Conditions. *J. Phys. A* **32**, L489.

- [12] N. L. Biggs (2001) A Matrix Method for Chromatic Polynomials. *J. Combinatorial Theory, Series B* **82**, 19.
- [13] N. L. Biggs (2002) Equimodular Curves. *Discrete Math.* **259**, 37.
- [14] G. D. Birkhoff (1912) A Determinant Formula for the Number of Ways of Colouring a Map. *Ann. of Math.* **14**, 42.
- [15] B. Bolobás (1998) *Modern Graph Theory*, Springer.
- [16] J. A. Bondy and U. S. R. Murty (2008) *Graph Theory*, Springer.
- [17] S.-C. Chang and R. Shrock (2000) Ground-State Entropy of the Potts Antiferromagnet with Next-Nearest-Neighbor Spin-Spin Couplings on Strips of the Square Lattice. *Phys. Rev. E* **60**, 4650.
- [18] S.-C. Chang and R. Shrock (2001) Ground State Entropy of the Potts Antiferromagnet on Triangular Lattice Strips. *Ann. Phys.* **290**, 124.
- [19] S.-C. Chang and R. Shrock (2001) Ground State Entropy of the Potts Antiferromagnet on Strips of the Square Lattice. *Physica A* **290**, 402.
- [20] S.-C. Chang and R. Shrock (2001) $T = 0$ Partition Functions for Potts Antiferromagnets on Lattice Strips with Fully Periodic Boundary Conditions. *Physica A* **292**, 307.
- [21] S.-C. Chang and R. Shrock (2001) Structural Properties of Potts Model Partition Functions and Chromatic Polynomials for Lattice Strips. *Physica A* **296**, 131.
- [22] S.-C. Chang and R. Shrock (2001) Exact Potts Model Partition Functions on Strips of the Honeycomb Lattice. *Physica A* **296**, 183.
- [23] S.-C. Chang and R. Shrock (2001) Potts Model Partition Functions for Self-Dual Families of Strip Graphs. *Physica A* **301**, 301.
- [24] S.-C. Chang and R. Shrock (2002) General Structural Results for Potts Model Partition Functions on Lattice Strips. *Physica A* **316**, 335.
- [25] S.-C. Chang and R. Shrock (2009) Some Exact Results on the Potts Model Partition Function in a Magnetic Field. *J. Phys. A* **42**, 385004.
- [26] S.-C. Chang and R. Shrock (2009) Structure of the Partition Function and Transfer Matrices for the Potts Model in a Magnetic Field on Lattice Strips. *J. Stat. Phys.* **137**, 667.

- [27] S.-C. Chang and R. Shrock (2009) Weighted Graph Colorings. *J. Stat. Phys.* **138**, 496.
- [28] X. Y. Chen and C. Y. Pan (1988) Finite Temperature Entropy of the Antiferromagnetic Potts Model. *Int. J. Mod. Phys. B* **2**, 1495.
- [29] F. M. Dong, K. M. Koh, K. L. Teo (2005) *Chromatic Polynomials and Chromaticity of Graphs*, World Scientific, Singapore.
- [30] R. Fernández and A. Procacci (2008) Regions Without Complex Zeros for Chromatic Polynomials on Graphs with Bounded Degree. *Combinatorics, Probability and Computing*, **17**, 225.
- [31] C. M. Fortuin and P. W. Kasteleyn (1972) On the Random-Cluster Model: I. Introduction and Relation to Other Models *Physica* **57**, 536.
- [32] W. F. Giauque and J. W. Stout (1936) The Entropy of Water and the Third Law of Thermodynamics. The Heat Capacity of Ice from 15 to 273°K. *J. Am. Chem. Soc.* **58**, 1144.
- [33] F. Harary(1969) *Graph Theory*, Addison-Wesley.
- [34] J. M. Harris, J. L. Hirst, M. J. Mossinghoff (2008) *Combinatorics and Graph Theory*, Springer.
- [35] B. Jackson (1993) A Zero-Free Interval for Chromatic Polynomials of Graphs. *Combinatorics, Probability and Computing* **2**, 235.
- [36] P. Lancaster and M. Tismenetsky (1985) *The Theory of Matrices, with Applications*, Academic Press, New York.
- [37] E. H. Lieb (1967) Residual Entropy of Square Ice. *Phys. Rev.* **162**, 162.
- [38] D. London (1966) Inequalities in Quadratic Forms. *Duke Math. J.* **33**, 511.
- [39] H. Minc (1988) *Nonnegative Matrices*, Wiley, New York.
- [40] J. F. Nagle (1971) A New Subgraph Expansion for Obtaining Coloring Polynomials for Graphs. *J. Combinatorial Theory, Series B* **10**, 42.
- [41] L. Pauling (1935) The Structure and Entropy of Ice and of Other Crystals with Some Randomness of Atomic Arrangement. *J. Am. Chem. Soc.* **57**, 2680.

- [42] R. B. Potts (1952) Some Generalized Order-Disorder Transformations. *Proc. Camb. Phil. Soc.* **48**, 106.
- [43] R. C. Read (1968) An Introduction to Chromatic Polynomials. *J. Combinatorial Theory* **4**, 52.
- [44] R. C. Read and W. T. Tutte (1988) Chromatic Polynomials. *Selected Topics in Graph Theory 3* (L.W. Beineke, R.J. Wilson, Eds.), Academic Press, New York, p.15-42.
- [45] R. C. Read and R. J. Wilson (1998) *An Atlas of Graphs*, Oxford University Press, Clarendon, 1998.
- [46] M. Roček, R. Shrock, S.-H. Tsai (1998) Chromatic Polynomials for Families of Strip Graphs and Their Asymptotic Limits. *Physica A* **252**, 505.
- [47] J. Salas and R. Shrock (2001) Exact $T = 0$ Partition Functions for Potts Antiferromagnets on Sections of the Simple Cubic Lattice. *Physica A* **259**, 315.
- [48] R. Shrock (1999) $T = 0$ Partition Functions for Potts Antiferromagnets on Möbius Strips and Effects of Graph Topology. *Phys. Lett. A* **261**, 57.
- [49] R. Shrock (2000) Exact Potts Model Partition Functions on Ladder Graphs. *Physica A* **283**, 388.
- [50] R. Shrock (2001) Chromatic Polynomials and Their Zeros and Asymptotic Limits for Families of Graphs. *Discrete Math.* **231**, 421.
- [51] R. Shrock (2011) Exact Potts/Tutte Polynomials for Polygon Chain Graphs. *J. Phys. A* **44**, 145002.
- [52] R. Shrock and S.-H. Tsai (1997) Asymptotic Limits and Zeros of Chromatic Polynomials and Ground-State Entropy of Potts Antiferromagnets. *Phys. Rev. E* **55**, 5165.
- [53] R. Shrock and S.-H. Tsai (1997) Upper and Lower Bounds for the Ground State Entropy of Antiferromagnetic Potts Models. *Phys. Rev. E* **55**, 6791.
- [54] R. Shrock and S.-H. Tsai (1997) Families of Graphs with Chromatic Zeros Lying on Circles. *Phys. Rev. E* **56**, 1342.
- [55] R. Shrock and S.-H. Tsai (1997) Ground-State Entropy of Potts Antiferromagnets: Bounds, Series, and Monte Carlo Measurements. *Phys. Rev. E* **56**, 2733.

- [56] R. Shrock and S.-H. Tsai (1997) Families of Graphs with $W_r(\{G\}, q)$ Functions That Are Nonanalytic at $1/q = 0$. *Phys. Rev. E* **56**, 3935.
- [57] R. Shrock and S.-H. Tsai (1997) Lower Bounds and Series for the Ground-State Entropy of the Potts Antiferromagnet on Archimedean Lattices and Their Duals. *Phys. Rev. E* **56**, 4111.
- [58] R. Shrock and S.-H. Tsai (1998) Ground State Entropy of Potts Antiferromagnets and the Approach to the Two-Dimensional Thermodynamic Limit. *Phys. Rev. E* **58**, 4332.
- [59] R. Shrock and S.-H. Tsai (1998) Ground State Entropy of Potts Antiferromagnets on Homeomorphic Families of Strip Graphs. *Physica A* **259**, 315.
- [60] R. Shrock and S.-H. Tsai (1998) Ground-State Degeneracy of Potts Antiferromagnets: Cases with Noncompact W Boundaries Having Multiple Points at $1/q = 0$. *J. Phys. A* **31**, 9641.
- [61] R. Shrock and S.-H. Tsai (1999) Ground State Entropy of Potts Antiferromagnets on Cyclic Polygon Chain Graphs. *J. Phys. A* **32**, 5053.
- [62] R. Shrock and S.-H. Tsai (1999) Ground-State Degeneracy of Potts Antiferromagnets: Homeomorphic Classes with Noncompact W Boundaries. *Physica A* **265**, 186.
- [63] R. Shrock and S.-H. Tsai (1999) Ground-State Degeneracy of Potts Antiferromagnets on Two-Dimensional Lattices: Approach Using Infinite Cyclic Strip Graphs. *Phys. Rev. E* **60**, 3512.
- [64] R. Shrock and S.-H. Tsai (1999) Ground-State Entropy of the Potts Antiferromagnet on Cyclic Strip Graphs. *J. Phys. A* **32**, L195.
- [65] R. Shrock and S.-H. Tsai (2000) Exact Partition Functions for Potts Antiferromagnets on Cyclic Lattice Strips. *Physica A* **275**, 429.
- [66] R. Shrock and Y. Xu (2010) Weighted-Set Graph Colorings. *J. Stat. Phys.* **139**, 27.
- [67] R. Shrock and Y. Xu (2010) Exact Results on Potts Model Partition Functions in a Generalized External Field and Weighted-Set Graph Colorings. *J. Stat. Phys.* **141**, 909.

- [68] R. Shrock and Y. Xu (2010) Lower Bounds on the Ground-State Entropy of the Potts Antiferromagnet on Slabs of the Simple Cubic Lattice. *Phys. Rev. E* **81**, 031134.
- [69] R. Shrock and Y. Xu (2011) Ground State Entropy of the Potts Antiferromagnet on Homeomorphic Expansions of Kagomé Lattice Strips. *Phys. Rev. E* **83**, 041109.
- [70] R. Shrock and Y. Xu (2012) Chromatic Polynomials of Planar Triangulations, the Tutte Upper Bound and Chromatic Zeros. *J. Phys. A* **45**, 055212.
- [71] R. Shrock and Y. Xu (2012) The Structure of Chromatic Polynomials of Planar Triangulations and Implications for Chromatic Zeros and Asymptotic Limiting Quantities. *J. Phys. A*, in press (arXiv:1201.4200).
- [72] A. D. Sokal (2001) Bounds on the Complex Zeros of (Di)Chromatic Polynomials and Potts-Model Partition Functions. *Combinatorics, Probability and Computing*, **10**, 41.
- [73] C. Thomassen (1997) The Zero-Free Intervals for Chromatic Polynomials of Graphs. *Combinatorics, Probability and Computing*, **6**, 497.
- [74] W. T. Tutte (1947) A Ring in Graph Theory. *Proc. Camb. Phil. Soc.* **43**, 26.
- [75] W. T. Tutte (1954) A Contribution to the Theory of Chromatic Polynomials. *Canad. J. Math.* **6**, 80.
- [76] W. T. Tutte (1970) On Chromatic Polynomials and the Golden Ratio. *J. Combinatorial Theory* **9**, 289.
- [77] W. T. Tutte (2004) Graph-polynomials. *Advances in Applied Math.* **32**, 5.
- [78] H. Whitney (1932) A Logical Expansion in Mathematics. *Bull. Amer. Math. Soc.* **38**, 572.
- [79] D. R. Woodall (1977) Zeros of Chromatic Polynomials. *Combinatorial Surveys*, Proc. Sixth British Combinatorial Conference (P. J. Cameron, ed.), Academic Press, London and New York, p. 199-223.
- [80] D. R. Woodall (1992) A Zero-Free Interval for Chromatic Polynomials. *Discrete Math.* **101**, 333.

- [81] D. R. Woodall (1997) The Largest Real Zero of the Chromatic Polynomial. *Discrete Math.* **172**, 141.
- [82] D. R. Woodall (2002) Email to B. Jackson, private communication.
- [83] D. R. Woodall (2004) Erratum to “A zero-free interval for chromatic polynomials” [Discrete Mathematics 101 (1992) 333-341]. *Discrete Math.* **275**, 385.
- [84] F. Y. Wu (1978) Percolation and the Potts Model. *J. Stat. Phys.* **18**, 115.
- [85] F. Y. Wu (1982) The Potts Model. *Rev. Mod. Phys.* **54**, 235.